

User Guide



Version 2.0

February 9, 2018

License

This document is licensed under
Creative Commons Attribution-NonCommercial-NoDerivs 3.0 Unported License
<http://creativecommons.org/licenses/by-nc-nd/3.0/legalcode>



Acknowledgments

The work leading to the preparation of this document has received funding from the European Research Council under the European Union's Seventh Framework Programme (FP7/2007-2013)/ERC Grant agreement n° 307499. The collaboration with Professor Fernando T. Pinho (University of Porto, Portugal), Professor Paulo J. Oliveira (University of Beira Interior, Portugal) and Dr Alexandre Afonso (University of Porto, Portugal) in the development of numerical methods for computational rheology is also acknowledged.

Disclaimer

This offering is not approved nor endorsed by ESI-Group, the producer of the OpenFOAM® software and owner of the OpenFOAM® trademark.

The recommendations expressed in this document are those of the authors and are not necessarily the views of, or endorsement by, third parties named in this document.

RheoTool, where this guide is included, is distributed in the hope that it will be useful, but WITHOUT ANY WARRANTY. See the GNU General Public License (<http://www.gnu.org/licenses/>) for more details.

Trademarks

Linux is a registered trademark of Linus Torvalds.

OpenFOAM is a registered trademark of ESI Group.

Paraview is a registered trademark of Kitware.

Typeset in L^AT_EX.

© 2016-2018 Francisco Pimenta, Manuel A. Alves

Contents

| | | |
|----------|---|-----------|
| 1 | Introduction | 1 |
| 1.1 | Motivation | 1 |
| 1.2 | Guide organization | 2 |
| 1.3 | Changelog | 3 |
| 1.4 | Citing <i>rheoTool</i> | 4 |
| 1.5 | Contacts | 4 |
| 2 | Installation | 5 |
| 2.1 | Folder organization | 5 |
| 2.2 | Compatibility with OpenFOAM® and foam-extend versions | 6 |
| 2.3 | System requirements | 6 |
| 2.4 | Downloading Eigen library | 6 |
| 2.5 | Installing <i>rheoTool</i> | 7 |
| 2.6 | Differences between versions | 8 |
| 3 | Theoretical background | 10 |
| 3.1 | Governing equations | 10 |
| 3.2 | Stabilization of viscoelastic fluid flow simulations | 11 |
| 3.2.1 | The both-sides-diffusion (BSD) technique | 11 |
| 3.2.2 | The log-conformation tensor approach | 11 |
| 3.3 | Coupling algorithms | 13 |
| 3.3.1 | Pressure-velocity coupling | 13 |
| 3.3.2 | Stress-velocity coupling | 14 |
| 3.4 | High-resolution schemes | 15 |
| 3.5 | Electrically-driven flow models | 16 |
| 3.5.1 | Poisson-Nernst-Planck model | 16 |
| 3.5.2 | Splitting the electric potential | 17 |
| 3.5.3 | Poisson-Boltzmann model | 18 |
| 3.5.4 | Debye-Hückel model | 18 |
| 3.5.5 | Slip model | 19 |
| 3.5.6 | Ohmic (leaky dielectric) model | 20 |
| 4 | Overview of <i>rheoTool</i> | 22 |
| 4.1 | The <i>constitutiveEquations</i> library | 22 |
| 4.1.1 | Available GNF and viscoelastic models | 22 |
| 4.1.2 | A note on FENE-type models | 26 |
| 4.1.3 | Multi-mode modeling | 28 |

| | | |
|----------|---|-----------|
| 4.1.4 | Analysis of a code sample | 28 |
| 4.1.5 | Advanced settings | 34 |
| 4.1.6 | Adding new viscoelastic or GNF models | 34 |
| 4.2 | The <i>EDFModels</i> library | 35 |
| 4.2.1 | Available EDF models | 35 |
| 4.2.2 | The potentials splitting approach and multi-species modeling in the PNP, PB and DH models | 37 |
| 4.2.3 | Electrokinetic coupling loop in the PNP model | 37 |
| 4.2.4 | Analysis of a code sample | 37 |
| 4.2.5 | Adding new EDF models | 44 |
| 4.3 | Solvers | 45 |
| 4.3.1 | <i>rheoFoam</i> | 46 |
| 4.3.2 | <i>rheoTestFoam</i> | 53 |
| 4.3.3 | <i>rheoInterFoam</i> | 55 |
| 4.3.4 | <i>rheoEFoam</i> | 56 |
| 4.4 | Boundary conditions | 57 |
| 4.4.1 | <i>linearExtrapolation</i> | 57 |
| 4.4.2 | <i>zeroIonicFlux</i> | 58 |
| 4.4.3 | <i>boltzmannEquilibrium</i> | 58 |
| 4.4.4 | <i>inducedPotential</i> | 58 |
| 4.4.5 | <i>slipSmoluchowski</i> | 59 |
| 4.4.6 | <i>slipSigmaDependent</i> | 59 |
| 4.4.7 | A note on wall boundary conditions for pressure | 59 |
| 4.5 | Utilities | 61 |
| 4.5.1 | <i>GaussDefCmpw</i> schemes for convective terms | 61 |
| 4.5.2 | Generic post-processing: <i>ppUtil</i> | 63 |
| 4.5.3 | <i>writeEfield</i> | 65 |
| 5 | Tutorials | 66 |
| 5.1 | <i>rheoFoam</i> | 67 |
| 5.1.1 | General guidelines | 67 |
| 5.1.2 | A note on <i>coded FunctionObjects</i> | 72 |
| 5.1.3 | Case 1: flow between parallel plates | 73 |
| 5.1.4 | Case 2: lid-driven cavity flow | 74 |
| 5.1.5 | Case 3: flow in a 4:1 planar contraction | 76 |
| 5.1.6 | Case 4: flow around a confined cylinder | 79 |
| 5.1.7 | Case 5: bifurcation in a 2D cross-slot flow | 81 |
| 5.1.8 | Case 6: blood flow simulation in a real-model aneurysm | 84 |
| 5.2 | <i>rheoTestFoam</i> | 87 |
| 5.2.1 | General guidelines | 87 |
| 5.2.2 | Case I: Herschel-Bulkley model | 90 |
| 5.2.3 | Case II: FENE-CR model | 91 |
| 5.3 | <i>rheoInterFoam</i> | 94 |
| 5.3.1 | General guidelines | 94 |
| 5.3.2 | Case 1: impacting drop | 95 |
| 5.3.3 | Case 2: planar die swell | 97 |

| | |
|---|------------|
| 5.4 <i>rheoEFoam</i> | 99 |
| 5.4.1 General guidelines | 99 |
| 5.4.2 Case I: EDF of power-law and PTT fluids in a microchannel . . | 102 |
| 5.4.3 Case II: induced-charge electroosmosis around a cylinder . . | 106 |
| 5.4.4 Case III: charge transport across an ion-selective membrane . | 108 |
| 5.4.5 Case IV: electrokinetic instabilities in a flow-focusing device . | 110 |
| 5.4.6 Case V: electrokinetic mixer | 114 |
| 5.4.7 Case VI: electro-elastic instabilities in cross-shaped geometries | 116 |
| Appendix A Parameters and variables in <i>rheoTool</i> | 119 |
| Bibliography | 124 |

Chapter 1

Introduction

1.1 Motivation

The open-source OpenFOAM® toolbox can be used as a versatile finite-volume solver for CFD simulations in general polyhedral grids. A number of constitutive equations for Generalized Newtonian Fluids (GNF) are already available in the toolbox for a long time. More recently, Favero et al. [1] created a library containing a wide range of constitutive equations to model viscoelastic fluids, along with a solver named *viscoelasticFluidFoam* which makes use of this library. However, *viscoelasticFluidFoam* presents stability issues in certain conditions, such as, for example, in the simulation of high Weissenberg number (Wi) flows or when there is no solvent viscosity contribution (e.g. in the upper-convected Maxwell model).

In Ref. [2], we attempted to minimize those issues by modifying critical points in the *viscoelasticFluidFoam* solver and in the handling of viscoelastic models. The modified solver was tested in benchmark flows and second-order accuracy, both in space and time, was observed, in addition to an enhanced stability [2]. The package that we present in this document – *rheoTool* – implements the method described in [2].

Afterwards, the capability to simulate electrically-driven flows was added to *rheoTool* [3] and is available since version 2.0.

rheoTool is more than a collection of solvers and libraries. In addition to robust solvers for the simulation of pressure- and electrically-driven flows of both GNF and viscoelastic fluids, we provide also tutorials and utilities that can be useful for the users starting to apply the OpenFOAM® toolbox in the simulation of complex fluid flows. In particular, some of the distinguishing features of *rheoTool* are:

- both GNF and viscoelastic models can be selected on run time and applied to single-phase laminar flows. A solver for two-phase flows is also being developed and an experimental (but fully functional) version is already available.
- the log-conformation tensor methodology [4] is available for a wide range of viscoelastic models. This minimizes the numerical instabilities frequently observed for high Weissenberg number flows.
- a stress-velocity coupling term can be selected on run time in order to avoid

checkerboard fields under specific conditions, such as in the simulation of the Upper-Conveyed Maxwell (UCM) model in strong extensional flows.

- high-resolution schemes for convective terms are available in a component-wise and deferred correction approach, avoiding numerical instabilities (see Ref. [2] for details). Additional schemes were added to the newly created library, which are not available by default in the OpenFOAM® toolbox.
- a solver (*rheoTestFoam*) is provided to compute the relevant material functions of each GNF/viscoelastic model included in the library. The user can select any canonical flow to be tested (shear flow, extensional flow, etc.).
- a number of models for electrically-driven flows is available and can be coupled with any rheological model. Mixed pressure- and electrically-driven flows are also allowed.
- transient flow solvers use the SIMPLEC algorithm for pressure-velocity coupling, instead of the PISO implementation. Large time-steps can be used without decoupling problems, and the use of under-relaxation is not required (except for pressure in some problems using non-orthogonal grids).
- the tool is provided with a user-guide (this document) and a selected set of tutorials reproducing relevant benchmark or real-life flow problems.
- *rheoTool* is available for both ¹OpenFOAM® and ²foam-extend versions.

1.2 Guide organization

The remainder of this guide is organized as follows:

- Chapter 2 describes the basic steps to install *rheoTool*.
- Chapter 3 provides a succinct overview of the theory behind the governing equations being solved. More details can be found in Refs. [2,3,5].
- Chapter 4 presents an overview of the functionalities available in *rheoTool*, and discusses technical details about the code implementation.
- Chapter 5 contains several tutorials, guiding the reader into the use of *rheoTool*.

The language and the content used in this guide assumes that the reader has a basic knowledge on the use of the OpenFOAM® toolbox and is familiar with the finite-volume method applied to CFD problems. Thus, it is out the scope of this document to serve as an introduction on those subjects.

Although *rheoTool* is available for different OpenFOAM® and foam-extend versions, Chapters 4 and 5 use OpenFOAM® version 2.2.2 to describe the contents.

¹<http://openfoam.org/>

²<http://www.extend-project.de/>

However, the small differences among different versions should not be an obstacle to the readers using any other version.

The readers interested in the theory behind *rheoTool* are strongly encouraged to first read Refs. [2] and [3] before this guide.

1.3 Changelog

Version 2.0

Released on 09/02/2018.

Electrically-driven flows

- Add: solvers, libraries, utilities and tutorials for electrically-driven flows.

Constitutive equations

- Add: the Rolie-Poly viscoelastic model has been added to the library of constitutive equations. Both the stress and log-conformation versions are available.
- Add: the (single-equation) eXtended Pom-Pom viscoelastic model has been added to the library of constitutive equations. Both the stress and log-conformation versions are available.
- Change: sPTT models have been generalized to their full form by replacing the upper-convected derivative by the Gordon-Schowalter derivative. It is now possible to simulate PTT models with non-affine deformation, in both the stress and log-conformation versions.
- Change: the stabilization method in viscoelastic simulations has been made general and run time selectable: *none*, *BSD* or *coupling*.
- Change: a verification step has been added to the *WhiteMetznerLog* model in order to prevent its incorrect use (see the note in the table displaying the constitutive equations).

Post-Processing

- Add: class *ppUtil* for post-processing purposes has been added to the versions for OpenFOAM® and the one existing for foam-extend has been modified. Enable the use of multiple *ppUtil* in simultaneous.
- Fix: sampling error was fixed for the tutorials of versions *of40* and *fe40*.

Multiphase flows

- Change: `(fvc::grad(U)&fvc::grad(etaS())*alpha))` has been replaced by `fvc::div(etaS())*alpha*dev2(T(fvc::grad(U))))` for the use in multiphase flows (`constitutiveEq.C`).

- Fix: call to *constrainPressure()* in *rheoInterFoam*, version *of40*, has been corrected for the SIMPLEC algorithm (*pEqn.H*). Added a section in the user-guide on how to use properly the *fixedFluxPressure* BC with *rheoInterFoam* in versions *of222* and *fe40*.
- Add: tutorials on the die swell problem.

Generic

- Change/Fix: code cleanup and bug fix (BC evaluation of the explicit *fvc::div(phi,X)* operator) in class *GaussDefCmpw*.
- Change/Add: replace boundary condition *extST* by the *Type*-independent *linearExtrapolation* boundary condition (no backward compatibility). Added optional second-order regression.
- Change: major update of the user guide to include electrically-driven flows. Other changes were made in its content and organization, and some typos were corrected.
- Change: ensure compatibility with foam-extend 4.0 and OpenFOAM® v4.1.

Version 1.0

Released on 6/12/2016.

Initial version.

1.4 Citing *rheo Tool*

If you found *rheo Tool* useful and want to cite it in your work, the following BibTex entry can be used for that purpose:

```
@misc{rheoTool,
  author = "F. Pimenta and M.A. Alves",
  title = "rheoTool",
  howpublished = "\url{https://github.com/fppimenta/rheoTool}",
  year = "2016"}
```

Since the underlying theory of *rheo Tool* has been mainly presented in technical papers (Refs. [2] and [3]), these can also be used for citation purposes.

1.5 Contacts

rheo Tool is under continuous development and new features will be added in the future. If you have any suggestions, comments or doubts regarding the tool, or if you found a bug or error, feel free to contact us:

✉ F. Pimenta: fpimenta@fe.up.pt

✉ M.A. Alves: mmalves@fe.up.pt

Chapter 2

Installation

2.1 Folder organization

The structure of *rheoTool* cloned or downloaded from the GitHub repository (<https://github.com/fppimenta/rheoTool>) is depicted in Fig. 2.1.

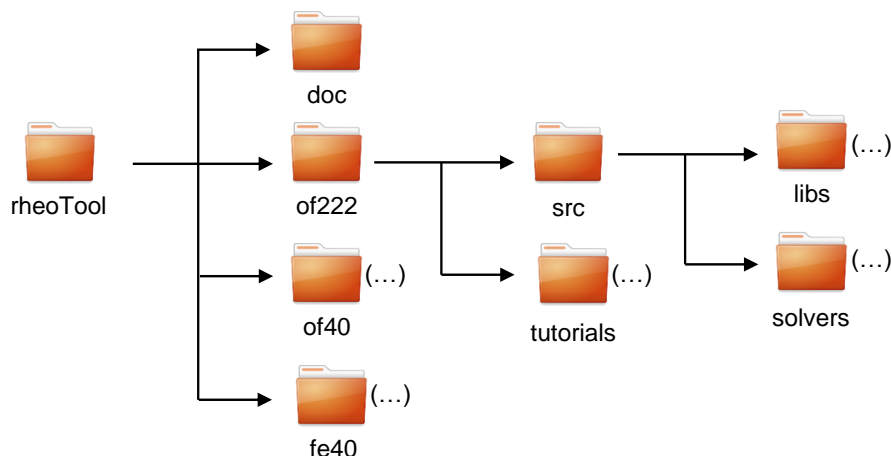


Figure 2.1: Directory organization of *rheoTool*.

The top-level directory of *rheoTool* contains the versions available for different OpenFOAM® (*of*) and foam-extend (*fe*) versions (see next section for compatibility issues). The folder **doc/**, containing the user-guide, is also in the top-level directory. Inside the folder for each version, there are two directories: **src/**, where the source-code can be found, and **tutorials/**, containing several tutorial cases showing the use of *rheoTool*. The **src/** directory is further subdivided in a directory with the applications (**solvers/**) and another one containing libraries (**libs/**).

After cloning/downloading *rheoTool*, the user is free to remove from the top-level directory all the versions not needed and keep only the one(s) of interest.

2.2 Compatibility with OpenFOAM® and foam-extend versions

The development and testing of *rheoTool* was mainly performed in OpenFOAM® version 2.2.2 (we will change to version 4.0/4.1 in a near future). However, an effort has been made to release *rheoTool* also running under other (more recent) versions of OpenFOAM® and foam-extend. Thus, compatible versions of *rheoTool* are provided for:

- OpenFOAM® v2.2.2 ([of222/](#)).
- OpenFOAM® v4.0, v4.1 ([of40/](#)).
- foam-extend 4.0 ([fe40/](#)).

Note that the list above includes the versions which were effectively tested. This means that a given version of *rheoTool* may be compatible with other OpenFOAM® or foam-extend versions not included in this list. The versions above were tested in a Ubuntu (12.04 or 16.04) environment, but other operating systems running OpenFOAM® can eventually support some version of *rheoTool*. However, the installation is only described here for a Linux OS.

2.3 System requirements

Only standard requirements are needed to install *rheoTool*:

- a compatible and functional version of OpenFOAM® or foam-extend should be already installed.
- the machine should be connected to the Internet.

After ensuring that these conditions are fulfilled, the user is ready to start the installation, which includes two major steps: downloading (no install) the open-source Eigen library [6] and installing *rheoTool*.

2.4 Downloading Eigen library

In the top-level directory of *rheoTool*, open a terminal and check that file `etc/bashrc` of your installed OpenFOAM® or foam-extend version has been sourced. This is particularly relevant if you have defined *alias* for different versions of OpenFOAM® or foam-extend. If this is the case, be sure that the alias pointing to the desired version has been typed. Shortly, you should only advance to the next step if a command like `~$ icoFoam -help` is recognized in the terminal. Note that in this document we use the prepending `~$` for any instruction to be typed in the command line (thus, `~$ icoFoam -help` means that you only type `icoFoam -help`). If this check is successful, run the script `downloadEigen` in that terminal:

```
~$ ./downloadEigen
```

This script downloads Eigen version 3.2.9 (other versions close to that would also work adequately) from the Internet (using *wget*), extracts it and moves it to directory:

```
$ WM_PROJECT_USER_DIR/ThirdParty/Eigen3.2.9
```

Eigen is used in *rheoTool* for computation of eigenvalues and eigenvectors and there is no need to install the library, since the inclusion of the required headers is enough for our purposes.

However, its location in the system must be defined and exported. This is achieved by attributing to variable **EIGEN_RHEO** – the one used and recognized by *rheoTool* – the actual path of Eigen. The command to do so has been displayed to the terminal after running script `downloadEigen` (if everything was ok) and looks like:

```
~$ echo "export EIGEN_RHEO=/home/user/OpenFOAM/user-4.0/ThirdParty/Eigen3.2.9">>/home/user/.bashrc
```

Do not copy this command, it is just an example of what is displayed to the screen. Instead, copy-paste and run the command appearing in your terminal.

If, for some reason, the user wants to move Eigen to another directory (or already has an Eigen version in another directory), then move Eigen to its final location (if already not) and define variable **EIGEN_RHEO** accordingly. **Note that Eigen only needs to be installed once per system.** Even if the user has installed multiple versions of *rheoTool* in the same system, the above procedure only needs to be run once (for the first version being installed), as long as the directory containing Eigen since the first installation is not deleted, or renamed.

2.5 Installing *rheoTool*

While Eigen needs to be saved in a specified directory to avoid any change in the code (because an absolute path is used), the folder containing *rheoTool* can be saved and compiled in any location on your machine. Nevertheless, a location with writing permission is recommended, otherwise you will need to use *sudo* mode to run all the commands. A good location for *rheoTool* is, for example, directory `$WM_PROJECT_USER_DIR`, which is defined by default when OpenFOAM® or foam-extend is installed.

After you move *rheoTool* to its final location, **open a new terminal** (to ensure that your system `~/.bashrc` is sourced and contains the path of Eigen) in the top-level directory of *rheoTool* (ensuring that the OpenFOAM® or foam-extend environment has been sourced, as previously) and enter the directory with the version of *rheoTool* that is compatible with your OpenFOAM® or foam-extend version, and then go to directory `src/`. For example, for OpenFOAM® v2.2.2, it would be:

```
~$ cd of222/src
```

Now, run the script `Allwmake` to build the libraries and applications of *rheoTool*:

```
~$ ./Allwmake
```

Both the libraries and applications installed with *rheoTool* can be cleaned by running the script `Allwclean`.

Since the user will probably not need the remaining versions of *rheoTool* that remain in the top-level directory, they can simply be deleted, if already not.

To check if the installation succeeded, the user should try to run one of the tutorials of Chapter 5.

2.6 Differences between versions

In order to make *rheoTool* compatible with each OpenFOAM®/foam-extend version, several modifications were required at the programming level for each case. On the other hand, the user-interface remained almost unchanged among the different versions. The main exception is on the *codedStream FunctionObjects* and *coded* boundary conditions, which are used in the tutorials of Chapter 5. Indeed, while these functionalities are available in OpenFOAM®, it is not the case for foam-extend. Thus, the *coded* boundary conditions and the utilities implemented as *codedStream FunctionObjects* in OpenFOAM® versions had to be assembled and compiled in a library for the foam-extend version.

A second point to be taken into account is that *rheoTool* may perform differently in each OpenFOAM®/foam-extend version, as it may happen with any other default solver of OpenFOAM®/foam-extend. This is naturally a consequence of the evolution of the core machinery of OpenFOAM®/foam-extend, transversal to many solvers and libraries. Fortunately, in most of the cases the differences will be small. All the discussion in this guide, including the results presented for the tutorials in Chapter 5, is for OpenFOAM® v2.2.2, as aforementioned. Taking this version as reference, the following issues were detected in the tests that we performed:

- there is some difference in the results for non-orthogonal grids, between *of222* and the other two versions tested. This issue can be observed, for example, in the tutorial of section 5.1.6, where the drag coefficient in a cylinder is computed. The difference is originated by a change which has been introduced since version 2.3.x in the computation of the cell-to-face distance at the boundaries, that is used, for example, in the *fvm::laplacian()* operator. The change can be found in file `src/finiteVolume/fvMesh/fvPatches/fvPatch/fvPatch.C`, in the function *fvPatch::delta()*, where the newer versions only account for the normal component of the cell-to-face vector.
- in general, a tutorial of *rheoTool* for versions *of40* or *of222* may be run either in serial or parallel while keeping the same numerical settings. However, in the tests using version *fe40*, it was observed that parallel runs are less stable than serial runs, usually requiring a lower time-step or some under-relaxation of the velocity (sometimes as low as 0.97).

Although the main development of *rheoTool* has been made using OpenFOAM® v2.2.2 for historical reasons, in general we recommend new users to prefer more recent distributions of OpenFOAM®, since several improvements and bug fixes have

been made since v2.2.2 (released in 2013). This is especially true for multiphase flows.

Chapter 3

Theoretical background

The equations governing pressure- and electrically-driven flows of incompressible, complex fluids are discussed in this Chapter, along with some important aspects related with their discretization in the finite-volume framework. Since a thorough discussion on this subject can be found in Refs. [2, 3], some intermediate steps are skipped and only the more relevant equations are presented.

3.1 Governing equations

The basic equations governing isothermal, single-phase, transient flows, under laminar conditions, for incompressible fluids, establish mass conservation (Eq. 3.1) and momentum balance (Eq. 3.2),

$$\nabla \cdot \mathbf{u} = 0 \quad (3.1)$$

$$\rho \left(\frac{\partial \mathbf{u}}{\partial t} + \mathbf{u} \cdot \nabla \mathbf{u} \right) = -\nabla p + \nabla \cdot \boldsymbol{\tau}' + \mathbf{f} \quad (3.2)$$

where \mathbf{u} is the velocity vector, t is the time, p is the pressure, $\boldsymbol{\tau}'$ is the extra-stress tensor and \mathbf{f} is any external body-force, such as the electric force discussed in Section 3.5. To simulate viscoelastic fluid flows, it is a common approach to split the total extra-stress tensor in a solvent contribution ($\boldsymbol{\tau}_s$) and a polymeric contribution ($\boldsymbol{\tau}$), $\boldsymbol{\tau}' = \boldsymbol{\tau} + \boldsymbol{\tau}_s$. In order to have a closed set of equations, a constitutive equation is required for each tensor contribution, which can be generally written as in Eqs. (3.3) and (3.4), for a wide range of models,

$$\boldsymbol{\tau}_s = \eta_s(\dot{\gamma})(\nabla \mathbf{u} + \nabla \mathbf{u}^T) \quad (3.3)$$

$$f(\boldsymbol{\tau})\boldsymbol{\tau} + \lambda(\dot{\gamma}) \overset{\nabla}{\boldsymbol{\tau}} + \mathbf{h}(\boldsymbol{\tau}) = \eta_p(\dot{\gamma})(\nabla \mathbf{u} + \nabla \mathbf{u}^T) \quad (3.4)$$

In Eqs. (3.3) and (3.4), η_s is the solvent viscosity, η_p is the polymeric viscosity coefficient, λ is the relaxation time, $\dot{\gamma}$ is the shear-rate, $f(\boldsymbol{\tau})$ is a general scalar function depending on an invariant of $\boldsymbol{\tau}$, $\mathbf{h}(\boldsymbol{\tau})$ is a tensor-valued function depending on $\boldsymbol{\tau}$ and $\overset{\nabla}{\boldsymbol{\tau}} = \frac{\partial \boldsymbol{\tau}}{\partial t} + \mathbf{u} \cdot \nabla \boldsymbol{\tau} - \boldsymbol{\tau} \cdot \nabla \mathbf{u} - \nabla \mathbf{u}^T \cdot \boldsymbol{\tau}$ represents the upper-convected

time derivative, which renders the models frame-invariant. Some models use the Gordon-Schowalter derivative ($\square \boldsymbol{\tau} = \nabla^2 \boldsymbol{\tau} + \zeta (\boldsymbol{\tau} \cdot \mathbf{D} + \mathbf{D} \cdot \boldsymbol{\tau})$, with $\mathbf{D} = \frac{1}{2}(\nabla \mathbf{u} + \nabla \mathbf{u}^T)$) instead of the upper-convected derivative, in order to take non-affine deformation into account (controlled by parameter ζ). In *rheoTool*, this is the case of PTT-type models. Other constitutive models exist, which can also make use of the lower-convected time derivative, but those are not explored here. The constitutive equation for a GNF is limited to Eq. (3.3), since elasticity is not considered ($\boldsymbol{\tau}' = \boldsymbol{\tau}_s$). In Table 4.1 presented in the next Chapter, Eqs. (3.3) and (3.4) are specified for several GNF and viscoelastic models.

Eqs. (3.1)–(3.4) represent the standard system of equations to be solved. However, due to numerical stability issues in viscoelastic fluid flow simulations, the system is rarely solved in that form. Indeed, several techniques are available for stabilization purposes (see, for instance, Ref. [7] for a comparison between the most popular techniques) and the ones used in *rheoTool* are addressed next.

3.2 Stabilization of viscoelastic fluid flow simulations

3.2.1 The both-sides-diffusion (BSD) technique

The both-sides-diffusion (BSD) is a technique already incorporated in the *viscoelasticFluidFoam* solver [1]. It consists in adding a diffusive term on both sides of momentum equation (Eq. 3.2), with the difference that one of them (left-hand side) is added implicitly, while the other one (right-hand side) is added explicitly. Once steady-state is reached, both terms cancel each other exactly. Such method increases the ellipticity of the momentum equation and, as such, has a stabilizing effect, mostly when there is no solvent contribution in the extra-stress tensor. Incorporating the terms arising from the both-sides-diffusion in the momentum equation, and making use of Eq. (3.3), then

$$\rho \left(\frac{\partial \mathbf{u}}{\partial t} + \mathbf{u} \cdot \nabla \mathbf{u} \right) - \nabla \cdot (\eta_s + \eta_p) \nabla \mathbf{u} = -\nabla p - \nabla \cdot (\eta_p \nabla \mathbf{u}) + \nabla \cdot \boldsymbol{\tau} + \mathbf{f} \quad (3.5)$$

Note that the added diffusive terms are scaled by the polymeric viscosity (η_p), which is a common choice in the literature (e.g. Ref. [7]), although not mandatory. In order to simplify the reading, the possible dependence of the viscosity and relaxation time on the shear-rate will be dropped in the respective symbols, as already done in Eq. (3.5), although this relation still holds to keep generality.

3.2.2 The log-conformation tensor approach

The log-conformation tensor approach consists in a change of variable when evolving in time the polymeric extra-stress and it was devised to tackle the numerical instability faced at high Weissenberg number flows [4, 8].

The polymeric extra-stress tensor is related with the conformation tensor (\mathbf{A}). For the Oldroyd-B model, for example, this relation is expressed as (see Table 4.1 for several viscoelastic models)

$$\boldsymbol{\tau} = \frac{\eta_p}{\lambda} (\mathbf{A} - \mathbf{I}) \quad (3.6)$$

In the log-conformation tensor methodology, a new tensor ($\boldsymbol{\Theta}$) is defined as the natural logarithm of the conformation tensor

$$\boldsymbol{\Theta} = \ln(\mathbf{A}) = \mathbf{R} \ln(\Lambda) \mathbf{R}^T \quad (3.7)$$

In Eq. (3.7), the conformation tensor was diagonalized ($\mathbf{A} = \mathbf{R} \Lambda \mathbf{R}^T$) because it is positive definite, where \mathbf{R} is a matrix containing in its columns the eigenvectors of \mathbf{A} and Λ is a matrix whose diagonal elements are the respective eigenvalues resulting from the decomposition of \mathbf{A} . Eq. (3.4) written in terms of ($\boldsymbol{\Theta}$) becomes [4]

$$\frac{\partial \boldsymbol{\Theta}}{\partial t} + \mathbf{u} \cdot \nabla \boldsymbol{\Theta} = \boldsymbol{\Omega} \boldsymbol{\Theta} - \boldsymbol{\Theta} \boldsymbol{\Omega} + 2\mathbf{B} + \frac{1}{\lambda} \mathbf{g}(\boldsymbol{\Theta}) \quad (3.8)$$

where $\mathbf{g}(\boldsymbol{\Theta})$ is a model-specific tensorial function depending on $\boldsymbol{\Theta}$ (see Table 4.1 for other viscoelastic models) and

$$\mathbf{B} = \mathbf{R} \begin{bmatrix} m_{xx} & 0 & 0 \\ 0 & m_{yy} & 0 \\ 0 & 0 & m_{zz} \end{bmatrix} \mathbf{R}^T \quad (3.9)$$

$$\boldsymbol{\Omega} = \mathbf{R} \begin{bmatrix} 0 & \omega_{xy} & \omega_{xz} \\ -\omega_{xy} & 0 & \omega_{yz} \\ -\omega_{xz} & -\omega_{yz} & 0 \end{bmatrix} \mathbf{R}^T \quad (3.10)$$

$$\mathbf{M} = \mathbf{R} \nabla \mathbf{u}^T \mathbf{R}^T = \begin{bmatrix} m_{xx} & m_{xy} & m_{xz} \\ m_{yx} & m_{yy} & m_{yz} \\ m_{zx} & m_{zy} & m_{zz} \end{bmatrix} \quad (3.11)$$

$$\omega_{ij} = \frac{\Lambda_j m_{ij} + \Lambda_i m_{ji}}{\Lambda_j - \Lambda_i} \quad (3.12)$$

After solving Eq. (3.8), $\boldsymbol{\Theta}$ is diagonalized in the form

$$\boldsymbol{\Theta} = \mathbf{R} \Lambda^\Theta \mathbf{R}^T \quad (3.13)$$

and the conformation tensor is recovered by the inverse relation of Eq. (3.7)

$$\mathbf{A} = \exp(\boldsymbol{\Theta}) = \mathbf{R} \exp(\Lambda^\Theta) \mathbf{R}^T \quad (3.14)$$

Finally, the polymeric extra-stress tensor can be computed from \mathbf{A} (Eq. 3.6) and used in the momentum equation.

Note that for PTT-type models, which may include non-affine deformation through the Gordon-Schowalter derivative, the tensor \mathbf{M} (Eq. 3.11) is computed differently: $\mathbf{M} = \mathbf{R} (\nabla \mathbf{u}^T - \zeta \mathbf{D}) \mathbf{R}^T$.

It is worth to mention that the log-conformation approach can be considered a particular case of the kernel-conformation method [9]. However, from our experience, the *log* kernel is frequently the optimal kernel (in terms of robustness and accuracy) for generic problems, so that only this one is widely used in *rheoTool*. Nevertheless, for the Oldroyd-B model, the root^{*k*} kernel [9] and the square-root transformation [10] are also included in *rheoTool* for demonstration purposes.

3.3 Coupling algorithms

3.3.1 Pressure-velocity coupling

Although the OpenFOAM® toolbox is already able to solve linear systems of equations in a coupled way, most of the solvers still rely on segregated solutions (this is a rule for transient solvers). In segregated solvers, the equations for each variable are solved sequentially. Even for a fully-implicit method, if the coupling between variables is weak, then numerical divergence is prone to occur.

In the OpenFOAM® toolbox, common algorithms for pressure-velocity coupling are SIMPLE and SIMPLEC for steady-state solvers and either PISO or PIMPLE (a combination of SIMPLE(C) and PISO) for transient solvers. From the benchmark cases performed in Ref. [2], it was observed that SIMPLEC was particularly suitable for transient viscoelastic fluid flows at low Reynolds numbers, regarding stability and accuracy.

The continuity equation, implicit in the pressure variable, derived for SIMPLEC (a more detailed derivation is presented in Ref. [2]) leads to

$$\nabla \cdot \left(\frac{1}{a_P - H_1} (\nabla p)_P \right) = \nabla \cdot \left[\frac{\mathbf{H}}{a_P} + \left(\frac{1}{a_P - H_1} - \frac{1}{a_P} \right) (\nabla p^*)_P \right] \quad (3.15)$$

where a_P are the diagonal coefficients from the momentum equation, $H_1 = - \sum_{nb} a_{nb}$ is an operator representing the negative sum of the off-diagonal coefficients from momentum equation, $\mathbf{H} = - \sum_{nb} a_{nb} \mathbf{u}_{nb}^* + \mathbf{b}$ is an operator containing the off-diagonal contributions, plus source terms (except the pressure gradient) of the momentum equation and p^* is the pressure field known from the previous time-step or iteration. Accordingly, the equation to correct the velocity after obtaining the continuity-compliant pressure field from Eq. (3.15) is

$$\mathbf{u} = \frac{\mathbf{H}}{a_P} + \left(\frac{1}{a_P - H_1} - \frac{1}{a_P} \right) (\nabla p^*)_P - \frac{1}{a_P - H_1} (\nabla p)_P \quad (3.16)$$

Importantly, in order to avoid the onset of checkerboard fields, the pressure gradient terms involved in the computation of face velocities, i.e., in Eqs. (3.15) and (3.16), are directly evaluated using the pressure on the cells straddling the face, in a Rhie-Chow-like procedure (more details in Ref. [2]). Nonetheless, when Eq. (3.16) is used to correct the cell-centered velocity field, the pressure gradient terms are computed "in the usual way", for example using Green-Gauss integration.

Rhie-Chow methods used to avoid checkerboard fields, as the one described in the previous paragraph, are known to be affected by the use of small time-steps and they also present time-step dependency on steady-state results [11]. In OpenFOAM® solvers, a common strategy to avoid such effects is to add a corrective term to face-interpolated velocities, through functions *ddtPhiCorr()* or *ddtCorr()*. Recently, in foam-extend the time-step dependency was solved in a different way, by removing the transient term contribution from the a_P coefficients of the momentum equation [12]. However, this approach may be problematic when used with the SIMPLEC algorithm, since a division by zero is prone to happen. In *rheoTool*, we keep using the added corrective term, although, as mentioned in Ref. [2], this term can be improved in order to more efficiently avoid the small time-step dependency of steady-state solutions.

3.3.2 Stress-velocity coupling

Stress-velocity decoupling problems can arise for similar reasons as those described for pressure-velocity: the cell-centered velocity loses the influence of the forces (either polymeric extra-stress or pressure gradient) of its direct neighborhood (cells sharing a face in common). This usually happens in the interpolation from cell-centered to face-centered fields. In the case of polymeric extra-stresses, it is the divergence term ($\nabla \cdot \boldsymbol{\tau}$) in the momentum equation, when $\boldsymbol{\tau}$ is linearly interpolated from cell centers to face centers, which can be responsible for the decoupling.

In Ref. [2], we described a new stress-velocity coupling method, where the polymeric extra-stresses at face centers are computed as

$$\boldsymbol{\tau}_f = \bar{\boldsymbol{\tau}}_f + \eta_p \left[(\nabla \mathbf{u} |_f + (\nabla \mathbf{u})^T |_f) - \left(\bar{\nabla \mathbf{u}} |_f + \bar{(\nabla \mathbf{u})^T} |_f \right) \right] \quad (3.17)$$

where terms with an overbar are linearly interpolated from cell-centered values, while the remaining velocity gradients are directly evaluated from the cell-centered velocities straddling the face. When the definition of $\boldsymbol{\tau}_f$ in Eq. (3.17) is inserted in the momentum equation with the both-sides-diffusion terms already present (Eq. 3.5), then we obtain

$$\rho \left(\frac{\partial \mathbf{u}}{\partial t} + \mathbf{u} \cdot \nabla \mathbf{u} \right) - \nabla \cdot (\eta_s + \eta_p) \nabla \mathbf{u} = -\nabla p - \bar{\nabla} \cdot \eta_p \bar{\nabla \mathbf{u}} + \nabla \cdot \bar{\boldsymbol{\tau}} + \mathbf{f} \quad (3.18)$$

where the term $\bar{\nabla} \cdot \eta_p \bar{\nabla \mathbf{u}}$ is a "special second-order derivative" (different from the *laplacian* operator of OpenFOAM®), defined as the divergence of the velocity gradient, where the velocity gradient at the faces is obtained by linear interpolation of the velocity gradient evaluated on the cell centers. More details are presented in Ref. [2], where it is shown that with mesh refinement Eq. (3.17) approaches $\boldsymbol{\tau}_f = \bar{\boldsymbol{\tau}}_f$ and the additional terms cancel out. Note that when inserting Eq. (3.17) in the momentum equation (resulting in Eq. 3.18), we drop the transpose velocity gradients for simplicity, since continuity imposes $\nabla \cdot \nabla \mathbf{u}^T = \mathbf{0}$.

3.4 High-resolution schemes

The discretization of convective terms within the finite-volume framework leads to

$$\int_V (\mathbf{u} \cdot \nabla \phi) dV = \sum_f \phi_f (\mathbf{u}_f \cdot \mathbf{S}_f) = \sum_f \phi_f F_f \quad (3.19)$$

where ϕ is a generic variable being advected, \mathbf{S}_f is the face-area vector and F_f is the volumetric flux crossing face f . While fluxes are known at the faces from the Rhee-Chow-like interpolation (Eq. 3.16), ϕ at face centers need to be interpolated from known values at cell centers. OpenFOAM® offers a wide range of schemes to perform such interpolation, from upwind – an unconditionally stable scheme, but only first-order accurate –, to central differences – a conditionally stable, second-order accurate scheme. A good compromise between both extremes is provided by High-Resolution Schemes (HRSs). When represented in a Normalized Variable Diagram (NVD), several HRSs are piecewise-linear functions and can be defined using the Normalized Weighting Factor (NWF) approach [13]:

$$\tilde{\phi}_f = \alpha \tilde{\phi}_C + \beta \quad (3.20)$$

where the following definitions hold

$$\tilde{\phi}_f = \frac{\phi_f - \phi_U}{\phi_D - \phi_U} \quad (3.21a)$$

$$\tilde{\phi}_C = \frac{\phi_C - \phi_U}{\phi_D - \phi_U} \quad (3.21b)$$

In Eq. (3.20), α and β are scalars specific to each HRS and they can be functions of $\tilde{\phi}_C$. Subscripts in Eqs. (3.21a,b) have the following meaning: for a given face, cell C is the cell from which the flux comes (upstream), cell D (downstream) is the cell to which the flux goes and cell U (far-upstream) is the cell upstream to cell C. In a general unstructured mesh, cell U cannot be identified unequivocally, and ϕ_U in Eqs. (3.21a,b) can be evaluated as [14]

$$\phi_U = \phi_D - 2(\nabla \phi)_C \cdot \mathbf{d}_{CD} \quad (3.22)$$

where \mathbf{d}_{CD} is the vector connecting the center of cells C and D. For a deferred correction implementation of HRSs, the upwind part of the HRS is discretized implicitly, while the remaining (difference between the HRS and the upwind differencing scheme) is discretized explicitly (cf. Ref. [2]), which, using Eqs. (3.20-3.22), results in

$$\phi_f = [\phi_C]_{\text{implicit}} + [(\alpha - 1)\phi_C + \beta\phi_D + (1 - \alpha - \beta)(\phi_D - 2(\nabla \phi)_C \cdot \mathbf{d}_{CD})]_{\text{explicit}} \quad (3.23)$$

Handling the HRSs in a deferred correction approach avoids, in some cases, numerical instabilities introduced by the central-differencing component of the HRS. Additionally, in Ref. [2] it was observed that the usual methodology of OpenFOAM® to apply HRSs to non-scalar variables (tensors and vectors) can locally introduce numerical instabilities in some viscoelastic flow problems. This

methodology consists in using a frame-invariant quantity for non-scalar variables, such as the squared magnitude for vectors, or the trace (or double-dot product) for tensors, to compute the α and β parameters in Eq. (3.23). It was observed that such artificial instabilities can be significantly damped with a component-wise handling of non-scalar variables [2], at the cost of losing frame-invariance, which however is very weak and vanishes with grid refinement. Accordingly, non-scalar variables are split into its components and Eq. (3.23) is applied independently to each one of them. Note that this approach still generates one single matrix of coefficients for such variables, since the upwind differencing scheme coefficients are common to all the components (they only depend on the flux). The differentiation between components is only introduced in the explicit part of Eq. (3.23), generating a different source term for each individual tensor/vector component. This is possible due to the use of a deferred correction approach.

3.5 Electrically-driven flow models

Consider now that the fluid under analysis is a weak electrolyte subjected to an electric field. In such conditions, the momentum equation (Eq. 3.2) should include the contribution from an electric body-force,

$$\mathbf{f} = \mathbf{f}_E = \nabla \cdot \left[\varepsilon \left(\mathbf{E} \mathbf{E} - \frac{\|\mathbf{E}\|^2}{2} \mathbf{I} \right) \right] = \rho_E \mathbf{E} - \frac{\|\mathbf{E}\|^2}{2} \nabla \varepsilon \quad (3.24)$$

where \mathbf{E} is the electric field, $\varepsilon = \varepsilon_0 \varepsilon_R$ is the electric permittivity and ρ_E is the charge density (per unit volume). In order to close the system of equations for electrically-driven flows (EDFs), additional relations must be provided to compute the terms in Eq. (3.24). Some options, the ones available in *rheoTool*, are presented next. Note that when referring generically to EDFs, we do not exclude the possibility of having any other external forcing (for example due to an imposed pressure difference), in addition to the electric forcing. When only an electric forcing exists, we call this flow as pure EDF.

The second term of Eq. (3.24) is only non-zero for a system of two fluids, each having a different electric permittivity.

3.5.1 Poisson-Nernst-Planck model

In the absence of magnetic effects, the electric potential (Ψ) can be computed by Gauss' law

$$\nabla \cdot (\varepsilon \nabla \Psi) = -\rho_E \quad (3.25)$$

where the electric field is $\mathbf{E} = -\nabla \Psi$ in electrostatics. By definition, the charge density is

$$\rho_E = F \sum_{i=1}^N z_i c_i \quad (3.26)$$

where F is Faraday's constant, z_i is the charge valence of specie i and c_i is the concentration of specie i (mol/m^3). The sum is over the N charged species in the electrolyte. The standard law governing the transport of charged species in a weak electrolyte, under the action of an electric field and neglecting any reaction, is embodied by the Nernst-Planck equation,

$$\frac{dc_i}{dt} + \mathbf{u} \cdot \nabla c_i = \nabla \cdot (D_i \nabla c_i) + \nabla \cdot \left[\underbrace{\left(D_i \frac{e z_i}{kT} \nabla \Psi \right) c_i}_{\mathbf{u}_{M,i}} \right] \quad (3.27)$$

which closes the system of equations for an EDF. In Eq. (3.27), D is the diffusion coefficient, e is the elementary charge, k is Boltzmann's constant and T is the absolute temperature. The last term of Eq. (3.27), representing the transport of charged species due to an electric field, can be thought as a standard convective term driven by an electromigration velocity ($\mathbf{u}_{M,i}$). However, it may also be considered as the Laplacian operator applied to field Ψ , with a space and time varying diffusion coefficient, $D_i \frac{e z_i}{kT} c_i$ (this last approach is used in *rheoTool* for discretization purposes).

The so-called Poisson-Nernst-Planck model (henceforth PNP model) is constituted by Eqs. (3.25)-(3.27) and, coupled with the continuity and momentum equations, is applicable to a wide range of EDFs. However, the coexistence of different scales of time and length in EDFs may originate a stiff system of equations when the PNP model is used. As such, several simplified models can be derived to mitigate these numerical issues, as described next. Note that the PNP model does not take into account molecular crowding effects (e.g., the number of ions near a surface may grow unbounded), so care must be taken when using it to simulate electrolytes of mild to high ionic strength.

In the PNP model, the electric-related unknowns are c_i and Ψ . Due to the convective term in Eq. (3.27), there is a two-way coupling between the PNP and the momentum equations.

3.5.2 Splitting the electric potential

Before proceeding to the derivation of other EDF models, we introduce here a useful approach to simulate EDF problems. In the PNP model, a single electric potential variable has been used, Ψ . However, in certain situations this can pose some difficulties when defining the boundary conditions to solve the Poisson equation. A common approach to avoid such issues is the decomposition of the electric potential in two variables: the externally imposed electric potential, ϕ_{Ext} , and the intrinsic electric potential, ψ , such that $\Psi = \phi_{\text{Ext}} + \psi$ [3]. Following this approach, Gauss' law is also decomposed in two equations,

$$\nabla \cdot (\varepsilon \nabla \phi_{\text{Ext}}) = 0 \quad (3.28a)$$

$$\nabla \cdot (\varepsilon \nabla \psi) = -\rho_E \quad (3.28b)$$

An additional simplification which can be used simultaneously with the splitting approach is to consider $\mathbf{f}_E = -\rho_E \nabla \phi_{Ext}$ in the momentum equation, i.e., the intrinsic electric potential contribution is ignored in the electric field definition. This can be justified by stating that this extra force not accounted for directly is balanced by a pressure gradient, which mutually cancel each other in the momentum equation [3], under the assumption that it would not affect the flow.

The splitting approach will be used in the derivation of the next two models.

3.5.3 Poisson-Boltzmann model

If we assume that the ions follow a Boltzmann equilibrium, then the PNP model can be simplified to the so-called Poisson-Boltzmann model (henceforth PB model), for which Gauss' law reads

$$\nabla \cdot (\varepsilon \nabla \psi) = -F \sum_{i=1}^N z_i c_{i,0} \exp\left(-\frac{e z_i}{kT} (\psi - \psi_0)\right) \quad (3.29)$$

with $c_{i,0}$ being a reference concentration of specie i , where the intrinsic potential is ψ_0 . Without loss of generality, we will assume that $c_{i,0}$ is the bulk ionic concentration, where the intrinsic potential is $\psi_0 = 0$.

Note that the right hand-side of Eq. (3.29) represents (minus) the charge density for the PB model. Thus, Eq. (3.29) provides the definition of Eq. (3.28b) for the PB model, under the splitting approach.

For this model, the only electric-related unknowns are the two electric potentials, ψ and ϕ_{Ext} , computed from Eqs. (3.28a) and (3.29). Furthermore, as can be seen from Eq. (3.29), there is no influence of flow variables in the PB model (one-way coupling).

In order to increase the implicitness of Eq. (3.29), its source term can be linearized by expansion in Taylor series up to the first-derivative, transforming the equation into

$$\nabla \cdot (\varepsilon \nabla \psi) + \psi F \sum_{i=1}^N (a_i b_i)^* = -F \sum_{i=1}^N (a_i)^* + \psi^* F \sum_{i=1}^N (a_i b_i)^* \quad (3.30)$$

with $b_i = -\frac{e z_i}{kT}$ and $a_i = z_i c_{i,0} \exp(b_i \psi)$. All the terms of Eq. (3.30) with a star are evaluated explicitly.

3.5.4 Debye-Hückel model

Considering the PB model, if we further simplify Eq. (3.29) assuming low electric potentials, $\frac{e z_i}{kT} \psi \ll 1$, then

$$\nabla \cdot (\varepsilon \nabla \psi) = -F \sum_{i=1}^N z_i c_{i,0} \left(1 - \frac{e z_i}{kT} \psi\right) \quad (3.31)$$

which is the equation governing the electric potential distribution in the so-called Debye-Hückel model (henceforth DH model).

As for the PB model, the only electric-related unknowns are the two electric potentials, ψ and ϕ_{Ext} , computed from Eqs. (3.28a) and (3.31). Also, there is no influence of flow variables in the DH model (one-way coupling).

3.5.5 Slip model

A common characteristic of electrokinetic problems is the spontaneous formation of an electric double layer (EDL) near a charged surface, upon contact with an electrolyte. The thickness of the EDL can be approximated by the Debye length (λ_D), a physical parameter appearing when solving the Poisson equation for the electric potential,

$$\lambda_D = \sqrt{\frac{\varepsilon kT}{Fe \sum_{i=1}^N z_i^2 c_{i,0}}} \quad (3.32)$$

In several practical applications, the charge density is mainly located in the EDL region, while the bulk electrolyte is neutral. If the Debye length is much smaller than the characteristic dimension of the system ($\frac{\lambda_D}{W} \ll 1$) and assuming a smooth, laminar flow inside the EDL, then it is possible to approximate the EDL effect by a slip velocity at the surface, avoiding the need to solve the flow inside the EDL. Such a case would be, for example, the pumping of a Newtonian electrolyte ($\lambda_D \sim \mathcal{O}(10^{-9} \text{ m})$) in a microchannel of arbitrary shape ($W \sim \mathcal{O}(10^{-6} \text{ m})$), by electroosmosis, at low voltage ($\frac{ez}{kT}\psi \ll 1$) – the last condition is usually relaxed. The Helmholtz-Smoluchowski theory is frequently used to approximate the slip velocity in such conditions,

$$\mathbf{u}_{\text{Sch}} = \mu \mathbf{E} \quad (3.33)$$

where $\mu = -\frac{\varepsilon \zeta}{\eta_0}$ is the electroosmotic mobility (ζ is usually the surface zeta-potential). Thus, when Eq. (3.33) is used as a boundary condition for velocity in the momentum equation, both the electroosmotic mobility and the electric field at the surface must be known. The electroosmotic mobility is assumed to be known a priori – it can be a fixed value over all the surface or have a known distribution. On the other hand, the electric field on the surface must be computed, making use of the initial assumption that no free charge exists in the bulk electrolyte, thus $\Psi = \phi_{\text{Ext}} + \psi = \phi_{\text{Ext}}$, and

$$\nabla \cdot (\varepsilon \nabla \Psi) = 0 \quad (3.34)$$

When the slip model is used, the electric body-force is not included in the momentum equation – electric effects contribute uniquely via the slip boundary condition on the wall.

Note that slip models do not resolve any phenomena occurring in the EDL. Thus, this approach is highly inaccurate for some flows, even though the condition $\frac{\lambda_D}{W} \ll 1$ is satisfied. For example, this kind of model is unable to predict the high values of shear-rate typically found in EDLs, which can trigger elastic instabilities

for complex fluid flows [15] – using a slip model would simply retrieve a smooth flow in such cases.

3.5.6 Ohmic (leaky dielectric) model

The so-called Ohmic model [16] is particularly useful to simulate fluids of different conductivities, although a generalized Ohmic model has been recently proposed for different types of problems [17]. The model can be derived from the PNP equations, rewritten in terms of the conductivity and free-charge density, and assuming additionally instantaneous charge relaxation and electroneutrality [16]. The interested reader is directed to Ref. [16] for the full derivation of the Ohmic model. Here, only the final equations are presented. Furthermore, and contrarily to what was done for the previous models, we will restrict our analysis to a binary electrolyte, i.e., an electrolyte composed of only one positive and one negative species, with $z_+ = -z_- = z$, but no restrictions in the relation between D_+ and D_- .

First, let's start defining the conductivity (σ) and free-charge density (ρ_E) for a binary electrolyte,

$$\sigma = \frac{F^2 z^2}{RT} (D_+ c_+ + D_- c_-) \quad (3.35)$$

$$\rho_E = Fz(c_+ - c_-) \quad (3.36)$$

where R is the universal gas constant. Imposing the conservation of each variable leads to (after the assumptions mentioned above; more details in Ref. [16])

$$\frac{\partial \sigma}{\partial t} + \mathbf{u} \cdot \nabla \sigma = D_{\text{eff}} \nabla^2 \sigma \quad (3.37)$$

$$\nabla \cdot (\sigma \nabla \Psi) = 0 \quad (3.38)$$

where the effective diffusivity is $D_{\text{eff}} = \frac{2D_- D_+}{D_- + D_+}$. The conductivity is transported through Eq. (3.37), while Eq. (3.38), derived from the conservation of charge-density (then simplified on the basis of electroneutrality), is actually used to compute the distribution of electric potential. The electric force entering the momentum equation assumes its standard form, taking into account that the charge density can be expressed as $\rho_E = -\nabla \cdot (\varepsilon \nabla \Psi)$ from Gauss' law, then

$$\mathbf{f}_E = \rho_E \mathbf{E} = \nabla \cdot (\varepsilon \nabla \Psi) \nabla \Psi \quad (3.39)$$

In order to close the Ohmic model, the EDL effect is commonly represented by a slip velocity, which avoids detailing the flow inside the EDL using a very fine mesh. Since the zeta-potential of a surface depends generally on the ionic conductivity, a σ -dependent slip velocity is typically used [16], such as

$$\mathbf{u}_{\text{Sch}}(\sigma) = \mu_0 \left(\frac{\sigma}{\sigma_0} \right)^m \mathbf{E} \quad (3.40)$$

where $\mu_0 = -\frac{\varepsilon\zeta_0}{\eta_0}$ is a reference electroosmotic mobility, at a reference conductivity (σ_0), and m is an exponent governing the power-law dependence of the zeta-potential on the conductivity ($m \in [-0.5, -0.3]$) is in agreement with several works, e.g. [16]). Note that \mathbf{E} in Eq. (3.40) is the electric potential at the surface where the slip velocity is computed.

Chapter 4

Overview of *rheoTool*

In the previous Chapter, the main theoretical points behind *rheoTool* were briefly discussed. This Chapter focus on the numerical implementation of the governing equations in the OpenFOAM® environment, providing an overview of the functionalities available in *rheoTool*.

4.1 The *constitutiveEquations* library

4.1.1 Available GNF and viscoelastic models

The *constitutiveEquations* library is a main component of *rheoTool*, since it contains all the viscoelastic and GNF constitutive equations, which can be called from the solvers. It was derived from the *viscoelasticTransportModels* library [1]. However, instead of restricting the library to viscoelastic models, we also extend it to include GNF models, most of them already present in OpenFOAM®. This was done in order to allow accessing both classes of models from a single library, hence from a single solver.

The models available in the *constitutiveEquations* library are displayed in Table 4.1, along with the respective expressions to be used in Eqs. (3.3), (3.4), (3.6) and (3.8).

Table 4.1: Available constitutive models in the *constitutiveEquations* library.

GNF models

| Model | ¹ Type Name | $\eta_s(\dot{\gamma})$ |
|---|------------------------|---|
| Newtonian | <i>Newtonian</i> | η |
| ² (Bounded) Power-Law | <i>PowerLaw</i> | $\max(\eta_{\min}, \min(\eta_{\max}, k \dot{\gamma}^{n-1}))$ |
| Carreau-Yasuda | <i>CarreauYasuda</i> | $\eta_\infty + (\eta_0 - \eta_\infty)[1 + (k\dot{\gamma})^a]^{\frac{n-1}{a}}$ |
| ² (Bounded) Herschel-Bulkley | <i>HerschelBulkley</i> | $\min(\eta_0, \tau_0 \dot{\gamma}^{-1} + k \dot{\gamma}^{n-1})$ |

¹ Corresponds to the name entry identifying the model in the source code.

² In the Power-Law and Herschel-Bulkley models special care is taken to avoid division by zero when $\dot{\gamma}$ is zero or very small and $n - 1 < 0$. For $\dot{\gamma} < VSMALL$, the value $\dot{\gamma} = VSMALL$ is used in the computation of the shear viscosity ($VSMALL = 10^{-300}$ for versions using double precision).

Notes:

- $\dot{\gamma} = \sqrt{\frac{\dot{\gamma} : \dot{\gamma}}{2}}$, with $\dot{\gamma} = \nabla \mathbf{u} + \nabla \mathbf{u}^T$.
- \mathbf{I} is the identity tensor and $\frac{D}{Dt}(\phi) = \frac{\partial \phi}{\partial t} + \mathbf{u} \cdot \nabla \phi$ represents the material derivative of the generic variable ϕ .
- $\overset{\nabla}{\tau} = \frac{\partial \tau}{\partial t} + \mathbf{u} \cdot \nabla \tau - \tau \cdot \nabla \mathbf{u} - \nabla \mathbf{u}^T \cdot \tau$ is the upper-convected derivative of τ .
- $\overset{\square}{\tau} = \overset{\nabla}{\tau} + \zeta(\tau \cdot \mathbf{D} + \mathbf{D} \cdot \tau)$ is the Gordon-Schowalter derivative of τ , with $\mathbf{D} = \frac{1}{2}(\nabla \mathbf{u} + \nabla \mathbf{u}^T)$.

Continuation of Table 4.1

Viscoelastic models solved in the standard extra-stress or conformation tensor variables

| Model | TypeName | $\eta_s(\dot{\gamma})$ | $\eta_p(\dot{\gamma})$ | $\lambda(\dot{\gamma})$ | Constitutive Equation |
|----------------------------------|-----------------------|------------------------|--|---|---|
| Oldroyd-B | <i>Oldroyd-B</i> | η_s | η_p | λ | $\boldsymbol{\tau} + \lambda \frac{\nabla}{\nabla} \boldsymbol{\tau} = \eta_p (\nabla \mathbf{u} + \nabla \mathbf{u}^T)$ |
| WhiteMetzner (Carreau-Yasuda) | <i>WhiteMetznerCY</i> | η_s | $\eta_p [1 + (K\dot{\gamma})^a]^{\frac{n-1}{a}}$ | $\lambda [1 + (L\dot{\gamma})^b]^{\frac{m-1}{b}}$ | $\boldsymbol{\tau} + \lambda(\dot{\gamma}) \frac{\nabla}{\nabla} \boldsymbol{\tau} = \eta_p(\dot{\gamma}) (\nabla \mathbf{u} + \nabla \mathbf{u}^T)$ |
| Giesekus | <i>Giesekus</i> | η_s | η_p | λ | $\boldsymbol{\tau} + \lambda \frac{\nabla}{\nabla} \boldsymbol{\tau} + \alpha \frac{\lambda}{\eta_p} (\boldsymbol{\tau} \cdot \boldsymbol{\tau}) = \eta_p (\nabla \mathbf{u} + \nabla \mathbf{u}^T)$ |
| PTT linear | <i>PTTlinear</i> | η_s | η_p | λ | $\left[1 + \frac{\varepsilon \lambda}{\eta_p} \text{tr}(\boldsymbol{\tau}) \right] \boldsymbol{\tau} + \lambda \frac{\square}{\square} \boldsymbol{\tau} = \eta_p (\nabla \mathbf{u} + \nabla \mathbf{u}^T)$ |
| PTT exponential | <i>PTTexp</i> | η_s | η_p | λ | $\left[e^{\frac{\varepsilon \lambda}{\eta_p} \text{tr}(\boldsymbol{\tau})} \right] \boldsymbol{\tau} + \lambda \frac{\square}{\square} \boldsymbol{\tau} = \eta_p (\nabla \mathbf{u} + \nabla \mathbf{u}^T)$ |
| FENE-CR | <i>FENE-CR</i> | η_s | η_p | λ | $\left[1 + \lambda \frac{D}{Dt} \left(\frac{1}{f} \right) \right] \boldsymbol{\tau} + \frac{\lambda}{f} \frac{\nabla}{\nabla} \boldsymbol{\tau} = \eta_p (\nabla \mathbf{u} + \nabla \mathbf{u}^T)$ where $f = \frac{L^2 + \frac{\lambda}{\eta_p} \text{tr}(\boldsymbol{\tau})}{L^2 - 3}$ |
| FENE-P | <i>FENE-P</i> | η_s | η_p | λ | $\boldsymbol{\tau} + \frac{\lambda}{f} \frac{\nabla}{\nabla} \boldsymbol{\tau} = \frac{a \eta_p}{f} (\nabla \mathbf{u} + \nabla \mathbf{u}^T) - \frac{D}{Dt} \left(\frac{1}{f} \right) [\lambda \boldsymbol{\tau} + a \eta_p \mathbf{I}]$ where $f = \frac{L^2 + \frac{\lambda}{a \eta_p} \text{tr}(\boldsymbol{\tau})}{L^2 - 3}$ and $a = \frac{L^2}{L^2 - 3}$ |
| ³ Rolie-Poly | <i>Rolie-Poly</i> | η_s | η_p | λ_D | $\lambda_D \frac{\nabla}{\nabla} \mathbf{A} = -(\mathbf{A} - \mathbf{I}) - 2k \frac{\lambda_D}{\lambda_R} \left(1 - \sqrt{3/\text{tr}(\mathbf{A})} \right) \left[\mathbf{A} + \beta \left(\frac{\text{tr}(\mathbf{A})}{3} \right)^{\delta} (\mathbf{A} - \mathbf{I}) \right]$ where $k = \frac{\left(3 - \frac{\chi^2}{\chi_{\max}^2} \right) \left(1 - \frac{1}{\chi_{\max}^2} \right)}{\left(1 - \frac{\chi^2}{\chi_{\max}^2} \right) \left(3 - \frac{1}{\chi_{\max}^2} \right)}$ and $\chi = \sqrt{\frac{\text{tr}(\mathbf{A})}{3}}$ |
| eXtended Pom-Pom | <i>XPomPom</i> | η_s | η_p | λ_B | $f \boldsymbol{\tau} + \lambda_B \frac{\nabla}{\nabla} \boldsymbol{\tau} + \alpha \frac{\lambda_B}{\eta_p} (\boldsymbol{\tau} \cdot \boldsymbol{\tau}) + \frac{\eta_p}{\lambda_B} (f - 1) \mathbf{I} = \eta_p (\nabla \mathbf{u} + \nabla \mathbf{u}^T)$ where $f = 2 \frac{\lambda_B}{\lambda_S} e^{\frac{2}{q} (\Lambda - 1)} \left(1 - \frac{1}{\Lambda} \right) + \frac{1}{\Lambda^2} \left[1 - \frac{\alpha}{3} \frac{\text{tr}(\boldsymbol{\tau} \cdot \boldsymbol{\tau})}{(\eta_p / \lambda_B)^2} \right]$ and $\Lambda = \sqrt{1 + \frac{\text{tr}(\boldsymbol{\tau})}{3 \eta_p / \lambda_B}}$ |

³ See Ref. [18]. This model is exclusively solved in the conformation tensor variable, which is then converted to $\boldsymbol{\tau}$ using, $\boldsymbol{\tau} = \frac{\eta_p}{\lambda_D} k(\mathbf{A} - \mathbf{I})$.

Continuation of Table 4.1

‡Viscoelastic models solved with the log-conformation approach

| Model | TypeName | $\Theta \rightarrow \tau$ | ^{4,5} Constitutive Equation |
|---|--------------------------|--|---|
| ⁶ Oldroyd-B | <i>Oldroyd-BLog</i> | $\tau = \frac{\eta_p}{\lambda} (e^\Theta - \mathbf{I})$ | $\Upsilon = \frac{1}{\lambda} (e^{-\Theta} - \mathbf{I})$ |
| ⁷ WhiteMetzner (Carreau-Yasuda) | <i>WhiteMetznerCYLog</i> | $\tau = \frac{\eta_p}{\lambda} (e^\Theta - \mathbf{I})$ | $\Upsilon = \frac{1}{\lambda(\dot{\gamma})} (e^{-\Theta} - \mathbf{I})$ |
| Giesekus | <i>GiesekusLog</i> | $\tau = \frac{\eta_p}{\lambda} (e^\Theta - \mathbf{I})$ | $\Upsilon = \frac{1}{\lambda} \left[(e^{-\Theta} - \mathbf{I}) - \alpha e^\Theta (e^{-\Theta} - \mathbf{I})^2 \right]$ |
| PTT linear | <i>PTTlinearLog</i> | $\tau = \frac{\eta_p}{\lambda(1-\zeta)} (e^\Theta - \mathbf{I})$ | $\Upsilon = \frac{1}{\lambda} \left\{ 1 + \frac{\varepsilon}{1-\zeta} [\text{tr}(e^\Theta) - 3] \right\} (e^{-\Theta} - \mathbf{I})$ |
| PTT exponential | <i>PTTexpLog</i> | $\tau = \frac{\eta_p}{\lambda(1-\zeta)} (e^\Theta - \mathbf{I})$ | $\Upsilon = \frac{1}{\lambda} e^{\frac{\varepsilon}{1-\zeta} (\text{tr}(e^\Theta) - 3)} (e^{-\Theta} - \mathbf{I})$ |
| FENE-CR | <i>FENE-CRLog</i> | $\tau = \frac{\eta_p f}{\lambda} (e^\Theta - \mathbf{I})$ | $\Upsilon = \frac{f}{\lambda} (e^{-\Theta} - \mathbf{I})$, where $f = \frac{L^2}{L^2 - \text{tr}(e^\Theta)}$ |
| FENE-P | <i>FENE-PLog</i> | $\tau = \frac{\eta_p}{\lambda} (f e^\Theta - a \mathbf{I})$ | $\Upsilon = \frac{1}{\lambda} (a e^{-\Theta} - f \mathbf{I})$, where $a = \frac{L^2}{L^2 - 3}$ and $f = \frac{L^2}{L^2 - \text{tr}(e^\Theta)}$ |
| ⁸ Rolie-Poly | <i>Rolie-PolyLog</i> | $\tau = \frac{\eta_p}{\lambda_D} k (e^\Theta - \mathbf{I})$ | $\Upsilon = -\frac{1}{\lambda_D} e^{-\Theta} \left\{ (e^\Theta - \mathbf{I}) + 2k \frac{\lambda_D}{\lambda_R} \left(1 - \sqrt{3/\text{tr}(e^\Theta)} \right) \left[e^\Theta + \beta \left(\frac{\text{tr}(e^\Theta)}{3} \right)^\delta (e^\Theta - \mathbf{I}) \right] \right\}$ |
| eXtended Pom-Pom | <i>XPomPomLog</i> | $\tau = \frac{\eta_p}{\lambda_B} (e^\Theta - \mathbf{I})$ | $\Upsilon = -\frac{1}{\lambda_B} e^{-\Theta} [(f - 2\alpha) e^\Theta + \alpha e^\Theta e^\Theta + (\alpha - 1) \mathbf{I}]$ where $f = 2 \frac{\lambda_B}{\lambda_S} e^{\frac{2}{q} (\Lambda - 1)} \left(1 - \frac{1}{\Lambda} \right) + \frac{1}{\Lambda^2} [1 - \alpha - \frac{\alpha}{3} \text{tr}(e^\Theta (e^\Theta - 2\mathbf{I}))]$ and $\Lambda = \sqrt{\frac{\text{tr}(e^\Theta)}{3}}$ |

‡ The solvent viscosity, the polymeric viscosity coefficient and the relaxation time for the models solved in variable Θ are the same as those for the models solved in variable τ or \mathbf{A} , in the previous page.

⁴ For the shortness of notation, we have introduced the operator: $\Upsilon = \frac{\partial \Theta}{\partial t} + \mathbf{u} \cdot \nabla \Theta - (\Omega \Theta - \Theta \Omega) - 2\mathbf{B}$.

⁵ The following equivalences hold true: $e^\Theta = \mathbf{A} = \mathbf{R} \mathbf{\Lambda} \mathbf{R}^T$ and $e^{-\Theta} = \mathbf{A}^{-1} = \mathbf{R} \mathbf{\Lambda}^{-1} \mathbf{R}^T$.

⁶ For this model, we also included the square-root conformation approach [10] (TypeName: *Oldroyd-B.Sqrt*) and the root^k kernel approach [9] (TypeName: *Oldroyd-BRootk*), for demonstration purposes.

⁷ This log-conformation tensor approach of the White-Metzner model is only applicable when $\frac{\eta_p(\dot{\gamma})}{\lambda(\dot{\gamma})} = \frac{\eta_p}{\lambda}$ is constant, i.e., for $K = L$, $a = b$ and $n = m$. The version based on the extra-stress tensor variable is more general and does not have this restriction.

⁸ The expression for k is the same as for the model solved in variable \mathbf{A} , in the previous page, considering that $\mathbf{A} = e^\Theta$.

In a footnote of Table 4.1, the (invariant) shear-rate used to compute shear-rate dependent variables was defined as

$$\dot{\gamma} = \sqrt{\frac{\dot{\gamma} : \dot{\gamma}}{2}} = \sqrt{2\mathbf{D} : \mathbf{D}}, \text{ with } \dot{\gamma} = \nabla \mathbf{u} + \nabla \mathbf{u}^T \text{ and } \mathbf{D} = \frac{1}{2}\dot{\gamma} \quad (4.1)$$

In the code, the shear-rate is returned by function *strainRate()* as

$$\text{strainRate}() = \text{sqrt}(2.0)*\text{mag}(\text{symm}(\text{fvc}::\text{grad}(U())))$$

and it is equivalent to Eq. (4.1). Indeed,

$$\text{symm}(\text{fvc}::\text{grad}(U())) = \frac{1}{2}(\nabla \mathbf{u} + \nabla \mathbf{u}^T) = \frac{1}{2}\dot{\gamma} = \mathbf{D}$$

thus,

$$\text{sqrt}(2.0)*\text{mag}(\text{symm}(\text{fvc}::\text{grad}(U()))) = \sqrt{2}\sqrt{\frac{1}{2}\dot{\gamma} : \frac{1}{2}\dot{\gamma}} = \sqrt{\frac{\dot{\gamma} : \dot{\gamma}}{2}} = \sqrt{2\mathbf{D} : \mathbf{D}}$$

which is equal to Eq. (4.1) – the definitions of operators *symm()*, *mag()* and *:* (double contraction) can be found in the OpenFOAM® programmers' guide. Note that the invariant computed in Eq. (4.1) is actually the magnitude of the rate-of-strain tensor, which is usually called shear rate or strain rate for shear-dominated or extensional-dominated flows, respectively.

All the viscoelastic models can be solved in the standard extra-stress tensor $\boldsymbol{\tau}$ (Eq. 3.4) or using the log-conformation approach (Eq. 3.8). The selection is made in dictionary **constitutiveProperties**, which should be located inside the folder **constant/** of the case (see more details in section 5.1.1). For the Oldroyd-B model, we provide two additional methods for demonstration purposes. One of them (TypeName: *Oldroyd-B.Sqrt*) consists in solving the constitutive equation using the square-root of the conformation tensor, according to Ref. [10]. The second approach (TypeName: *Oldroyd-B.Rootk*) allows to apply a general root^k kernel, as described in Ref. [9]. Both can be used in 2D or 3D simulations, as any other model in the library. Since both models are only illustrative, their implementation and theory are not described in this guide, although both can be easily understood after a close inspection of the source code and taking as reference the literature cited for each one. Furthermore, tutorials for both methodologies are included in *rheoTool* (see the tutorial of Section 5.1.7).

4.1.2 A note on FENE-type models

The Finite Extendable Non-linear Elastic (FENE) models were originally developed based on the representation of polymer molecules by elastic dumbbells [5]. In such analysis, the end-to-end vector for each molecule is naturally related with the conformation tensor, such that the constitutive equations for this family of models is frequently written and handled as a function of the conformation tensor. The polymeric contribution to the momentum equation is then accounted for by transforming the conformation tensor (\mathbf{A}) in the extra-stress tensor ($\boldsymbol{\tau}$), using the relations in Table 4.1 (for the models expressed in the log-conformation approach, considering that $e^\Theta = \mathbf{A}$). The same applies for the Roly-Polie model.

In order to write the constitutive equation for FENE-type models as a function of $\boldsymbol{\tau}$, some terms arise, which may compromise the numerical stability. Furthermore, the computational cost to evaluate the resulting expression is higher than for the original model. As such, some authors simplify the constitutive equation by neglecting certain terms [19]. For the FENE-CR and FENE-P models, the complete constitutive equation written as a function of \mathbf{A} and $\boldsymbol{\tau}$ and the modified formulation in $\boldsymbol{\tau}$ are:

- FENE-CR

- Complete in \mathbf{A} :

$$\lambda \overset{\nabla}{\mathbf{A}} = -f(\text{tr}(\mathbf{A}))(\mathbf{A} - \mathbf{I}), \text{ where } f(\text{tr}(\mathbf{A})) = \frac{L^2}{L^2 - \text{tr}(\mathbf{A})}$$

- Complete in $\boldsymbol{\tau}$ (see Table 4.1):

$$\left[1 + \lambda \frac{D}{Dt} \left(\frac{1}{f}\right)\right] \boldsymbol{\tau} + \frac{\lambda}{f} \overset{\nabla}{\boldsymbol{\tau}} = \eta_p (\nabla \mathbf{u} + \nabla \mathbf{u}^T), \text{ where } f = \frac{L^2 + \frac{\lambda}{\eta_p} \text{tr}(\boldsymbol{\tau})}{L^2 - 3}$$

- Modified in $\boldsymbol{\tau}$ (usually known as FENE-MCR):

$$\boldsymbol{\tau} + \frac{\lambda}{f} \overset{\nabla}{\boldsymbol{\tau}} = \eta_p (\nabla \mathbf{u} + \nabla \mathbf{u}^T), \text{ where } f = \frac{L^2 + \frac{\lambda}{\eta_p} \text{tr}(\boldsymbol{\tau})}{L^2 - 3}$$

- FENE-P

- Complete in \mathbf{A} :

$$\lambda \overset{\nabla}{\mathbf{A}} = -[f(\text{tr}(\mathbf{A}))\mathbf{A} - a\mathbf{I}], \text{ where } f(\text{tr}(\mathbf{A})) = \frac{L^2}{L^2 - \text{tr}(\mathbf{A})} \text{ and } a = \frac{L^2}{L^2 - 3}$$

- Complete in $\boldsymbol{\tau}$ (see Table 4.1):

$$\boldsymbol{\tau} + \frac{\lambda}{f} \overset{\nabla}{\boldsymbol{\tau}} = \frac{a\eta_p}{f} (\nabla \mathbf{u} + \nabla \mathbf{u}^T) - \frac{D}{Dt} \left(\frac{1}{f}\right) [\lambda \boldsymbol{\tau} + a\eta_p \mathbf{I}], \text{ where } f = \frac{L^2 + \frac{\lambda}{a\eta_p} \text{tr}(\boldsymbol{\tau})}{L^2 - 3}$$

and $a = \frac{L^2}{L^2 - 3}$

- Modified in $\boldsymbol{\tau}$:

$$\boldsymbol{\tau} + \frac{\lambda}{f} \overset{\nabla}{\boldsymbol{\tau}} = \frac{a\eta_p}{f} (\nabla \mathbf{u} + \nabla \mathbf{u}^T), \text{ where } f = \frac{L^2 + \frac{\lambda}{a\eta_p} \text{tr}(\boldsymbol{\tau})}{L^2 - 3} \text{ and } a = \frac{L^2}{L^2 - 3}$$

In *rheoTool*, all the formulations are available and can be used (see Section 5.1.1 to know how to select each one). The steady material functions evaluated for canonical flows are the same for all the formulations. However, this is not true when evaluating the transient material functions: the modified formulations have a different behavior comparing with the complete ones, which are themselves similar. For a generic flow, the complete formulations, either in \mathbf{A} or $\boldsymbol{\tau}$, should provide similar results, since they are mathematically equivalent. Due to discretization errors and stability issues, this may not be true. Regarding the modified formulations, they are not expected to behave exactly as the complete ones, even in the limit of highly refined grids.

From our experience, we strongly recommend using the formulations written and solved as a function of \mathbf{A} for FENE-type models. Those are the most stable, the most accurate regarding the original theory presented in [5] and the ones for which there is direct correspondence with the models solved with the log-conformation approach, since those were derived from the constitutive equations written as a function of the conformation tensor. Note that the FENE-CR and FENE-P models available in the *viscoelasticTransportModels* library of *viscoelasticFluidFoam* [1] are expressed in the modified form presented above.

4.1.3 Multi-mode modeling

Similarly to the *viscoelasticTransportModels* library [1], the *constitutiveEquations* library also supports multi-mode modeling for viscoelastic models. In such cases, the total extra-stress tensor is the sum of the extra-stress tensor resulting from each k^{th} mode

$$\boldsymbol{\tau}' = \sum_{k=1}^N (\boldsymbol{\tau}^k + \boldsymbol{\tau}_s^k) \quad (4.2)$$

In practice, this is achieved by assembling and solving one constitutive equation for each k^{th} mode, that is, Eq. (3.3) – solvent contribution – and Eq. (3.4) or (3.8) – polymer contribution – are built and solved N times each time-step. A warning should be made at this point, since this approach is probably not the most conventional. Indeed, $\boldsymbol{\tau}_s$ in Eq. (4.2) is commonly placed outside the summation symbol, since multiple modes are only assigned to the polymeric contribution. To achieve this in *rheoTool*, and considering the expression for $\boldsymbol{\tau}_s$ in Eq. (3.3), **the user must split the "single-solvent viscosity" by the N modes considered**, in any way, such that this "single-solvent viscosity" is recovered summing all these N values in Eq. (4.2).

4.1.4 Analysis of a code sample

For the readers still initiating their journey in OpenFOAM®, we will explore in this section the implementation of the Oldroyd-B constitutive model, solved with the log-conformation tensor approach. This example will establish the link between part of the theory described in Chapter 3 and its implementation in the source code.

The source code displayed in Listing 4.1 is taken from file `src/libs/constitutiveEquations/constitutiveEqs/Oldroyd-B/Oldroyd-BLog/Oldroyd_BLog.C`. Let's analyze the most important lines:

- lines **1-91**: this section initializes the variables used in the constitutive model. In terms of field variables, we have (lines 23-84): `tau_(\tau)`, `theta_(\Theta)`, `eigVals_(\Lambda)` and `eigVecs_(\mathbf{R})`. All those fields must be defined by the user when starting a simulation, except `eigVals_` and `eigVecs_`, which can be defined or not. If defined (typical of a restart from a previous simulation), they are used in the first time-step; otherwise, they are both initialized as the identity

tensor/matrix, corresponding to a null extra-stress tensor ($\boldsymbol{\tau}$). Afterwards, the fluid properties are read from a dictionary (lines 85-88), along with the stabilization method selected by the user (line 90): none, BSD or the stress-velocity coupling described in Section 3.3.2.

- lines **94-151**: this section implements the member function *correct()*, whose purpose is to update the polymeric extra-stress field, by evolving Θ according to the constitutive equation. From line 96 to 105, variables \mathbf{M} , $\boldsymbol{\Omega}$ and \mathbf{B} , defined in Eqs. (3.9)–(3.11), are computed. The function *decomposeGradU()* is a member function of the base class *constitutiveEq* (find it in the file `constitutiveEq.C`), since it is used by all the models based on the log-conformation tensor approach. Then, in lines 107-140, the constitutive equation (Eq. 3.8) is built and solved, after which Θ is diagonalized to compute its eigenvectors/eigenvalues (line 144). The function doing this task (*calcEig()*) is also a member function of the class *constitutiveEq* and the algorithm being used by default for that purpose is the QR method provided by the Eigen library [6]. Another method is also available, as discussed in Section 4.1.5. Note that the eigenvalues retrieved by function (*calcEig()*) are already **exponentiated**, so that they correspond to $\Lambda = \exp(\Lambda^\Theta)$. Finally, with the currently computed eigenvectors/eigenvalues, the polymeric extra-stress tensor ($\boldsymbol{\tau}$) is recovered from the conformation tensor (line 148), according to the relation established in Eqs. (3.6) and (3.14) (check Table 4.1 for other models), and will be used in the *divTau()* function described below.
- in the *viscoelasticTransportModels* library [1] each model was in charge to define its own contribution to the momentum equation, i.e., the term $(\nabla \cdot \boldsymbol{\tau}')$. In the *constitutiveEquations* library there is a default definition of this term in the base class. In fact, the function *divTau()* is now defined in class *constitutiveEq* and can be found in file `constitutiveEq.C`, Listing 4.2. This function starts by distinguishing between GNF and viscoelastic models in line 7. For a GNF model (lines 8-14), the extra-stress contribution is $\nabla \cdot \boldsymbol{\tau}' = \nabla \cdot \eta(\dot{\gamma}) \nabla \mathbf{u} + \nabla \mathbf{u} \cdot \nabla \eta(\dot{\gamma})$, divided by the density to be compliant with the usual strategy of OpenFOAM® for single-phase, incompressible fluid flows. Note that the second term is included to account for a shear-rate dependent viscosity coefficient. By definition, a GNF fluid has no elasticity, thus $\boldsymbol{\tau} = \mathbf{0}$. For a viscoelastic fluid (lines 17-49), the output depends on the stabilization method selected (see function *checkForStab()* in `constitutiveEq.C` for the correspondence between indexes and the method): if *none*, there is no added stabilization and $\nabla \cdot \boldsymbol{\tau} = \nabla \cdot \bar{\boldsymbol{\tau}} - \nabla \cdot \eta_s \nabla \mathbf{u}$; if *BSD*, then the both-sides-diffusion technique is used and $\nabla \cdot \boldsymbol{\tau} = \nabla \cdot \bar{\boldsymbol{\tau}} - \nabla \cdot \eta_p \nabla \mathbf{u} + \nabla \cdot (\eta_s + \eta_p) \nabla \mathbf{u}$ (Eq. 3.5); otherwise (if *coupling*), the stress-velocity coupling technique of Eq. (3.17) is used and $\nabla \cdot \boldsymbol{\tau} = \nabla \cdot \bar{\boldsymbol{\tau}} - \overline{\nabla \cdot \eta_p \nabla \mathbf{u}} + \nabla \cdot (\eta_s + \eta_p) \nabla \mathbf{u}$. Note that using the *coupling* stabilization is the method recommended for most of the cases, being the one used by default if no information is provided by the user. However, some cases may require the use of no stabilization, as for example the simulation of multimode models with $\eta_p \gg \eta_s$ – the amount of artificial

diffusion may mask the real phenomena in transient simulations. For the cases using stabilization, the explicit behavior effects on transient results can be minimized by performing inner iterations at each time-step, a subject discussed later in this guide (see Section 4.3.1). In file `constitutiveEq.C`, a function `divTauS()` is also included, which retrieves part of the extra-stress contribution to the momentum equation, when solving two-phase flows (this topic will be discussed later).

```

        ),
45      U.mesh()
),
47      eigVals_
(
49      IOobject
(
51          "eigVals" + name,
52          U.time().timeName(),
53          U.mesh(),
54          IOobject::READ_IF_PRESENT,
55          IOobject::AUTO_WRITE
),
56      U.mesh(),
57      dimensionedTensor
(
58          "I",
59          dimless,
60          pTraits<tensor>::I
),
61      zeroGradientFvPatchField<tensor>::typeName
),
62      eigVecs_
(
63      IOobject
(
64          "eigVecs" + name,
65          U.time().timeName(),
66          U.mesh(),
67          IOobject::READ_IF_PRESENT,
68          IOobject::AUTO_WRITE
),
69      U.mesh(),
70      dimensionedTensor
(
71          "I",
72          dimless,
73          pTraits<tensor>::I
),
74      zeroGradientFvPatchField<tensor>::typeName
),
75      rho_(dict.lookup("rho")),
76      etaS_(dict.lookup("etaS")),
77      etaP_(dict.lookup("etaP")),
78      lambda_(dict.lookup("lambda")),
79  {
80      checkForStab(dict);
81  }
82
83 // * * * * * Member Functions * * * * *
84 // *
85 void Foam::Oldroyd_BLog::correct()
86 {
87     // Decompose grad(U).T()
88
89     volTensorField L = fvc::grad(U());
90
91
92
93
94
95
96
97

```

```
99      dimensionedScalar c1( "zero", dimensionSet(0, 0, -1, 0, 0, 0,
100                           0), 0.);
101      volTensorField    B = c1 * eigVecs_;
102      volTensorField    omega = B;
103      volTensorField    M = (eigVecs_.T() & L.T() & eigVecs_);
104
105      decomposeGradU(M, eigVals_, eigVecs_, omega, B);
106
107      // Solve the constitutive Eq in theta = log(c)
108
109      dimensionedTensor Itensor
110      (
111          "Identity",
112          dimensionSet(0, 0, 0, 0, 0, 0, 0),
113          tensor::I
114      );
115
116      fvSymmTensorMatrix thetaEqn
117      (
118          fvm::ddt(theta_)
119          + fvm::div(phi(), theta_)
120          ==
121          symm
122          (
123              (omega&theta_)
124              - (theta_&omega)
125              + 2.0 * B
126              + (1.0/lambda_)
127              *
128                  (
129                      eigVecs_ &
130                      (
131                          inv(eigVals_)
132                          - Itensor
133                      )
134                      & eigVecs_.T()
135                  )
136          )
137      );
138
139      thetaEqn.relax();
140      thetaEqn.solve();
141
142      // Diagonalization of theta
143
144      calcEig(theta_, eigVals_, eigVecs_);
145
146      // Convert from theta to tau
147
148      tau_ = (etaP_/lambda_) * symm( (eigVecs_ & eigVals_ & eigVecs_
149                           .T()) - Itensor);
150
151      tau_.correctBoundaryConditions();
```

151 }

Listing 4.1: Source code for the *Oldroyd-BLog* constitutive model (*Oldroyd_BLog.C*)

```

1 tmp<fvVectorMatrix> constitutiveEq::divTau
2 (
3     const volVectorField& U
4 ) const
5 {

6     if (isGNF())
7     {
8         return
9         (
10            fvm::laplacian( eta() / rho(), U, "laplacian(eta,U)"
11            + (fvc::grad(U) & fvc::grad(eta() / rho())))
12        );
13    }
14 else
15    {
16        if (stabMeth_ == 0) // none
17        {
18
19            return
20            (
21                fvc::div(tau() / rho(), "div(tau)")
22                + fvm::laplacian(etaS() / rho(), U, "laplacian(eta,U"
23                    ))
24            );
25
26        }
27        else if (stabMeth_ == 1) // BSD
28        {
29
30            return
31            (
32                fvc::div(tau() / rho(), "div(tau)")
33                - fvc::laplacian(etaP() / rho(), U, "laplacian(eta,U"
34                    ))
35                + fvm::laplacian( (etaP() + etaS()) / rho(), U, "
36                    laplacian(eta,U"))
37            );
38
39        }
40
41        return
42        (
43            fvc::div(tau() / rho(), "div(tau)")
44            - (etaP() / rho()) * fvc::div(fvc::grad(U))
45            + fvm::laplacian( (etaP() + etaS()) / rho(), U, "
46                laplacian(eta,U"))
47        );

```

47

49 } }

Listing 4.2: Source code of the virtual function `divTau()` defined in file `constitutiveEq.C`

4.1.5 Advanced settings

As aforementioned, the eigenvectors/eigenvalues used in the models based on the log-conformation approach are computed, by default, using the QR algorithm provided by the Eigen library [6]. However, there is also the possibility to use an iterative Jacobi method [20]. While both options offer good accuracy and stability, the QR algorithm was seen to be slightly faster and this is the reason of being the default option. Switching between either methods is not run time selectable, but hard-coded, instead. This can be controlled in member function `calcEig()` of class `constitutiveEq`, located in file `constitutiveEq.C`. The Jacobi method can be selected by uncommenting the currently commented block (*// Eigen decomposition using the iterative jacobi algorithm*) and commenting the block (*// Eigen decomposition using a QR algorithm of Eigen library*), i.e., all the remaining lines inside the function. The source-code of `jacobi()` function is located in `utils/jacobi.H`. Note that, independently of which method is used in function `calcEig()`, this function will return the eigenvectors of the input tensor, and the **exponential** of the eigenvalues of the same tensor. After re-compiling the library with those modifications, all the log-conformation-based models will be affected by those changes.

4.1.6 Adding new viscoelastic or GNF models

For the users with minimal programming skills in OpenFOAM®, adding new viscoelastic or GNF models should be a straightforward task. The main steps are:

- copy-paste the folder of an existing model (that we will call template model) in directory `src/libs/constitutiveEquations/constitutiveEqs/` for viscoelastic models, or `src/libs/constitutiveEquations/constitutiveEqs/GNF/` for GNF models. Rename the folder and the files inside it (`.C` and `.H` files) with the new model's name. Remove the `.dep` file inside the folder, as well as the folder for the log-implementation (if not needed), in case of viscoelastic models.
 - inside the source `.C` and header `.H` files, find-replace the old model's name by the new one (e.g. *Ctrl + H* in *gedit*). This is to change the name of the class, which is usually equal to the name given to the respective source file. However, it is a good idea to always check first the name given to the class of the template model.
 - add the source code of the new model to the compilation list of the library. For that, edit file `src/libs/constitutiveEquations/Make/files`

by adding the path for the source code (see the entries for the other models already there).

- make a first compilation of the new model, by running the script *Allwmake* in directory `src/`. Note that, until this point, the source code of the new model is the one from the original template model, where only the name of the class has been changed. Thus, the model should compile without errors. If not, something wrong occurred in the previous steps.
- the last step is to change the source code of the model in order to implement the desired constitutive equation. Typically, the changes will be in three main places: (i) the header file, where the new variables and parameters of the model have to be declared (delete the ones from the template model that are not needed); (ii) the constructor in the source file, where those new entries should be added and initialized (delete the ones not needed); (iii) function *correct()*, which is aimed to either update the viscosity (GNF) or the polymeric extra-stresses (viscoelastic model). Note that you may also need to define functions *divTau()* and *divTauS()* for your new model, if the ones defined and used by default in the base class (see `constitutiveEq.C`) are not adequate. After all the changes on the code had been completed, compile again by running script *Allwmake*.

If all the steps listed above were successfully executed, then the new model is now available to all the solvers of *rheoTool*. In order to use library *constitutiveEquations* in any solver other than the ones provided with *rheoTool*, the user should:

- add the header `#include "constitutiveModel.H"` to the main solver.
- create a *constitutiveModel* object by calling the constructor, with the correct arguments, for example: `constitutiveModel constEq(U, phi)`.
- add the library *constitutiveEquations* to the Make/options, and specify its path (check the Make/options of the solvers in *rheoTool* for an example).

4.2 The *EDFModels* library

4.2.1 Available EDF models

The list of runtime selectable EDF models is presented in Table 4.2.

Table 4.2: Available models for electrically-driven flows in the *EDFModels* library. The last column indicates the section in the user guide where the model has been described.

| Model | ¹ TypeName | ^{2,3,4} \mathbf{f}_E | ⁵ Governing Equations | Section |
|--------------------------------|-------------------------|--|---|---------------|
| Poisson-Nernst-Planck (PNP) | <i>NernstPlanck</i> | $- \left(F \sum_{i=1}^N z_i c_i \right) (\nabla \Psi - \mathbf{E}_a)$ | $\begin{cases} \nabla \cdot (\varepsilon \nabla \phi_{\text{Ext}}) = 0 \\ \nabla \cdot (\varepsilon \nabla \psi) = -F \sum_{i=1}^N z_i c_i \\ \frac{\partial c_i}{\partial t} + \mathbf{u} \cdot \nabla c_i = \nabla \cdot (D_i \nabla c_i) + \nabla \cdot \left[(D_i \frac{e z_i}{kT} \nabla \Psi) c_i \right] \end{cases}$ | Section 3.5.1 |
| Poisson-Boltzmann (PB) | <i>PoissonBoltzmann</i> | $\left[-F \sum_{i=1}^N z_i c_{i,0} \exp(-\frac{e z_i}{kT} \psi) \right] (\nabla \Psi - \mathbf{E}_a)$ | $\begin{cases} \nabla \cdot (\varepsilon \nabla \phi_{\text{Ext}}) = 0 \\ \nabla \cdot (\varepsilon \nabla \psi) + \psi F \sum_{i=1}^N (a_i b_i)^* = -F \sum_{i=1}^N (a_i)^* + \psi^* F \sum_{i=1}^N (a_i b_i)^* \\ \text{with } b_i = -\frac{e z_i}{kT} \text{ and } a_i = z_i c_{i,0} \exp(b_i \psi) \end{cases}$ | Section 3.5.3 |
| Debye-Hückel (DH) | <i>DebyeHuckel</i> | $\left[-F \sum_{i=1}^N z_i c_{i,0} \left(1 - \frac{e z_i}{kT} \psi \right) \right] (\nabla \Psi - \mathbf{E}_a)$ | $\begin{cases} \nabla \cdot (\varepsilon \nabla \phi_{\text{Ext}}) = 0 \\ \nabla \cdot (\varepsilon \nabla \psi) = -F \sum_{i=1}^N z_i c_{i,0} \left(1 - \frac{e z_i}{kT} \psi \right) \end{cases}$ | Section 3.5.4 |
| Slip velocity | <i>slipSmoluchowski</i> | 0 | $\nabla \cdot (\varepsilon \nabla \phi_{\text{Ext}}) = 0$ | Section 3.5.5 |
| Ohmic | <i>Ohmic</i> | $[\nabla \cdot (\varepsilon \nabla \phi_{\text{Ext}})] (\nabla \phi_{\text{Ext}} - \mathbf{E}_a)$ | $\begin{cases} \frac{\partial \sigma}{\partial t} + \mathbf{u} \cdot \nabla \sigma = D_{\text{eff}} \nabla^2 \sigma \\ \nabla \cdot (\sigma \nabla \phi_{\text{Ext}}) = 0 \end{cases}$ | Section 3.5.6 |

¹ Corresponds to the name entry identifying the model in the source code.

² \mathbf{f}_E is the electric body-force entering the momentum equation.

³ \mathbf{E}_a is an optional argument - a single vector - representing a uniform electric field.

⁴ When the splitting of potentials approach is selected for the PNP, PB and DH models, the user may choose to use $(\nabla \phi_{\text{Ext}} - \mathbf{E}_a)$, instead of $(\nabla \Psi - \mathbf{E}_a)$. Recall that the splitting of potentials is given by $\Psi = \phi_{\text{Ext}} + \psi$ (cf. Section 3.5.2).

⁵ For the PNP, PB and DH models, the equations are presented according to the splitting of potentials approach, which is optional. When a single electric potential is intended to be used, then replace ψ by Ψ and ignore the equations in terms of ϕ_{Ext} .

4.2.2 The potentials splitting approach and multi-species modeling in the PNP, PB and DH models

The possibility of splitting the electric potential into two variables, as described in Section 3.5.2, is available for the PNP, PB and DH models. When used, one Poisson equation for ψ and one Laplace equation for ϕ_{Ext} are solved, as shown in Table 4.2. In practice, the choice between using one or two potentials is achieved in the following way: if only one potential ($\text{psi} \Leftrightarrow \Psi$) is present in the starting-time folder, then it is assumed than a unique potential is to be used, while if two potentials ($\text{phiE} \Leftrightarrow \phi_{\text{Ext}}$ and $\text{psi} \Leftrightarrow \psi$) are defined, then the splitting approach is assumed. Under the splitting approach, the user still has the option to include or not the contribution of the intrinsic potential in the electric field definition of the body-force entering the momentum equation. The choice is through the variable *psiContrib*, which should be defined in a dictionary, as explained later in Section 5.4.1.

All the PNP, PB and DH models support multi-species modeling, with an arbitrary number of species, each having different properties (charge valence, and diffusivity, when it applies). On the other hand, the Ohmic model is only implemented for a binary, symmetric electrolyte, although the two species may have different diffusion coefficients.

4.2.3 Electrokinetic coupling loop in the PNP model

The PNP model has a loop for the coupling between the Nernst-Planck equations (ionic concentration) and the Poisson equation (electric potential). This loop was seen to be required to keep the second-order accuracy in time of the PNP model [3]. Furthermore, it also allows the use of higher time-steps, while ensuring the conservation of ions. Although it is allowed to select one single iteration for this loop, we recommend the use of at least two iterations in any generic case. Moreover, two coupling iterations is the default behavior for this model if no information is provided by the user.

4.2.4 Analysis of a code sample

As previously done in Section 4.1.4 for the *constitutiveEquations* library, in this Section we analyze a piece of code from the *EDFModels* library in order to illustrate the connection between the code and the theory previously discussed. However, we should note that the differences, at the code level, between the different models of the *EDFModels* library are bigger than in the *constitutiveEquations* library, as can be deduced from Table 4.2.

The piece of code selected for that purpose, Listing 4.3, represents the implementation of the PNP model and can be found in `src/libs/EDFModels/models/NernstPlanck/NernstPlanck.c`. Let's start the analysis to the most important parts:

- lines 11-33: this is the constructor of a subclass (*NPSpecie*), nested in the main class (*NernstPlanck*). Remember that the PNP, PB and DH models

were all presented in a multi-species formulation, which is the form available in the code. The *NPSpecie* subclass is exactly each specie of the PNP model. For **each new** specie, we can see the initialization of the following attributes (members): the concentration field (*ci*), the charge valence (*zi*) and the diffusivity (*Di*). The *NernstPlanck* class may have *N* instances of the *NPSpecie* subclass, as much as defined by the user.

- lines **35-107**: this is the constructor of the main class, where the several fields and variables are initialized. The call to function *checkForPhiE()* in line 44, which is implemented in the base class (see *EDFEquation.C*), is checking for the existence of field *phiE* in the folder corresponding to the starting time. If it is found, the code will interpret that the electric potential should be split into 2 variables (*phiE* $\Leftrightarrow \phi_{\text{Ext}}$ and *psi* $\Leftrightarrow \psi$), otherwise, the code will consider that only a single potential should be used (*psi* $\Leftrightarrow \Psi$). This is how we identify if the splitting of potentials approach should be used. We also highlight lines 89-107, where each specie of the PNP model is being constructed and saved in a *PtrList <>*, named *species_*.
- lines **110-156**: as suggested by the function's name (*Fe*), these lines implement the function returning the electric body-force for the momentum equation. The charge density (*rhoE*) is computed in lines 114-120 (compare with Eq. 3.26), and multiplied by the electric field in lines 122-155 (compare with Eq. 3.24 and Table 4.2). The computation of the electric field may include, or not, the contribution from the intrinsic potential, as discussed in Section 3.5.2 – this is a user selection. Furthermore, the vector *extraE_* is an extra, uniform electric field, which can be optionally defined by the user (see Table 4.2 and its footnotes).
- lines **158-252**: it is inside this function, named *correct()*, that the electric-related equations are solved for. The function is generally prepared to use the splitting approach, in which case three equations are solved: the Laplace equation for the external potential (lines 172-186), the Poisson equation for the intrinsic (or full, unique) potential (lines 188-218) and the Nernst-Planck transport equation for each ionic specie (220-250) – all these equations can be seen in Table 4.2. Each equation is inserted in a *while* loop controlled by the number of cycles and by the initial residual of the equation solved for. This is to optionally converge the explicit terms inside each equation, for each inner-iteration. In addition, and as discussed in Section 4.2.3, all the equations are solved inside an electrokinetic coupling loop (lines 161-251), whose number of iterations is controlled by variable *nIterPNP_*, that is read from dictionary *fvSolution* (line 86). If the variable is not specified by the user, 2 iterations are carried out by default.

All the other EDF models also have the functions *Fe()* and *correct()* in their structure, which are defined according to the given model. We believe that the readers/users will easily understand those functions by reading the comments included in the code, and by comparing the code with Table 4.2.

```
1 #include "NernstPlanck.H"
2 #include "addToRunTimeSelectionTable.H"
3
4 // * * * * * * * * * * Static Data Members * * * * * * * * //
5 namespace Foam
6 {
7     defineTypeNameAndDebug(NernstPlanck, 0);
8     addToRunTimeSelectionTable(EDFEquation, NernstPlanck, dictionary);
9 }
10
11 // * * * * * * * * * * Constructors * * * * * * * * //
12 Foam::NernstPlanck::NPSpecie::NPSpecie
13 (
14     const word& name,
15     const surfaceScalarField& phi,
16     const dictionary& dict
17 )
18 :
19     ci_
20     (
21         IOobject
22         (
23             name,
24             phi.time().timeName(),
25             phi.mesh(),
26             IOobject::MUST_READ,
27             IOobject::AUTO_WRITE
28         ),
29         phi.mesh()
30     ),
31     zi_(dict.lookup("z")),
32     Di_(dict.lookup("D"))
33 {
34 }
35
36 // * * * * * * * * * * Constructors * * * * * * * * //
37 Foam::NernstPlanck::NernstPlanck
38 (
39     const word& name,
40     const surfaceScalarField& phi,
41     const dictionary& dict
42 )
43 :
44     EDFEquation(name, phi),
45     solvePhiE_(checkForPhiE(name, phi)),
46     psi_
47     (
48         IOobject
49         (
50             "psi" + name,
51             phi.time().timeName(),
52             phi.mesh(),
53             IOobject::MUST_READ,
54             IOobject::AUTO_WRITE
55         ),
56         phi.mesh()
57     ),
58     phiE_
```

```

58     (
59         IOobject
60         (
61             "phiE" + name,
62             phi.time().timeName(),
63             phi.mesh(),
64             IOobject::READ_IF_PRESENT,
65             solvePhiE_ == false ? (IOobject::NO_WRITE) : (IOobject::
66             AUTO_WRITE)
67         ),
68         phi.mesh(),
69         dimensionedScalar
70         (
71             "zero",
72             psi_.dimensions(),
73             pTraits<scalar>::zero
74         ),
75         zeroGradientFvPatchField<scalar>::typeName
76     ),
77     relPerm_(dict.lookup("relPerm")),
78     T_(dict.lookup("T")),
79     extraE_(dict.lookupOrDefault<dimensionedVector>("extraEFfield",
80             dimensionedVector("0", dimensionSet(1, 1, -3, 0, 0, -1, 0),
81             vector::zero))),
82     psiContrib_(dict.lookupOrDefault<bool>("psiContrib", true)),
83     phiEEqRes_(phi.mesh().solutionDict().subDict("electricControls").
84             subDict("phiEEqn").lookupOrDefault<scalar>("residuals", 1e-7)),
85     psiEqRes_(phi.mesh().solutionDict().subDict("electricControls").
86             subDict("psiEqn").lookupOrDefault<scalar>("residuals", 1e-7)),
87     ciEqRes_(phi.mesh().solutionDict().subDict("electricControls").
88             subDict("ciEqn").lookupOrDefault<scalar>("residuals", 1e-7)),
89     maxIterPhiE_(phi.mesh().solutionDict().subDict("electricControls").
90             subDict("phiEEqn").lookupOrDefault<scalar>("maxIter", 50)),
91     maxIterPsi_(phi.mesh().solutionDict().subDict("electricControls").
92             subDict("psiEqn").lookupOrDefault<scalar>("maxIter", 50)),
93     maxIterCi_(phi.mesh().solutionDict().subDict("electricControls").
94             subDict("ciEqn").lookupOrDefault<scalar>("maxIter", 50)),
95     nIterPNP_(phi.mesh().solutionDict().subDict("electricControls").
96             lookupOrDefault<int>("nIterPNP", 2)),
97     species_(),
98     nSpecies_(0)
99 {
100     PtrList<entry> specEntries(dict.lookup("species"));
101     nSpecies_ = specEntries.size();
102     species_.setSize(nSpecies_);
103
104     forAll (species_, specI)
105     {
106         species_.set
107         (
108             specI,
109             new NPSpecie
110             (
111                 specEntries[specI].keyword(),
112                 phi,
113                 specEntries[specI].dict()
114             )

```

```

106     );
107 }
108 // * * * * * Member Functions * * * * *
109 Foam::tmp<Foam::volVectorField> Foam::NernstPlanck::Fe() const
110 {
111     volScalarField rhoE( psi_ * dimensionedScalar("norm", epsilonK_
112                           dimensions()/dimArea, 0.) );
113
114     forAll (species_, i)
115     {
116         rhoE
117         += (
118             species_[i].zi()*species_[i].ci()*FK_
119             );
120     }
121
122     if (solvePhiE_)
123     {
124         if (psiContrib_)
125         {
126             return
127             (
128                 -rhoE * ( fvc::grad(phiE_+psi_) - extraE_ )
129             );
130         }
131         else
132         {
133             return
134             (
135                 -rhoE * ( fvc::grad(phiE_) - extraE_ )
136             );
137         }
138     }
139     else
140     {
141         if (psiContrib_)
142         {
143             return
144             (
145                 -rhoE * ( fvc::grad(psi_) - extraE_ )
146             );
147         }
148     }
149     else
150     {
151         return
152             (
153                 -rhoE * (-extraE_ )
154             );
155     }
156 }
157
158 void Foam::NernstPlanck::correct()
159 {
160 }
```

```
// Electrokinetic coupling loop
162 for (int j=0; j<nIterPNP_; j++)
{
164     Info << "PNP Coupling iteration: " << j << endl;
166     scalar res=GREAT;
168     scalar iter=0;

170 //-- Equation for the external potential (loop for the case
//    of non-orthogonal grids)
172 if (solvePhiE_)
{
174     while (res > phiEEqRes_ && iter < maxIterPhiE_)
    {
176         fvScalarMatrix phiEEqn
        (
178             fvm::laplacian(phiE_)
        );
180
        phiEEqn.relax();
182     res=phiEEqn.solve().initialResidual();

184     iter++;
    }
186 }

188 //-- Equation for the intrinsic potential

190 res=GREAT;
iter=0;
192
    volScalarField souE(psi_ * dimensionedScalar("norm1",dimless/dimArea
        ,0.));
194
    forAll (species_, i)
{
    souE +=
198    (
        -species_[i].zi()*species_[i].ci()*FK_
200    /(relPerm_*epsilonK_)
    );
202 }

204 while (res > psiEqRes_ && iter < maxIterPsi_)
{
206
    fvScalarMatrix psiEqn
(
208    (
        fvm::laplacian(psi_)
210    ==
        souE
212    );
214
    psiEqn.relax();
    res=psiEqn.solve().initialResidual();
216}
```

```

218     iter++;
219 }

220 //-- Nernst-Planck equation for each ionic specie

222 forAll (species_, i)
{
224     res=GREAT;
225     iter=0;
226
227     volScalarField& ci = species_[i].ci();
228
229     dimensionedScalar cf(species_[i].Di() * eK_ * species_[i].zi() / (kbK_
230             *T_) );
231
232     while (res > ciEqRes_ && iter < maxIterCi_)
233     {
234         fvScalarMatrix ciEqn
235         (
236             fvm::ddt(ci)
237             +fvm::div(phi(), ci, "div(phi,ci)")
238             ==
239                 fvm::laplacian(species_[i].Di(), ci, "laplacian(D,ci)")
240                 +fvc::laplacian(ci*cf, phiE_+psi_, "laplacian(elecM)")
241             );
242
243         ciEqn.relax(phi().mesh().equationRelaxationFactor("ci"));
244         res=ciEqn.solve(phi().mesh().solver("ci")).initialResidual();
245
246         ci = Foam::max( dimensionedScalar("lowerLimit",ci.dimensions(), 0.),
247             ci );
248         iter++;
249     }
250 }
251 }
252 }
```

Listing 4.3: Source code of the Poisson-Nernst-Planck model in file *NernstPlanck.C*.

4.2.5 Adding new EDF models

The steps required to add new EDF models are similar to the ones described previously, in Section 4.1.6, for GNF and viscoelastic models. The main steps are:

- copy-paste the folder of an existing model (that we will call template model) in directory `src/libs/EDFModels/models/`. Rename the folder and the files inside it (`.C` and `.H` files) with the new model's name. Remove the `.dep` file inside the folder. We recommend to use model *slipSmoluchowski* as template, since it is the simplest one and does not contain other sub-classes, which would also need to be renamed in the next step.
- inside the source `.C` and header `.H` files, find-replace the old model's name by the new one (e.g. *Ctrl + H* in *gedit*). This is to change the name of the class, which is usually equal to the name given to the respective source file. However, it is a good idea to always check first the name given to the class of the template model.
- add the source code of the new model to the compilation list of the library. For that, edit file `src/libs/EDFModels/Make/files` by adding the path for the source code (see the entries for the other models already there).
- make a first compilation of the new model, by running the script *Allwmake* in directory `src/`. Note that, until this point, the source code of the new model is the one from the original template model, where only the name of the class has been changed. Thus, the model should compile without errors. If not, something wrong occurred in the previous steps.
- the last step is to change the source code of the model in order to implement the desired EDF model. Depending on the characteristics of the new model, several parts of the source and header files might need to be changed. Our recommendation is to look to the closest model among the ones available. After all the changes on the code had been completed, compile again by running script *Allwmake*.

If all the steps listed above were successfully executed, then the new model is now available to solver *rheoEFoam* (only). In order to use library *EDFModels* in any solver other than *rheoEFoam*, the user should:

- add the header `#include "EDFModel.H"` to the main solver.
- create an *EDFModel* object by calling the constructor with the correct arguments, for example: *EDFModel elecM(phi)*.
- add the library *EDFModels* to the *Make/options*, and specify its path (check the *Make/options* of *rheoEFoam* for an example).

4.3 Solvers

The solvers available in *rheoTool* are summarized in Table 4.3. Each one is discussed in detail in the following sections.

Table 4.3: Brief description of the solvers available in *rheoTool*.

| Name | Description |
|----------------------|--|
| <i>rheoFoam</i> | Transient solver for pressure-driven, single-phase, laminar, isothermal flows. Selection of rheology is general among all the available GNF and viscoelastic models. |
| <i>rheoInterFoam</i> | Transient solver for pressure-driven, two-phase, laminar, isothermal flows, using the volume-of-fluid (VOF) approach. Selection of rheology for each phase is general among all the available GNF and viscoelastic models. |
| <i>rheoTestFoam</i> | Application to compute steady and transient material properties for any of the available GNF and viscoelastic models. |
| <i>rheoEFoam</i> | Transient solver for electrically-driven, single-phase, laminar, isothermal flows. Mixed electric-/pressure-driven flows are also allowed. Selection of rheology is general among all the available GNF and viscoelastic models. |

4.3.1 *rheoFoam*

The solver *rheoFoam* implements the transient, incompressible Navier-Stokes equations for single-phase flows of GNF or viscoelastic fluids. Figure 4.1 displays the solving sequence.

The solver has three main loops: *L1*, which is advancing the time; *L2*, which is an inner-loop used to converge the solution at each time-step; and *L3*, a loop which can be enabled for non-orthogonal grids, in order to update (inside each time-step and each inner-iteration) the explicit correction of the pressure Laplacian, avoiding stability problems and reducing the error in transient computations. More than understanding each step identified in Fig. 4.1, we want to help the reader to identify them in the source code and relate them with the theory presented in the previous Chapter. With this purpose in mind, we will do a tour to the source code of the solver and the most important points will be discussed, skipping the lines not essential to understand the algorithm.

The solver *rheoFoam* is composed of one main file (*rheoFoam.C*) and four associated header files (*createFields.H*, *createPPUtil.H*, *UEqn.H*, *pEqn.H*, *CEqn.H*), which can be found in directory `src/solvers/rheoFoam/`. All the header files are included from the main .C file. We will start by digging into *rheoFoam.C*, whose source code is displayed in Listing 4.4.

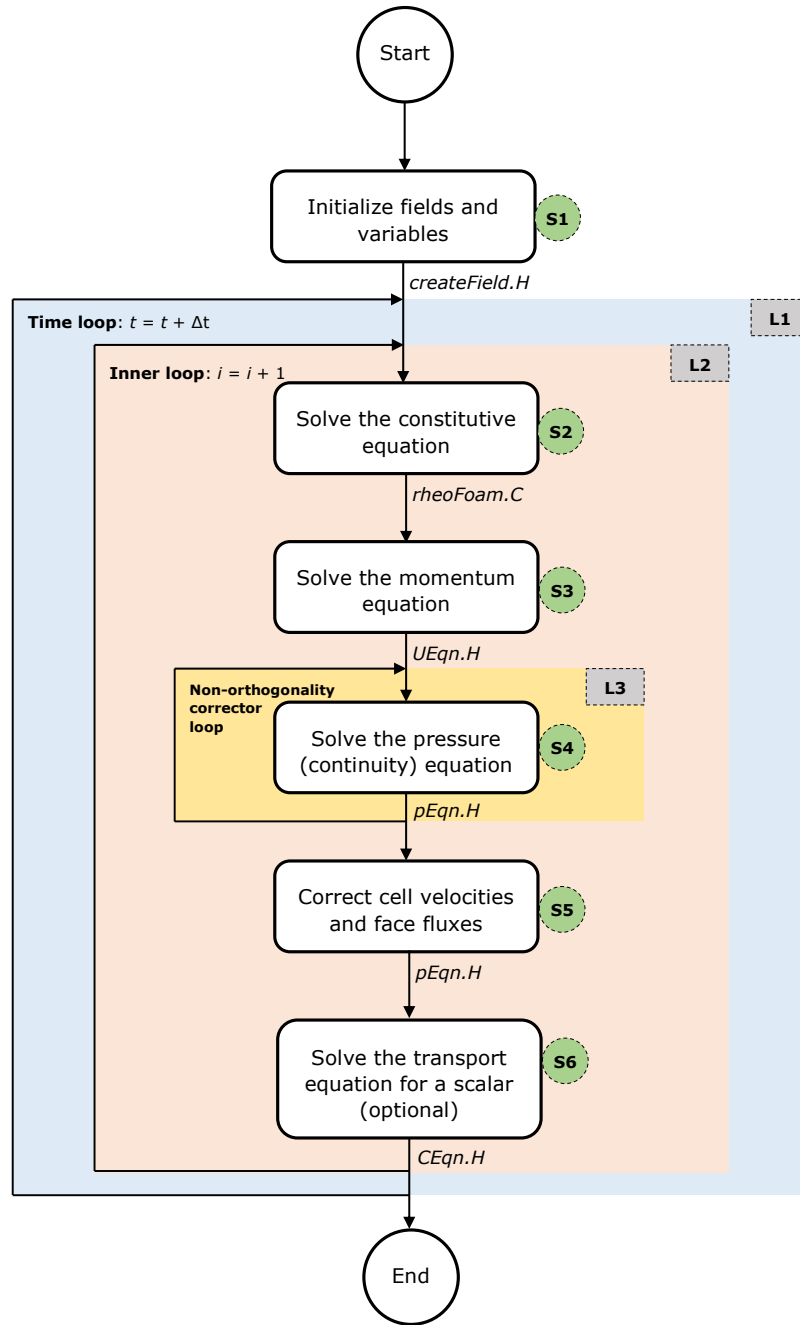


Figure 4.1: Solving sequence of *rheoFoam*.

- lines **1-5**: those *# include* lines load classes used by OpenFOAM® for standard tasks, transversal to most of the OpenFOAM® solvers.
- line **6**: this *# include* is providing access to a library of post-processing utilities, that we discuss later in Section 4.5.2.
- line **7**: this *# include* allows the solver to access the models defined in the

constitutiveEquations library.

- lines **13-21**: fields, variables, controls and the mesh are created (step *S1* of Fig. 4.1). Lines 16 and 18 point to the header files `createFields.H` and `createPPUtil.H`, respectively, located in the same directory as `rheoFoam.C`. The later is responsible for the creation of post-processing utilities.
- lines **27-65**: represents the time loop, i.e., *L1* of Fig. 4.1. The solver will keep running until the final specified time is reached or once the residuals of the solved variables drop below some tolerance (this dual criterion is specific of class *simpleControl*).
- lines **31-33**: those includes allow automatic time-step adjustment, based on the maximum Courant number specified by the user. This control can be switched off by the user (more details in Section 5.1.1).
- lines **36-55**: this is the inner loop, *L2*, of Fig. 4.1. Inside this loop, all the conservation equations are solved *nIter* times inside the same time-step. This reduces the explicitness of the method, which exists, for example, in the non-linear convective term of the momentum equation, in the both-sides-diffusion technique and in several terms of the constitutive equation (for a given equation, only the terms introduced through a `fvm::` operator are implicit). Furthermore, these iterations also strengthen the coupling between velocity and pressure.
- line **43**: the function *correct()* of the constitutive model is called. As seen before, this function updates variable τ by solving the constitutive equation(s).
- line **46**: the momentum equation is solved. The header file `UEqn.H` (Listing 4.5) will be explored later.
- line **47**: the pressure equation is solved. The header file `pEqn.H` (Listing 4.6) will be explored later.
- line **51-54**: the equation for a passive scalar is optionally solved, depending on a user-defined selection (more details in Section 5.1.1). The header file `CEqn.H` (Listing 4.7) will be explored later.
- lines **57-58**: this is where the post-processing utilities are evaluated, if any has been selected by the user.

```

1 #include "fvCFD.H"
2 #include "IFstream.H"
3 #include "OFstream.H"
4 #include "simpleControl.H"
5 #include "fvIOoptionList.H"
6 #include "ppUtilInterface.H"
7 #include "constitutiveModel.H"
8

```



```

64         s"
65         << nl << endl;
66     }
67
68     Info<< "End\n" << endl;
69
70     return 0;
71 }
```

Listing 4.4: Source code of *rheoFoam.C*.

The source code in file *createFields.H* will not be discussed, since it mainly contains standard declaration/initialization of fields and variables. However, it is worth mentioning the creation of a *constitutiveModel* object, named *constEq*, which stores the data of the constitutive equation selected.

According to the SIMPLEC algorithm, the momentum equation is first solved to obtain an estimated velocity field, using the pressure field of the previous inner-iteration or time-step. Then, we solve for the pressure field enforcing continuity. Finally, using the correct pressure field, the previously estimated velocity is corrected, both on faces and cell centers. This is what is being executed in *UEqn.H* and *pEqn.H*. We follow the discussion by analyzing the content of *UEqn.H*, whose code is displayed in Listing 4.5.

- lines **3-10**: this is where the momentum equation is built. We can identify the transient term in line 5, the convective term in line 6, an extra momentum source term in line 8 (term \mathbf{f} in Eqs. 3.5 and 3.18) and the extra-stress divergence in line 9 ($\nabla \cdot \boldsymbol{\tau}'$), containing both the solvent and the polymeric contributions (remember the output of *divTau()* function, analyzed in Section 4.1.4).
- line **16**: the momentum equation is solved considering the pressure gradient contribution, where the pressure field from the last time-step or inner-iteration is used. This term was not added before in order for operator \mathbf{H} obtained from the momentum equation to be free of such contribution, as discussed in Section 3.3.1. This is required to avoid the onset of checkerboard fields, since a traditional Rhie-Chow interpolation is not used (cf. Ref. [2]).

```

// Momentum predictor
2
3     tmp<fvVectorMatrix> UEqn
4     (
5         fvm::ddt (U)
6         +
7         fvm::div(phi, U)
8         ==
9         fvOptions (U)
10        +
11        constEq.divTau(U)
12    );
13
14    UEqn().relax();
15
16    fvOptions.constrain(UEqn());
17 }
```

```

16     solve(UEqn() == -fvc::grad(p));
18     fvOptions.correct(U);

```

Listing 4.5: Source code of *UEqn.H*.

After having a guessed (non-conservative) velocity field, we will see how it is used inside *pEqn.H* (Listing 4.6):

- lines **1-19**: variables required to solve the pressure equation (Eq. 3.15) are assembled. The sequence of steps can be easily understood, keeping in mind that *UEqn().A()* retrieves diagonal coefficients (a_P) and that *UEqn().H()* and *UEqn().H1()* stand for operators \mathbf{H} and H_1 , respectively. As previously discussed in Section 3.3.1, pressure gradient terms entering the definition of face fluxes (line 18) are directly evaluated on cell faces to avoid checkerboard fields. Also, in line 9 there is the addition of the corrective term for time-step dependency, described in Section 3.3.1.
- lines **24-39**: this is the non-orthogonality corrector loop ($L3$) displayed in Fig. 4.1. The goal is similar to the one of the inner loop: minimizing the explicitness of the algorithm. At this point, the reader may be asking why do this loop exists if the inner loop is already there doing a similar task? To clarify this point, it should be noted that the non-orthogonality corrector loop only makes sense to exist for non-orthogonal meshes. For those meshes, the *laplacian* operator in line 28 is not completely handled in an implicit way, but an explicit corrective term is added. For highly non-orthogonal meshes, this term has an important contribution and, due to being explicit, the pressure resulting from solving line 37 will not be continuity-compliant, which can afterwards introduce continuity problems and lead the simulation to diverge. For this reason, in such cases the implicitness of the Laplacian term is increased by continuously solving that equation with the updated pressure-field, and the fluxes are only corrected at the last iteration of this loop (lines 35-38). Is the non-orthogonal corrector loop absolutely necessary when dealing with non-orthogonal meshes? No, as long as the simulation does not diverge and if only steady-state results are required. Otherwise, this loop should be active. For a number of cases, doing 2-3 non-orthogonal iterations keeps the solver stable, without the need of under-relaxing the pressure. Even if only one non-orthogonal correction is performed, the Laplacian term should still be discretized with the corrective term to keep the accuracy in non-orthogonal meshes.
- lines **28,33**: the pressure equation (Eq. 3.15) is assembled (line 28) and solved (line 33).
- line **37**: this is the equation which corrects the face fluxes (Eq. 3.16 interpolated to the faces). Again, pressure gradient terms are directly evaluated on cell faces: the *snGrad()* operator in line 18, when building *phiHbyA*, and the one coming from the *laplacian()* operator in line 28, from which the *flux()* operator is derived.

- line 47: this is the equation which corrects the cell-centered velocity field (Eq. 3.16).

```

2      volScalarField rAU(1.0/UEqn().A());
3      volVectorField HbyA("HbyA", U);
4      HbyA = rAU*UEqn().H();
5
6      surfaceScalarField phiHbyA
7      (
8          "phiHbyA",
9          (fvc::interpolate(HbyA) & mesh.Sf())
10         + fvc::ddtPhiCorr(rAU, U, phi)
11     );
12
13      fvOptions.relativeFlux(phiHbyA);
14      adjustPhi(phiHbyA, U, p);
15
16      tmp<volScalarField> rAtU(rAU);
17
18      rAtU = 1.0/(1.0/rAU - UEqn().H1());
19      phiHbyA += fvc::interpolate(rAtU() - rAU)*fvc::snGrad(p)*mesh.
20          magSf();
21      HbyA -= (rAU - rAtU())*fvc::grad(p);
22
23      UEqn.clear();
24
25      // Non-orthogonal pressure corrector loop
26      while (simple.correctNonOrthogonal())
27      {
28          fvScalarMatrix pEqn
29          (
30              fvm::laplacian(rAtU(), p, "laplacian(p|(ap-H1))") ==
31                  fvc::div(phiHbyA)
32          );
33
34          pEqn.setReference(pRefCell, pRefValue);
35
36          pEqn.solve();
37
38          if (simple.finalNonOrthogonalIter())
39          {
40              phi = phiHbyA - pEqn.flux();
41          }
42
43          #include "continuityErrs.H"
44
45          // Explicitly relax pressure for momentum corrector
46          p.relax();
47
48          // Momentum corrector
        U = HbyA - rAtU()*fvc::grad(p);
        U.correctBoundaryConditions();
        fvOptions.correct(U);

```

Listing 4.6: Source code of pEqn.H.

After `pEqn.H` is executed, both the pressure and the face fluxes are continuity-compliant, but not the cell-centered velocity field. The conservative fluxes can now be used to solve any transport equation. In *rheoFoam*, we offer the possibility to solve a transport equation for a passive scalar. The governing equation, included in file `CEqn.H`, is simply a convection-diffusion transport equation, as can be seen in lines 5-11 of Listing 4.7.

```

1 // Transport of passive scalar
2
3 dimensionedScalar D_ = cttProperties.subDict("passiveScalarProperties").lookup("D");
4
5 fvScalarMatrix CEqn
6 (
7     fvm::ddt(C)
8     + fvm::div(phi, C)
9     ==
10    fvc::laplacian(D_, C)
11 );
12
13 CEqn.relax();
14 CEqn.solve();
15
16 if (U.time().outputTime())
17 {
18     C.write();
19 }
```

Listing 4.7: Source code of `CEqn.H`.

4.3.2 *rheoTestFoam*

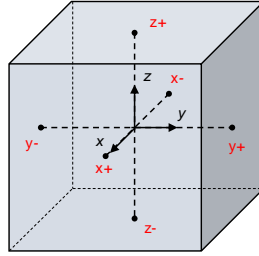
The main purpose of solver *rheoTestFoam* is to evaluate the behavior of the constitutive models for a user-defined $\nabla\mathbf{u}$ tensor. At the same time, it can also be envisaged as a basic debugging tool to check for the correct implementation of the constitutive models, since an analytical or semi-analytical solution usually exists, which can be used for comparison.

Shortly, *rheoTestFoam* solves for the solvent and polymeric constitutive equations, Eqs. (3.3) and (3.4), respectively, for a prescribed $\nabla\mathbf{u}$ tensor, assuming homogeneous flow conditions ($\nabla \cdot \boldsymbol{\tau} = \mathbf{0}$; $\mathbf{u} \cdot \nabla \boldsymbol{\tau} = \mathbf{0}$). Since there are no approximations related with spatial discretization, the resulting steady-state solution $\boldsymbol{\tau}' = \boldsymbol{\tau} + \boldsymbol{\tau}_s$ is exact, and OpenFOAM® is simply acting as a nonlinear matrix solver. To obtain unsteady solutions, the temporal discretization introduces numerical errors during the transient period, which can be reduced using a small time-step.

The computational domain used with this solver is composed of a single cell: a cube with unitary edge length (1 m). The boundary conditions for \mathbf{u} are internally manipulated inside the code, in order to get the tensor $\nabla\mathbf{u}$ defined by the user, Fig. 4.2. Thus, **the default mesh and boundary conditions should not be changed** by the user when working with *rheoTestFoam*. We note that the

following definition holds in this guide (and in OpenFOAM®, in general):

$$(\nabla \mathbf{u})_{ij} = \frac{\partial u_j}{\partial x_i} = \begin{bmatrix} \frac{\partial u}{\partial x} & \frac{\partial v}{\partial x} & \frac{\partial w}{\partial x} \\ \frac{\partial u}{\partial y} & \frac{\partial v}{\partial y} & \frac{\partial w}{\partial y} \\ \frac{\partial u}{\partial z} & \frac{\partial v}{\partial z} & \frac{\partial w}{\partial z} \end{bmatrix} \quad (4.3)$$



$$\begin{aligned} \mathbf{u}_{x-} &= \left(\kappa_1 - \left(\frac{\partial u_x}{\partial x} \right) \frac{\delta x}{2}, \kappa_2 - \left(\frac{\partial u_y}{\partial x} \right) \frac{\delta x}{2}, \kappa_3 - \left(\frac{\partial u_z}{\partial x} \right) \frac{\delta x}{2} \right) & \mathbf{u}_{x+} &= \left(\kappa_1 + \left(\frac{\partial u_x}{\partial x} \right) \frac{\delta x}{2}, \kappa_2 + \left(\frac{\partial u_y}{\partial x} \right) \frac{\delta x}{2}, \kappa_3 + \left(\frac{\partial u_z}{\partial x} \right) \frac{\delta x}{2} \right) \\ \mathbf{u}_{y-} &= \left(\kappa_1 - \left(\frac{\partial u_x}{\partial y} \right) \frac{\delta y}{2}, \kappa_2 - \left(\frac{\partial u_y}{\partial y} \right) \frac{\delta y}{2}, \kappa_3 - \left(\frac{\partial u_z}{\partial y} \right) \frac{\delta y}{2} \right) & \mathbf{u}_{y+} &= \left(\kappa_1 + \left(\frac{\partial u_x}{\partial y} \right) \frac{\delta y}{2}, \kappa_2 + \left(\frac{\partial u_y}{\partial y} \right) \frac{\delta y}{2}, \kappa_3 + \left(\frac{\partial u_z}{\partial y} \right) \frac{\delta y}{2} \right) \\ \mathbf{u}_{z-} &= \left(\kappa_1 - \left(\frac{\partial u_x}{\partial z} \right) \frac{\delta z}{2}, \kappa_2 - \left(\frac{\partial u_y}{\partial z} \right) \frac{\delta z}{2}, \kappa_3 - \left(\frac{\partial u_z}{\partial z} \right) \frac{\delta z}{2} \right) & \mathbf{u}_{z+} &= \left(\kappa_1 + \left(\frac{\partial u_x}{\partial z} \right) \frac{\delta z}{2}, \kappa_2 + \left(\frac{\partial u_y}{\partial z} \right) \frac{\delta z}{2}, \kappa_3 + \left(\frac{\partial u_z}{\partial z} \right) \frac{\delta z}{2} \right) \end{aligned}$$

Figure 4.2: Boundary conditions manipulation in the single-cell mesh used with *rheoTestFoam*. The constants currently used to represent the cell-centered velocity are $\kappa_1 = \kappa_2 = \kappa_3 = 0$, although any other values could be used. The edge length of the cubic cell is set to $\delta x = \delta y = \delta z = 1\text{m}$.

Two operation modes are available with this solver:

- **ramp mode:** the user defines a list of $\nabla \mathbf{u}$ tensors and the solver will retrieve the steady solution for each entry. In this mode, the solver automatically selects the ideal time-step value to be used and the steady-state is also automatically detected (either the relative variation of the extra-stress magnitude drops below 10^{-8} , or after a predefined number of time-steps has been exceeded – this last condition is used to avoid infinite loops).
- **transient mode:** the user defines one single $\nabla \mathbf{u}$ tensor and the solver will return the evolution over time of the monitored variables. In this case, both the time-step and the end time are controlled by the user. This mode allows to determine the transient material functions of the constitutive model selected.

As default behavior, *rheoTestFoam* writes a file named `Report` containing all the components of the total extra-stress tensor, $\boldsymbol{\tau}'$ (remember that $\boldsymbol{\tau}' = \boldsymbol{\tau} + \boldsymbol{\tau}_s$ is

the total extra-stress tensor, including both solvent and polymeric contributions). In ramp mode, also the status (*Converged* or *Exceed_Niter*) is returned, along with the relative error. The user can compute any relevant material function from the tensor components retrieved. If for some reason the status *Exceed_Niter* is retrieved for any $\nabla\mathbf{u}$ entry in *ramp* mode, we recommend to run *rheoTestFoam* in *transient* mode for that same $\nabla\mathbf{u}$, using a small time-step – at convergence, the steady material properties will be obtained. This may happens, for example, when using a multimode model with very different modes, for which the automatic time-stepping procedure fails to choose a stable time-step for the given $\nabla\mathbf{u}$. On the other hand, some viscoelastic models are naturally unbounded under certain flow conditions, such as the UCM and Oldroyd-B models for $Wi \geq 0.5$ in extensional flow. Care should be taken for such situations, since the solver will most likely retrieve a non-physical solution close to those limits and eventually diverge.

Note that *rheoTestFoam* is only adapted to work optimally in ramp mode with the models implemented in the extra-stress tensor variable, which excludes the models solved with the log-conformation approach or with the conformation tensor (FENE-type). However, the material functions for a given model are the same independently of the variable in which it is solved for, as long as all the terms are accounted for. Thus, it is possible to extract the material functions of all the models provided in *rheoTool*.

In a future release of *rheoTool*, we anticipate that the solver *rheoTestFoam* will be able to fit the available constitutive models to experimental data input by the user and return the best-fit model, along with the best-fit parameters (λ, η, \dots). This will allow to run simulations with a numerical model reproducing properly the material functions of real fluids.

4.3.3 *rheoInterFoam*



Section 4.3.3 is under development.

The solver *rheoInterFoam* is a generalization of *rheoFoam* for two-phase flows, using the Volume of Fluid (VOF) method of OpenFOAM® to represent the interface between the two phases.

Currently, *rheoInterFoam* solves a constitutive equation for each phase and the extra-stress tensor contributing to the momentum equation is the weighted average of the extra-stress tensor for each phase, where the weighing is ensured by the indicator function used in VOF. This approach allows to have phases represented by different constitutive equations, although this is possibly not the most accurate and stable way to do the computations. Additionally, the SIMPLEC algorithm used for single-phase flows may need to be improved when used in *rheoInterFoam*. Other aspects are still under test, which makes the current version of *rheoInterFoam* still experimental. Nonetheless, this version is fully functional.

4.3.4 *rheoEFoam*

The solver *rheoEFoam* is the extension of *rheoFoam* to electrically-driven flows – note the additional *E* in the solver name, which points to its *Electric* component. Thus, with no surprise, both solvers share the same basic structure and only minor differences exist between both at the code level. For this reason, we will not discuss again the common parts. Instead, we refer the reader to Section 4.3.1 to eventually recall the structure of *rheoFoam* and in this Section we only highlight the main differences introduced in *rheoEFoam*. Note that *rheoEFoam* allows the combination of both electrically- and pressure-driven flows with no restrictions. Pure pressure-driven flows can be also simulated with *rheoEFoam*, for which the solver becomes functionally equivalent to *rheoFoam*, although directly using *rheoFoam* is the more efficient option in these situations.

Starting by the file `createFields.H`, there is an extra line for the creation of the electric model, as shown in Listing 4.8.

```
1 // Create the electric model
  EHDEKModel elecM(phi);
```

Listing 4.8: Line in the file `createFields.H` of *rheoEFoam*, where the electric model is created.

In file `rheoEFoam.C`, the header `# include "EDFModel.H"` has been added in order to enable the use of the *EDFModels* library, whose path had also to be added to file `Make/options`. The other change is in the inner-iteration loop, which now starts by solving the electric-related equations (line 11, Listing 4.9), calling the function `correct()` of the electric model (recall an example of that function in lines 188-281 of Listing 4.3). The user may also choose to not solve the equations governing the fluid flow (see the *if* condition in line 13 of Listing 4.9). This is useful when only the electric component of the problem is of interest.

```
// --- Inner loop iterations ---
2
3     for (int i=0; i<nInIter; i++)
4     {
5
6         Info<< "Inner iteration: " << i << nl << endl;
7
8         // --- Pressure-velocity SIMPLEC corrector
9         {
10            // ---- Update electric terms ----
11            elecM.correct();
12
13            if (solveFluid)
14            {
15                // ---- Solve constitutive equation ----
16                constEq.correct();
17
18                // ---- Solve U and p ----
19                #include "UEqn.H"
20                #include "pEqn.H"
21            }
22        }
```

```

24          // --- Passive Scalar transport
25          if (sPS)
26          {
27              #include "CEqn.H"
28          }
29      }
30  }
```

Listing 4.9: Inner-iteration loop of *rheoEFoam* (source code: *rheoEFoam.C*).

Finally, the last change at the code level is in file *UEqn.H*, containing the momentum equation, which has been modified to include the electric body-force (line 8, Listing 4.10) – it can be a null vector, depending on the EDF model selected.

```

tmp<fvVectorMatrix> UEqn
1   (
2       fvm::ddt (U)
3       + fvm::div(phi, U)
4       ==
5       fvOptions (U)
6       + constEq.divTau(U)
7       + elecM.Fe() / constEq.rho()
8   );
```

Listing 4.10: Momentum-balance equation in *rheoEFoam* (source code: *UEqn.H*).

4.4 Boundary conditions

4.4.1 *linearExtrapolation*

TypeName: *linearExtrapolation*

Type: fixed-value (any type field).

Formula: $T_{ij,f} = T_{ij,P} + (\nabla T_{ij})_P \cdot \mathbf{d}_{Pf}$, where T_{ij} is the ij component of the generic field T (scalar, vector or tensor), indices f and P represent the boundary face and the cell owning that face, respectively, and \mathbf{d}_{Pf} is the vector connecting their geometrical centers.

Description: linear extrapolation of each field component from boundary cells to boundary faces. Shortly, this boundary condition starts by computing the gradient of each component at the center of the cell owning the boundary face (using the previous iteration/time-step known values on the boundary face). Then, with both the value and the gradient of each component at those locations, the components at the boundary faces are estimated by linear extrapolation. The discretization scheme to compute the gradients enrolled in the process is run time selectable and can be adjusted in dictionary *fvSchemes*, through the entry *linExtrapGrad* followed by the selected scheme, in the *gradSchemes* subDict. In general, using

linear extrapolation for the polymeric extra-stress tensor on walls should be preferred in relation to a zero-gradient boundary condition, which has a lower order of accuracy [2].

Since version 2.0, an optional second-order accurate linear regression [21] can be selected by adding the entry *useRegression true* to the dictionary defining the BC, i.e., below keyword *type*, for example. If not present, the solver will execute by default the linear extrapolation defined above.

4.4.2 *zeroIonicFlux*

TypeName: *zeroIonicFlux*

Type: fixed-gradient (scalar).

Formula: $\nabla c_i|_f \cdot \mathbf{n}_f = -c_{i,f} \frac{e z_i}{kT} \nabla \psi|_f \cdot \mathbf{n}_f$, with $c_{i,f} = c_{i,P} \exp\left[-\frac{e z_i}{kT}(\psi_f - \psi_P)\right]$. Indices f and P represent the boundary face and the cell owning that face (see the definition of the other variables in Section 3.5.1).

Description: imposing a no-flux condition for an ionic specie, in the Poisson-Nernst-Planck model. This boundary condition results from the balance of diffusion and electromigration at the patch, assuming that a no-penetration condition holds there. The expression being used has been derived from a Robin-type boundary condition [3].

4.4.3 *boltzmannEquilibrium*

TypeName: *boltzmannEquilibrium*

Type: fixed-value (scalar).

Formula: $c_{i,f} = c_{i,0} \exp\left[\frac{e z_i}{kT}(\psi_f - \psi_0)\right]$, where $c_{i,0}$ is the reference concentration (user-defined) at which the intrinsic electric potential is ψ_0 (user-defined; see the definition of the other variables in Section 3.5.1). A common choice is to set $c_{i,0}$ as the bulk concentration of ions and $\psi_0 = 0$.

Description: ionic concentration derived from the assumption of Boltzmann equilibrium near the patch. This boundary condition is intended to be used when the electric potential is split, in which case only the intrinsic potential is used in the formula. This boundary condition does not guarantee the zero-flux of a given specie in all the situations, and, in general, it is not accurate for transient simulations.

4.4.4 *inducedPotential*

TypeName: *inducedPotential*

Type: fixed-value (scalar).

Formula: $\psi_f = -\phi_{Ext,f} + \psi_{Fix} + \left(\frac{1}{\sum_{f=1}^{N_f} |\mathbf{S}_f|} \right) \sum_{f=1}^{N_f} \phi_{Ext,f} |\mathbf{S}_f|$, where ψ_{Fix} is the bias voltage (user-defined) of the patch, i.e., the electric potential of the surface in the absence of an external electric field.

Description: intrinsic potential induced in a conducting surface placed over an electric field and having a bias voltage [22]. The last term in the formula represents the area-averaged external electric potential over the surface. This boundary condition can be used with the Poisson-Boltzmann and Debye-Hückel models, under the potentials splitting approach.

4.4.5 *slipSmoluchowski*

TypeName: *slipSmoluchowski*

Type: fixed-value (vector).

Formula: $\mathbf{u}_{Sch,f} = \mu(-\nabla\phi_{Ext,f})$, where μ is the electroosmotic mobility (user-defined), as defined in Section 3.5.5.

Description: slip velocity derived from the Helmholtz-Smoluchowski theory (Section 3.5.5). Although this boundary condition can be used with any EDF model for which ϕ_{Ext} is defined, it is primarily intended to be used with the slip model.

4.4.6 *slipSigmaDependent*

TypeName: *slipSigmaDependent*

Type: fixed-value (vector).

Formula: $\mathbf{u}_{Sch,f} = \mu_0 \left(\frac{\sigma_f}{\sigma_0} \right)^m (-\nabla\phi_{Ext,f})$, as defined in Section 3.5.6. Parameters μ_0 , σ_0 and m are user-defined.

Description: slip velocity derived from the Helmholtz-Smoluchowski theory for a space-variable conductivity field (Section 3.5.6). This boundary condition can be used with the Ohmic model.

4.4.7 A note on wall boundary conditions for pressure

In the simulation of incompressible flows, it is a common approach to assign a zero-gradient boundary condition for the pressure at walls. This approach is efficient to ensure no-penetration in the wall (continuity equation), but it results in a lower-order approximation for the pressure gradient in the momentum equation and, in some cases, it may significantly unbalance the remaining sources of momentum. A more general approach is to derive the pressure gradient at the boundary from the continuity equation, by enforcing the no-penetration condition. Indeed, if Eq.

(3.16) is interpolated to the faces of a bounding wall, then setting the velocity, or more correctly the flux, to zero (no-penetration condition) results in

$$\mathbf{u}_f \cdot \mathbf{n} = 0 \Rightarrow (\nabla p)_f \cdot \mathbf{n} = (a_P - H_1) \left[\frac{H_f}{a_P} + \left(\frac{1}{a_P - H_1} - \frac{1}{a_P} \right) (\nabla p^*)_f \right] \cdot \mathbf{n} \quad (4.4)$$

Eq. (4.4) is generic since it does not depend on a specific form of the momentum equation. It can also be seen that if both sides of Eq. (4.4) are forced to be zero – the zero-gradient approach –, the equality is still satisfied and the no-penetration condition is still valid. The advantage in using Eq. (4.4) is that the resulting normal pressure gradient is going to effectively balance the remaining local forces in the momentum equation. In practice, the difference between using Eq. (4.4) or the zero-gradient approximation is only noticeable when the stresses at the wall are significant (high $\frac{H_f}{a_P}$), as for example in EDFs, where a strong electric force normal to the wall may exists. In the tutorials provided with *rheoTool*, the zero-gradient approximation is frequently used.

Since OpenFOAM® version 4.0, the boundary equation embodied by Eq. (4.4) is available by default under the name *fixedFluxExtrapolatedPressure*. However, this boundary condition may not be usable in some cases, as for example in cases with a zero velocity assigned to all boundaries. In such cases, there is a conflict created by function *adjustPhi()* when it attempts to artificially adjust the fluxes. This issue can be avoided by commenting the line where function *adjustPhi()* is called in the code (typically inside file *pEqn.H*), provided the user is sure that the set of boundary conditions under use verifies continuity. This limitation in the boundary condition might be eventually solved in future releases of OpenFOAM®.

Importantly, in multiphase flows with non-zero surface tension and/or gravity effects, the zero-gradient condition for pressure is generally incorrect. Indeed, for such flows it is usual to compute the fluxes in two steps in OpenFOAM®, i.e., the term $\frac{H_f}{a_P}$ in Eq. (4.4) is built in two steps. The last step adds the flux contribution from surface-tension and gravity without enforcing a null contribution at the wall. Thus, in general the right hand-side of Eq. (4.4) is non-null in these cases and simply setting $(\nabla p)_f \cdot \mathbf{n} = 0$ creates a local mass imbalance. The boundary conditions *fixedFluxPressure* (available in OpenFOAM® and foam-extend) and *fixedFluxExtrapolatedPressure* (only available in OpenFOAM® starting from version 4.0) solve this issue by equating the normal pressure gradient to this extra flux, and they should be employed in such situations. In addition, for *rheoTool* versions running OpenFOAM® v2.2.2 or foam-extend, when the SIMPLEC algorithm is selected for pressure-velocity coupling, the *fixedFluxPressure* BC requires that the entry *Dp* is defined and set to "rAtU" (check the tutorials provided). This is not needed for the PIMPLE coupling algorithm, or when using OpenFOAM® v4.x.

4.5 Utilities

4.5.1 *GaussDefCmpw* schemes for convective terms

The component-wise and deferred correction handling of HRSs, described in Section 3.4, is included as a library in *rheoTool*. If the installation procedure presented in Chapter 2 has been followed, this new class of schemes will only be available when using the family of solvers provided with *rheoTool*. However, there are several ways to make the schemes available to any solver of OpenFOAM®. One option (not requiring compilation) is to include this library (`libgaussDefCmpwConvectionSchemes.so`) as a *lib* entry of `controlDict` in the case directory. Another option is to compile the class inside library `finiteVolume`, which is included by most OpenFOAM® solvers. To access this class from a specific solver, `lgaussDefCmpwConvectionSchemes` should be added to the `Make/options` file of that solver, along with its path. We note that the component-wise and deferred correction handling of HRSs improved significantly the stability of viscoelastic fluid flow simulations [2], but its performance and advantage when used in other type of flows need to be tested (by no way we argue that this is a magic bullet for all purposes).

The new group of HRSs is accessible from class *GaussDefCmpw* and its use is similar to the standard HRSs of OpenFOAM®. For example, the CUBISTA scheme can be used by simply defining in dictionary `fvSchemes`: *GaussDefCmpw cubista*; in front of the divergence term being discretized (remember that keywords in OpenFOAM® are case-sensitive). To obtain a list of all the schemes available, simply type *GaussDefCmpw*; without any additional argument and you will obtain all the possibilities, listed in Table 4.4. There is a scheme named *none*, which corresponds to removing the convective term from the equation being discretized. Note that all the limiters implemented in class *GaussDefCmpw* are totally independent from the already existing limiters of OpenFOAM® and all are defined in file `limiters.H`. For example, you will have now *GaussDefCmpw minmod* and *Gauss Minmod*, which are two different schemes, or, actually, two different implementations of the same high-resolution scheme.

Details on the implementation of this class of schemes will not be presented in this guide, although the interested reader will easily find the analogy between the equations presented in Section 3.4 and the source code in files `gaussDefCmpwConvectionScheme.C` and `limiters.H`. Nevertheless, for documentation purposes, we summarize next the operations being executed by each member function of class *GaussDefCmpw*:

- *phifDefC()*: depending on the boolean value of *onlyDCphi*, this function returns either the interpolated variable on the faces – Eq. (3.23), with all the terms explicitly evaluated –, or the deferred correction to the upwind scheme – only the explicit term of Eq. (3.23).
- *lims()*: this function retrieves three variables: *alpha*, is a list containing α for each interval of the function defined in Eq. (3.20); *beta* is a list containing β for each interval of the function defined in Eq. (3.20); *bounds* is a list of ϕ_C

Table 4.4: Available High-Resolution schemes for convective terms in class *gaussDefCmpw*. The schemes are defined using the NWF approach (Eq. 3.20).

| Scheme | ¹ TypeName | ² Equation |
|----------------------------|-----------------------|--|
| Upwind | <i>upwind</i> | $[\alpha, \beta] = [1, 0]$ |
| CUBISTA | <i>cubista</i> | $[\alpha, \beta] = \begin{cases} [1, 0] & \tilde{\phi}_C \leq 0 \vee \tilde{\phi}_C \geq 1 \\ [7/4, 0] & 0 < \tilde{\phi}_C < 3/8 \\ [3/4, 3/8] & 3/8 \leq \tilde{\phi}_C \leq 3/4 \\ [1/4, 3/4] & 3/4 < \tilde{\phi}_C < 1 \end{cases}$ |
| MINMOD | <i>minmod</i> | $[\alpha, \beta] = \begin{cases} [1, 0] & \tilde{\phi}_C \leq 0 \vee \tilde{\phi}_C \geq 1 \\ [3/2, 0] & 0 < \tilde{\phi}_C < 1/2 \\ [1/2, 1/2] & 1/2 \leq \tilde{\phi}_C < 1 \end{cases}$ |
| SMART | <i>smart</i> | $[\alpha, \beta] = \begin{cases} [1, 0] & \tilde{\phi}_C \leq 0 \vee \tilde{\phi}_C \geq 1 \\ [3, 0] & 0 < \tilde{\phi}_C < 1/6 \\ [3/4, 3/8] & 1/6 \leq \tilde{\phi}_C \leq 5/6 \\ [0, 1] & 5/6 < \tilde{\phi}_C < 1 \end{cases}$ |
| WACEB | <i>waceb</i> | $[\alpha, \beta] = \begin{cases} [1, 0] & \tilde{\phi}_C \leq 0 \vee \tilde{\phi}_C \geq 1 \\ [2, 0] & 0 < \tilde{\phi}_C < 3/10 \\ [3/4, 3/8] & 3/10 \leq \tilde{\phi}_C \leq 5/6 \\ [0, 1] & 5/6 < \tilde{\phi}_C < 1 \end{cases}$ |
| SUPERBEE | <i>superbee</i> | $[\alpha, \beta] = \begin{cases} [1, 0] & \tilde{\phi}_C \leq 0 \vee \tilde{\phi}_C \geq 1 \\ [1/2, 1/2] & 0 < \tilde{\phi}_C < 1/2 \\ [3/2, 0] & 1/2 \leq \tilde{\phi}_C \leq 2/3 \\ [0, 1] & 2/3 < \tilde{\phi}_C < 1 \end{cases}$ |
| ³ no convection | <i>none</i> | — |

¹ Corresponds to the name entry identifying the scheme in the source code.² See Eq. (3.20).³ When this option is used, the convective term is deleted.

values, for which there is a change of branch in the function defined in Eq. (3.20). Thus, function *lims()* defines Eq. (3.20) for the selected scheme.

- *fvmDiv()*: this function also exists for *Gauss* schemes and returns the matrix of coefficients and the source term resulting from the discretization of the implicit convective operator *fvm::div()*. Function *phifDefC()* is called from here, whenever the selected scheme is different from *upwind* or *none*. Note that both *Gauss* and *GaussDefCmpw* classes implement the *upwind* scheme in the same way – it is the only scheme for which this happens.
- *fvcDiv()*: evaluates explicitly the operator *fvc::div()*.
- *interpolate()*: returns face-interpolated values, by simpling calling *phifDefC()*,

with the adequate boolean value.

- *flux()*: returns the field interpolated on face centers multiplied by the flux on each face (*phi*).

The class *GaussDefCmpw* easily allows modifying or adding a new piecewise-linear HRS, by simply adding a new instance or modifying an existing one in function *lims()*, in file *limiters.H*. It is also possible to include HRSs not defined as piecewise-linear functions, although this also requires modifying function *phifDefC()*.

4.5.2 Generic post-processing: *ppUtil*

In version 1.0 of *rheoTool* for OpenFOAM® versions, the computation and writing of quantities of interest after and/or during the simulations of the tutorial cases was mainly exemplified by the use of *coded FunctionObjects*. The reader will easily notice this throughout Chapter 5, where we even included a short Section devoted to those utilities (Section 5.1.2). On the other hand, the same tasks accomplished by such *coded FunctionObjects* were assembled in a library for the *rheoTool* version running in foam-extend, since *coded FunctionObjects* are not available there. While we recognize that *coded FunctionObjects* are a very useful tool, it is also true that they do not allow the efficient execution of some advanced tasks. Therefore, since *rheoTool* version 2.0 we generalized the post-processing dedicated library already present for foam-extend versions to all *rheoTool* versions, while still keeping the examples making use of *coded FunctionObjects*.

The post-processing library is named *libpostProcessingRheoTool* and it can be found in directory *src/libs/postProcessing/postProcUtils/*. The base class is named *ppUtil* and it is accessible from all the solvers included in *rheoTool* through the *ppUtilInterface* class. Creating a new *ppUtil* is straightforward for a user with some knowledge on OpenFOAM® programming:

- copy and paste the folder of an already existing *ppUtil* and give it a new name of your choice. Delete the *.dep* file in that folder.
- *find & replace* the old name of the *ppUtil* by the name that you gave to the folder. This should be done for both the *.C* and *.H* files (there are several ways to do it automatically, for example, *Ctrl + H* in *gedit*).
- modify the source code in order to do what you want.
- add the source file that was just created to the list of files for compilation in the *Makefile* of the library.
- run the *Allwmake* script in *src/* to compile, and it should be ready to use.

Several *ppUtil* can be used simultaneously in a given simulation. They should be defined in subDict *PostProcessing*, located in dictionary *fvsolution*. Each *ppUtil* should be provided as a different entry of group *functions*, as shown in Listing 4.11. In this example, two *ppUtil* are selected and a name is given to each one (*ciMonitor* and *jMonitor*; any name can be attributed).

```

1 PostProcessing
{
3
functions
5 (
7 ciMonitor
{
9   funcType      calcBalance;
11  enabled       true;
13  evaluateInterval 100;
15 }
17 jMonitor
19 {
21   funcType      calcJpatch;
23   ListOfPatches
25   (
27     "cylinder"
);
29   enabled       true;
31   evaluateInterval 100;
33 }
35 );
37 }

```

Listing 4.11: Example of a *PostProcessing* subDict.

For each *ppUtil* selected, at least three keywords must be defined:

- *funcType*: should specify the *TypeName* of the given *ppUtil*. To obtain a full list of all the available utilities, simply insert any random letter.
- *enabled*: should be *true* or *false* and it determines whether the *ppUtil* is active or not;
- *evaluateInterval*: should be any integer value > 0 and corresponds to the number of time-steps between consecutive calls to the given *ppUtil*. Currently, the execution interval can be only controlled by the number of time-steps.

When a given *ppUtil* is active and programmed to write some quantity (or several) of interest, a folder named `rheoToolPP/startTimeName/ppUtilName/` is created in the case directory and the output is forwarded to there.

The class *ppUtil* not only allows to create case-specific post-processing tools, as it also offers the possibility to build generic post-processing applications. In Table 4.5 we present some generic *ppUtil* which are included in *rheoTool* and that can be useful in a number of cases.

Table 4.5: General-purpose *ppUtil* available in *rheoTool*.

| Type | Name | Description |
|--------------------|------|--|
| <i>calcWSS</i> | | Computes the wall shear-stress magnitude for any constitutive equation: $WSSmag = \mathbf{n} \cdot \boldsymbol{\tau}' - \mathbf{n}(\mathbf{n} \cdot \boldsymbol{\tau}' \cdot \mathbf{n}) $ (Pa), where we remember that $\boldsymbol{\tau}'$ represents the total extra-stress tensor (see Section 3.1). This <i>ppUtil</i> is used in the tutorial of Section 5.1.8. |
| <i>calcJpatch</i> | | Computes the surface-averaged current density, for each ionic specie, in the patches specified by the user: $J_i = \frac{z_i F}{ \mathbf{S}_{\text{patch}} } \sum_{f=1}^{N_f} [(c_{i,f} \mathbf{u}_f - D_i \nabla c_{i,f} - D_i \frac{e z_i}{kT} c_{i,f} \nabla \Psi_f) \cdot \mathbf{S}_f]$ (A/m ²). This <i>ppUtil</i> is only meaningful for the PNP model (an example can be found in the tutorial of Section 5.4.4). |
| <i>calcBalance</i> | | Computes the average concentration for each ionic specie: $\bar{c}_i = \frac{1}{V_{\text{domain}}} \sum_{j=1}^{N_C} c_{i,j} V_j$ (mol/m ³). It also retrieves the net, surface-averaged flux of each ionic specie through all the domain boundaries (equivalent to run <i>calcJpatch</i> for all the boundaries, sum the fluxes and divide by $z_i F$). This <i>ppUtil</i> is only meaningful for the PNP model (an example can be found in the tutorial of Section 5.4.3). |

4.5.3 *writeEfield*

By default, the solver *rheoEFoam* does not write the electric field to the time directories. The purpose of utility *writeEfield* is to read the electric potential variable(s) and write the electric field, for each time directory. This means that this utility can only be called after the simulation has been run. The utility sums up all the electric potential variables available in the directories: Ψ (*psi*), ϕ_{Ext} (*phiE*) and/or ψ (*psi*).

The utility can be used by typing *writeEfield* in the terminal, without any other requirements, except that at least one electric potential variable must exist in the time directories. In addition, the time directories can not be decomposed among processors (reconstruct the case if it is decomposed).

Note that the electric field can be also computed from the electric potential in most of the visualization software, as for example Paraview, since a simple differentiation operation is required.

Chapter 5

Tutorials

In this Chapter, we provide a step-by-step guide on how to use the solvers of *rheoTool*. For each solver, general guidelines are first discussed, regarding the new fields and dictionaries required by that application. Then, specific tutorials are presented, which will illustrate the application of *rheoTool* to relevant problems. These tutorials cover the full process to obtain results, from the mesh generation to the post-processing stage.

The approach used in this Chapter assumes that the reader is familiar with the typical folder organization of OpenFOAM® cases and has basic knowledge on how to run simulations in OpenFOAM®.

A Some of the tutorials included in *rheoTool*, and described in this Chapter, make use of either *coded FunctionObjects* or *codedFixedValue* functionalities of OpenFOAM®, which allow to use run time compilable code from within the case directory. In some (older) versions of OpenFOAM® (e.g. v2.2.2), those features are not allowed to be executed by default and an error reporting this problem is retrieved. The instructions to change the default behavior are displayed in the error description printed in the screen. Shortly, the user should switch on variable *allowSystemOperations* in file `etc/controlDict` located in the OpenFOAM® installation directory.

i The tutorials in this Chapter are mainly intended for learning purposes. It is not our primary goal to obtain highly accurate results with such examples, but solely to show how to run the solvers, preferably using fast-running cases. Higher accuracy can be obtained in all the cases by increasing the resolution in space and time.

5.1 *rheoFoam*

5.1.1 General guidelines

Before proceeding, we note that the sequence of operations required to prepare a case in OpenFOAM® does not need to be ordered as presented next (`constant/` → `0/` → `system/`). This sequence was organized in such a way to be (hopefully) logic and easy to follow and execute.

`constant/`

Inside folder `constant/` there are two main components of the simulation: the mesh, in folder `polyMesh/`, and the dictionary `constitutiveProperties`, which is a dictionary specific of `rheoTool`. Since the mesh is an element required by almost all OpenFOAM® solvers, it will not be discussed here and we assume that a valid mesh already exists in folder `polyMesh/`.

The dictionary `constitutiveProperties` used by `rheoFoam` includes information about the constitutive model and the passive scalar transport which can optionally be activated in the simulation (Listing 5.1).

```

1 parameters
{
3     type          Oldroyd-BLog;
5     rho           rho [1 -3 0 0 0 0] 1.;
6     etaS          etaS [1 -1 -1 0 0 0] 0.01;
7     etaP          etaP [1 -1 -1 0 0 0] 0.99;
8     lambda        lambda [0 0 1 0 0 0] 1.;
9
10    stabilization coupling;
11 }

13 passiveScalarProperties
{
14     solvePassiveScalar off;
15     D                  D [ 0 2 -1 0 0 0 ] 1e-9;
16 }
17 }
```

Listing 5.1: Example of a `constitutiveProperties` dictionary used with `rheoFoam`.

The dictionary `constitutiveProperties` has two different sub-dictionaries (subDict), which must necessarily exist: *parameters*, with information on the constitutive model, and *passiveScalarProperties*, related with the scalar-transport equation.

Regarding subDict *parameters*, in line 3 we define the TypeName of the constitutive model to be used, which can be found in Table 4.1. In the example displayed in Listing 5.1, we are using the Oldroyd-B model, solved with the log-conformation approach (*Oldroyd-B + Log*). If we would like to use the same model without solving it with the log-conformation approach (solving the constitutive equation for the extra-stress tensor), then the type would be simply *Oldroyd-B* – this naming rule is valid for all viscoelastic models. Lines 5 to 8 specify the fluid properties

required by the constitutive model being solved. The density is a property common to all models (it is not related with the constitutive equation) and should always be present, while the model-dependent properties can be checked in Table 4.1. Anyway, if some required parameter is not specified, the solver will retrieve an error complaining for its absence.

The reader might be surprised with the unphysical parameters displayed in Listing 5.1 (even just being an example), particularly the density of the fluid, which is not realistic for any known viscoelastic liquid. The use of a unitary density ($\rho = 1 \text{ kg/m}^3$) and many other unitary variables is simply to facilitate the calculations. In the tutorials presented next, we frequently make use of this kind of approach, since the computation of dimensionless parameters does not require physically realistic quantities.

At line 10, the stabilization method is selected (recall that C++ is case-sensitive): *none* for no stabilization; *BSD* to use the both-sides-diffusion technique; *coupling* to use the stress-velocity coupling discussed in Section (3.3.2). Note that this option is only meaningful for viscoelastic models.

For multi-mode viscoelastic models, the TypeName is *multimode* and lines 3-10 need to be included for each mode, enclosed in a dictionary identified with the mode's name. An example is provided in the tutorials (tutorials/rheoFoam/OtherTests/).

For the FENE-type models not using the log-conformation approach, several formulations are available, as discussed in Section 4.1.2. The selection between them is also performed in subDict *parameters*. If nothing is specified, FENE models are evaluated using the (complete) formulation in **A**. In order to solve the complete formulation in τ , the keyword *solveInTau* should be defined and set to *true*. If the modified formulation in τ is intended, both *solveInTau* and *modifiedForm* keywords should be defined and set to *true*. Some examples are provided in the tutorials (tutorials/rheoFoam/OtherTests/). Note that the selection between the available formulations of FENE-type models is **not** achieved by specifying different TypeNames for each one: the TypeName is the same for all the formulations within the same model (FENE-CR or FENE-P) and the selection is based on the keywords just described.

Focusing now on subDict *passiveScalarProperties*, only two entries are present. In line 15, the user can select to solve (*on*, *true* or *yes*), or not (*off*, *false* or *no*), the transport equation of a passive scalar. If the equation is solved, then line 16 should specify the diffusion coefficient and field *C* (the name of the scalar being transported) should be defined in the folder corresponding to the start-time. Otherwise, none of these two actions is required. Importantly, if the option to solve the transport equation is enabled, but field *C* is not provided, then *rheoFoam* will solve a transport equation (you can confirm it on the solver output) for a scalar not present in the domain (its concentration will remain null over all the simulation time), since this is how the field is internally initialized when there is no entry for it in the start-time folder.

0/

At this point, both the mesh and the fluid are defined and some decisions have been made about the numerical method. It is now time to create and define the

initial and boundary conditions for the variables used in the simulation, which will depend on the constitutive equation selected. At least three scenarios are possible:

- **GNF fluid:** those cases only require defining pressure (divided by the density), p (in this guide represented by $\frac{p}{\rho}$), and velocity, U (in this guide represented by \mathbf{u}) fields. For all the GNF models, except for the Newtonian case, the solver will automatically write the shear-rate dependent viscosity at subsequent times.
- **viscoelastic model using the standard extra-stress approach:** those cases require defining pressure (divided by the density), p , velocity, U , and the polymeric extra-stress field, τ_{au} (in this guide represented by $\boldsymbol{\tau}$). The novelty relative to the GNF cases is in variable τ_{au} , which is of type *symmTensor*. All the three variables will be automatically written at future times. When a multi-mode viscoelastic model is used, each mode owns a variable τ_{au} , which should be present in folder `0/`. The name given to each variable should be consistent with the names attributed to each mode in `constitutiveProperties`, i.e., this name should be appended at the end of name τ_{au} . For example, having defined mode names `M1` and `M2`, then the names for the respective τ_{au} should be `tauM1` and `tauM2`.
- **viscoelastic model using the log-conformation approach:** comparing with the previous case, it requires defining the additional variable `theta`, which represents the natural logarithm of the conformation tensor (in this guide represented by Θ), which is also a *symmTensor*. In order to define boundary conditions for `theta`, we suggest the reader to take a look at Eqs. (3.6) and (3.7). For example, if the polymeric extra-stress (τ_{au}) is a null tensor, then variable `theta` is also a null tensor. At subsequent times, the solver will automatically write fields p , U , τ_{au} , `theta` and both the eigenvectors, `eigVecs` (in this guide represented by \mathbf{R}), and eigenvalues, `eigVals` (in this guide represented by Λ), which are obtained from the diagonalization of the conformation tensor. Note that the fields `eigVecs` and `eigVals` do not need to be present to start a simulation, although they are read if they are present (for example, to restart a simulation from the exact point where it finished). For a multi-mode model, the same considerations previously described apply, including for variable `theta`.

When using FENE-type models solved in the conformation tensor, without the logarithmic transformation (see Section 4.1.2), the conformation tensor field (\mathbf{A}) can be optionally defined in folder `0/`, being read by the solver in that case. However, if not defined, the solver automatically initializes the conformation tensor field from $\boldsymbol{\tau}$, that should always be present. Independently of being or not present in the starting time folder, field \mathbf{A} will be written to the case directory for the remaining of the simulation.

For any of the previous cases, if the option to solve the transport equation of a passive scalar has been enabled, then a field C should also be present in folder `0/`. The utility `setFields` of OpenFOAM® can be particularly helpful to initialize

this field, since it allows to assign different values of C in different regions of the domain.

system/

The last steps before starting the simulation are related with the dictionaries located in folder `system/`, which mainly control the numerical method. In particular, we will focus our attention on the following dictionaries: `controlDict`, `fvSchemes` and `fvSolution`. All the three dictionaries must be present for the simulation to run, as required by most of the OpenFOAM® solvers. Since most of the entries in those dictionaries are transversal to both *rheoFoam* and any OpenFOAM® solver, we will limit our description to the new features introduced by *rheoFoam*.

In `controlDict` dictionary, the options allowing to automatically control the time-step by imposing a Courant number limit are available in *rheoFoam* and can be used (following the same principles of other OpenFOAM® solvers). Those options are `adjustTimeStep (on/off)`, `maxCo` (the value of the limiting Courant number) and `maxDeltaT` (the maximum admissible time-step). Furthermore, and although not being a feature exclusive of *rheoFoam*, *coded functionObjects* can be defined in `controlDict` and used with *rheoFoam* to extract and monitor quantities of interest (this is not possible in *foam-extend*). This kind of functions are frequently used in the tutorials of this Chapter.

Regarding dictionary `fvSchemes`, we remember that *GaussDefCmpw* schemes (Section 4.5.1) are available for selection and can be used to discretize any convective term with the generic form `div(phi,variable)`, where `variable` is either `U`, `tau`, `theta` or `C`. Still in the `divSchemes` subDict, the term `div(grad(U))` is part of the stress-velocity coupling algorithm (see line 44 of Listing 4.2) and should (always) be discretized using a central differencing scheme (*Gauss linear*), if used. In the `gradSchemes` subDict, the entry `linExtrapGrad` is for the gradient of the tensor components when using linear extrapolation of polymeric extra-stress at a given boundary, as discussed in Section 4.4.1. Apart from this, the remaining entries in `fvSchemes` should be familiar to the user and the selection of appropriate discretization schemes for each one is essential to keep the numerical method accurate and stable.

The dictionary `fvSolution` is the only remaining to be adjusted before running the simulation. In subDict *solvers*, the matrix solver for each equation being solved should be specified (remember that there will be N equations to solve for `theta/tau` in a model using N modes; wildcard characters are useful in those cases). If the user forgets to specify any, the solver will retrieve an error message asking for it. Only the pressure equation results in a symmetric matrix of coefficients, while all the others generate non-symmetric matrices. The only exception is the momentum equation without the convective term included, which also results in a symmetric matrix. This should be taken into account when selecting the type of matrix solver, since some are specific for some type of matrices. In the *SIMPLE* subDict, there is a new entry specific of *rheoFoam*, which is `nInIter`. This variable was defined in Section 4.3.1 and controls the number of inner-iterations (see Fig. 4.1). If not defined, the solver will execute 1 inner-iteration as the default behavior. Still in the *SIMPLE* subDict, the entry `residualControl` allows the

solver to automatically stop the simulation once the residuals for all the specified variables drop below the prescribed value. This is mainly a characteristic of steady-state solvers of OpenFOAM® and it can be also used in *rheoFoam*. However, if the goal is to run *rheoFoam* until the *endTime* specified in *controlDict*, simply leave this entry empty. The last subDict in *fvSolution* is the *relaxationFactors*, that determines the amount of explicit (*fields*) and implicit (*equations*) under-relaxation for each field or equation. When using the SIMPLEC algorithm for pressure-velocity coupling, as a rule of thumb, the pressure does not need to be explicitly under-relaxed to correct the velocity (see Ref. [2]). The only exception occurs for non-orthogonal grids, where a small amount of under-relaxation may eventually be needed for pressure. The under-relaxation factor, ranging between 1 (no under-relaxation) and 0 (total under-relaxation, pressure does not evolve in time), is case-specific and should be as high as possible (it can be conditioned by stability issues). Regarding implicit under-relaxation (*equations*), it only makes sense to be used with steady-state solvers, where the absence of a time-derivative term requires under-relaxation for stability reasons. Since *rheoFoam* is by default a transient solver, where time-derivatives are present in all the transport equations, implicit under-relaxation is not needed. In practice, it is possible to run *rheoFoam* without those time-derivatives by selecting a default steady-state discretization scheme in the *ddtSchemes* subDict of *fvSchemes* and, by this way, *rheoFoam* will run as a typical steady-state solver of OpenFOAM®, requiring implicit under-relaxation. However, in some situations (viscoelastic models solved with the log-conformation approach) the user will probably face stability issues, due to the poor diagonal dominance of the base matrix of coefficients. For this reason, unless the user is experienced and knows what is doing, we strongly recommend to use *rheoFoam* in transient mode. Note that, if it exists, the steady-state will be reached after some time of a transient simulation (typically after several relaxation times, of the order of 10 or above for higher Wi , for viscoelastic models). If the transient analysis is not important, a high Courant number ($\gg 1$) can be defined to reach this state faster, as long as the computations remain stable.

In all the tutorials presented next, a steady-state is reached for the range of parameters used in the examples. However, in none of them we use the residuals as the termination criteria. Indeed, we prefer to set a very long *endTime* and monitor a relevant variable at sensitive points over time. It can be the extra-stress near a singular point, the drag coefficient over a surface, a vortex length, or any other relevant quantity for the problem at hand. This is usually achieved either through a *probe* (when the variable exists within the solver) or a *ppUtil* or *codedFunctionObject* (when the variable does not exist within the solver and needs to be computed), in dictionary *controlDict*. The termination criteria is then based on this variable. Of course, we have set the *endTime* in the tutorials based on that analysis. The residuals displayed on the screen should not be used alone as the termination criteria.

As mentioned in Section 4.5.2, the *PostProcessing* subDict enabling the use of the *ppUtil* class is also defined in dictionary *fvSolution*. A detailed discussion on this subject can be found in Section 4.5.2.

5.1.2 A note on *coded FunctionObjects*

Most of the tutorials presented next use a *coded FunctionObject*. This is a run time compilable code, executing run time functions coded by the user, which can be defined in dictionary `controlDict`.

These functions allow to access almost all the data of the case, from field variables to information about the mesh. The frequency at which they are evaluated can be controlled using the keywords `outputControl` and `outputInterval`. It is also possible to disable these functions by setting the keyword `enabled` to `off`.

The *coded FunctionObjects* included in the tutorials are usually divided in three sections: a section which reads data, a section which computes quantities of interest from this data and a writing section. Usually, we create a dynamic list to accommodate the data to be written, so that any extra quantity can be easily added to the list. This also eases the writing step. The meaning of each column of the data being written is usually displayed as a comment in the source code of the *coded FunctionObject*, being of course dependent on the tutorial case.

Among the several possibilities to write the variables computed by *coded FunctionObjects*, we chose to use a `.sh` executable, named `writeData`. This executable simply receives as arguments the name of the file to write to (the user can change it in the `codedStream functionObjects`), along with the data to be written, both provided by a system call from the *coded FunctionObject*. If the executable is not present in the case directory, but it is being called by the *FunctionObject*, a warning is displayed in the terminal informing about this situation (it is also possible to copy this script to a location loaded by default in each OpenFOAM® session, in order to avoid the need of having it in the case directory). Keep in mind that this `.sh` executable only writes to a file the data it receives as argument, so that it is unlikely that the user would need to change it.

One main advantage of *coded FunctionObjects* is that they are case-specific, instead of solver-specific, which means that the code of the solver does not need to be changed. They are probably also a good entry point to start programming in OpenFOAM®, since the compilation steps are automatically handled.

Note for foam-extend users: as mentioned in Section 2.6, *coded* objects are not available in foam-extend. For these versions, functions executing the same tasks as the *coded* objects are available in a dedicated post-processing library, as discussed in Section 4.5.2.

The boundary conditions implemented in OpenFOAM® versions as *coded* functions were added to library `libBCRheoTool.so` in the foam-extend version.

i For most of the tutorials presented next, the commands required to run them are specified. It is instructive for the less experienced users to type each one in the command line, in order to exactly know what is being done. However, in the directory for each tutorial we also provide a script named `Allrun` that automatically runs all these commands. On the other hand, the script `Allclean` also included cleans the directory, deleting everything that has been created.

5.1.3 Case 1: flow between parallel plates

 [tutorials/rheoFoam/Channel/Oldroyd-BLog/](#)

❖ Overview

In this tutorial, the flow between two infinite parallel plates is simulated for an Oldroyd-B fluid. Although apparently simple, this case can pose formidable difficulties using the UCM and Oldroyd-B models at high Weissenberg number flows [23]. This example also shows that the log-conformation approach is effective in solving this stability issue, while retrieving the predicted analytical profiles.

Following Ref. [24], the Reynolds number for this problem is defined as $Re = \frac{\rho U w}{\eta_0}$ and the Weissenberg number as $Wi = \frac{\lambda U}{w}(1 - \beta)$, where $\beta = \frac{\eta_s}{\eta_s + \eta_p} = \frac{\eta_s}{\eta_0}$. The case reproduced in the tutorial is for $Re = 0$ (the convective term in the momentum equation is suppressed), $Wi = 0.99$ and $\beta = 0.01$.

❖ Geometry & Mesh

The geometry is a planar channel (two parallel plates) with half-width w , Fig. 5.1. The mesh is composed of 50 cells in the x -direction and 60 cells in the y -direction, uniformly distributed in both directions.

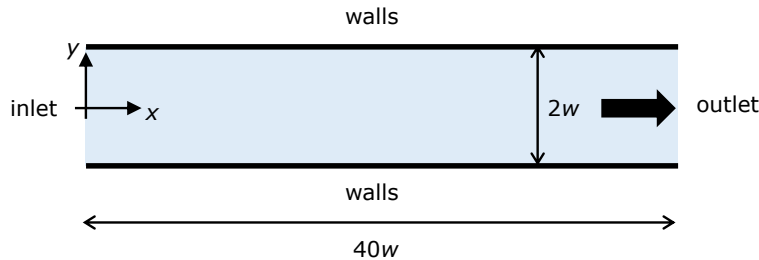


Figure 5.1: Planar channel geometry.

❖ Boundary conditions

This flow is 2D, being solved in the xy -plane. A uniform velocity profile (U) is set at the inlet, along with zero-gradient for pressure and polymeric extra-stress components. At the outlet, fully-developed flow conditions are assumed (zero-gradient for all variables, except pressure, which is fixed to a constant value, $p = 0$). A no-slip boundary condition is assigned at the walls (velocity is null, polymeric extra-stress components are linearly extrapolated and a zero-gradient is assumed for pressure in the normal direction to the wall).

❖ Command-line

1–Build the mesh:

```
~$ blockMesh
```

2–Run the solver:

```
~$ rheoFoam
```

3—Extract profiles for \mathbf{u} and $\boldsymbol{\tau}$ along line $x = 35$:

```
~$ sample
```

❖ Results

Figure 5.2 presents the fully-developed profiles at line $x = 35$. The variables were normalized as follows: length is normalized with w , time with w/U , velocity with U and polymeric components of the extra-stress with $\frac{\eta_0 U}{w}$, as in Ref. [24]. A good agreement is observed between the numerical results and the analytical solution written in dimensionless form [24]:

$$\begin{aligned} u_x &= \frac{3}{2}(1 - y^2) \\ \tau_{xy} &= -3(1 - \beta)y \\ \tau_{xx} &= 18Wi(1 - \beta)y^2 \end{aligned}$$

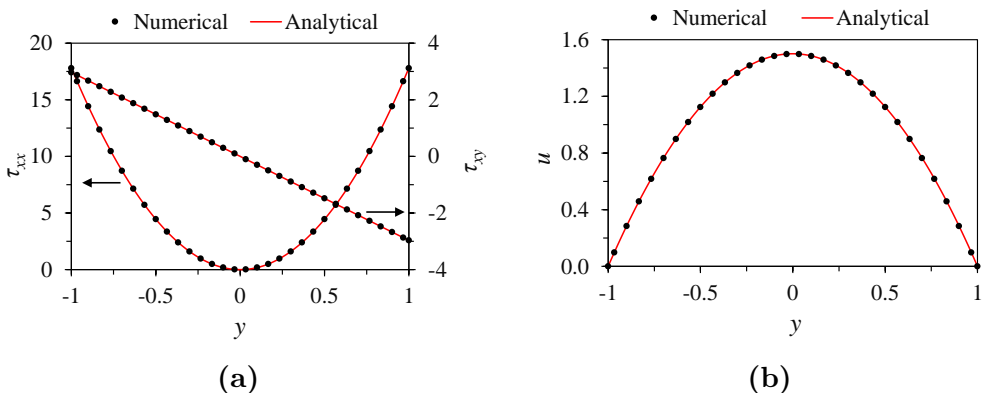


Figure 5.2: (a) Polymeric extra-stress components and (b) velocity, at $x = 35$, for $Re = 0$, $Wi = 0.99$ and $\beta = 0.01$.

The user can test the solver with a UCM fluid ($\beta = 0$) and confirm that an accurate solution is still achieved, without facing any numerical issue. However, running the same cases without the log-conformation approach leads to numerical divergence (try it!).

This tutorial probes a point in the flow over time (to check for convergence), which has been specified in `controlDict` dictionary. The data is written to a directory named `probes/`, whose location in the case directory depends on the OpenFOAM® version.

5.1.4 Case 2: lid-driven cavity flow

❖ `tutorials/rheoFoam/Cavity/Oldroyd-BLog/`

❖ Overview

The flow in a lid-driven cavity is a common benchmark for numerical solvers, for both Newtonian and viscoelastic fluids, being one of the mostly used geometries for such purposes. One reason explaining the popularity is its simple geometry: a square in 2D or a cube in 3D.

For viscoelastic fluids, stress boundary layers develop at the walls and, at high Deborah numbers, the flow becomes time-dependent. A similar behavior is observed with Newtonian fluids at high Reynold numbers.

The case reproduced in this tutorial is for an Oldroyd-B fluid with $\beta = \frac{\eta_s}{\eta_s + \eta_p} = 0.5$. The Deborah number is defined here as $De = \frac{\lambda U}{L}$, while the Reynolds number is $Re = \frac{\rho UL}{\eta_0}$. In this tutorial, we set $De = 1$ and $Re = 0.01$, so that the creeping flow assumption is still adequate, notwithstanding the finite Re .

Geometry & Mesh

The planar lid-driven cavity is simply a square, with side length L , Fig. 5.3. The coordinate axis is located at the bottom-left corner. The mesh consists of one single block with 127 cells uniformly distributed in both directions.

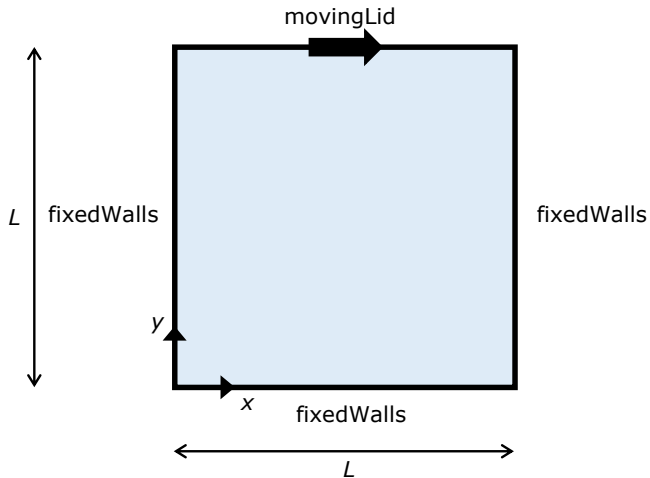


Figure 5.3: Geometry for the lid-driven cavity flow.

Boundary conditions

The flow is assumed to be 2D, being solved in the xy -plane. For the three stationary walls, a no-slip boundary condition is assigned, with null velocity, linearly extrapolated polymeric extra-stresses and zero normal gradient for pressure. At the moving lid wall, the same boundary conditions are used for pressure and polymeric extra-stresses. Regarding the velocity, a time-space dependent condition is employed in order to impose a smooth start of the flow, and to avoid a local singularity with infinite acceleration at the top-right and top-left corners [8]:

$$U_{\text{lid}}(x, t) = 8U [1 + \tanh \{8(t - 0.5)\}] x^2(1 - x)^2 \quad (5.1)$$

Eq. (5.1) is directly implemented as a *codedFixedValue* boundary condition in file 0/U. The variables were normalized as follows: length is normalized with L , time with L/U , velocity with U , and polymeric extra-stresses with $\frac{\eta_0 U}{L}$.

❖ Command-line

1–Build the mesh:

```
~$ blockMesh
```

2–Run the solver:

```
~$ rheoFoam
```

3–Extract profiles for \mathbf{u} and $\boldsymbol{\tau}$ along lines $x = 0.5$ and $y = 0.75$:

```
~$ sample
```

❖ Results

Figure 5.4 presents spatial profiles for the x -component of the velocity and for Θ_{xy} , along with the evolution over time of the volume-averaged "kinetic energy", defined as

$$E_k = \frac{1}{2V_t} \int |\mathbf{u}|^2 dV = \frac{1}{2V_t} \sum_{k=1}^N |\mathbf{u}_k|^2 V_k = \frac{1}{2N} \sum_{k=1}^N |\mathbf{u}_k|^2 \quad (5.2)$$

where N is the number of cells of the mesh and $V_t = NV_k$ for a uniform mesh. A good agreement is observed between the results obtained by *rheoFoam* and the reference data [8], which shows the good accuracy of the solver, both in space and time. The contour maps for the components of $\boldsymbol{\Theta}$ are also provided in Fig. 5.5, together with the flow streamlines.

The "kinetic energy" is written on run time to the case directory, using a *codedFunctionObject*, defined in dictionary `controlDict`. The reader can check in this function how Eq. (5.2) has been implemented.

5.1.5 Case 3: flow in a 4:1 planar contraction

 `tutorials/rheoFoam/Contraction41/Oldroyd-BLog/`

❖ Overview

The 4:1 planar contraction is another traditional benchmark flow problem for viscoelastic fluid flow solvers. The existence of singular points at the re-entrant corners, where stresses grow exponentially as the corner is approached, make this problem challenging from a numerical perspective.

This tutorial reproduces the work that we developed in Ref. [2] using an early version of *rheoFoam*, where an Oldroyd-B fluid ($\beta = \frac{1}{9}$) was studied for $De = 0-12$. The `constitutiveProperties` dictionary is adjusted to reproduce the case for $De = 1$ and $Re = 0.01$.

❖ Geometry & Mesh

The geometry for this case is reproduced in Fig. 5.6. The mesh corresponds to mesh M1 of Ref. [2].

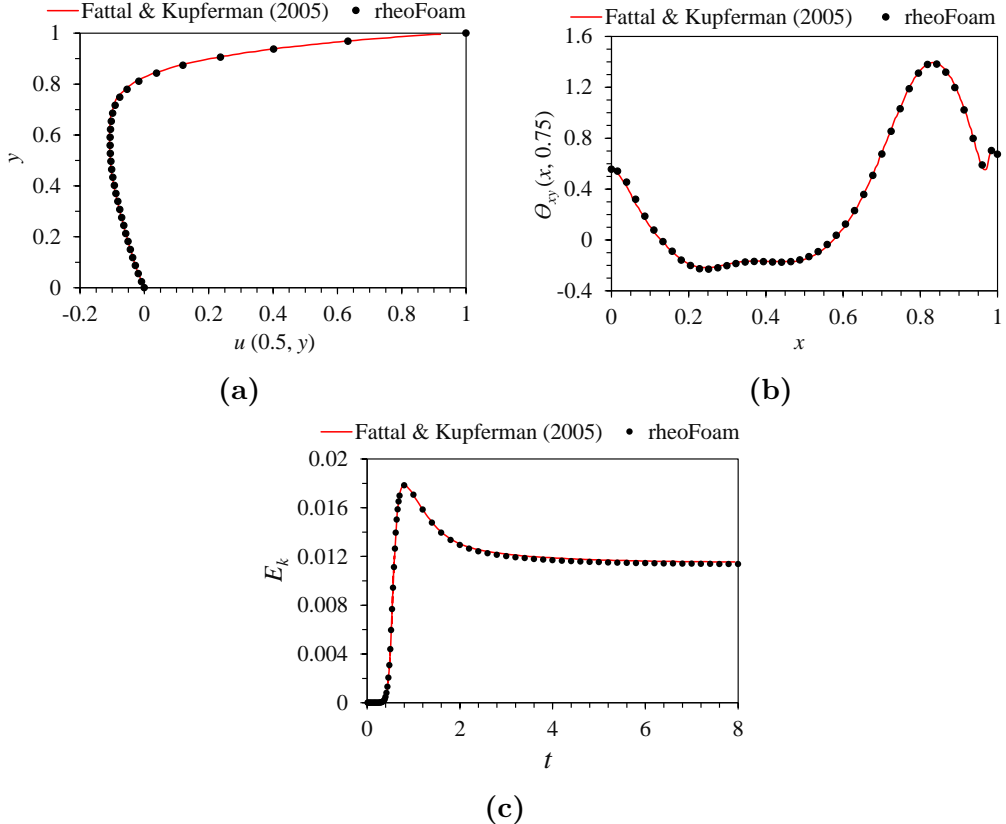


Figure 5.4: (a) Velocity profile along line $x = 0.5$ (at $t = 8$), (b) Θ_{xy} profile along line $y = 0.5$ (at $t = 8$) and (c) evolution of the average "kinetic energy" over time. All the results are for $Re = 0.01$, $De = 1$ and $\beta = 0.5$.

❖ Boundary conditions

The boundary conditions used are described in Ref. [2]. It is worth mentioning that the time-varying inlet velocity is implemented as a *codedFixedValue* boundary condition in file 0/U. The function is implemented as

$$\mathbf{u}(t) = \begin{cases} \frac{1-\cos(\pi t)}{fac} \mathbf{dirN} & t \leq tlim \\ \mathbf{Uav} & t > tlim \end{cases} \quad (5.3)$$

where **Uav** and **dirN** are vectors, and *fac* and *tlim* are scalar parameters. For **Uav** = (0.25, 0, 0), **dirN** = (1, 0, 0), *fac* = 8 and *tlim* = 1, this generates an inlet velocity profile aligned with the x -axis and whose magnitude increases from 0, at $t = 0$, to 0.25, at $t = 1$.

❖ Command-line

1–Build the mesh:

```
~$ blockMesh
```

2–Run the solver:

```
~$ rheoFoam
```

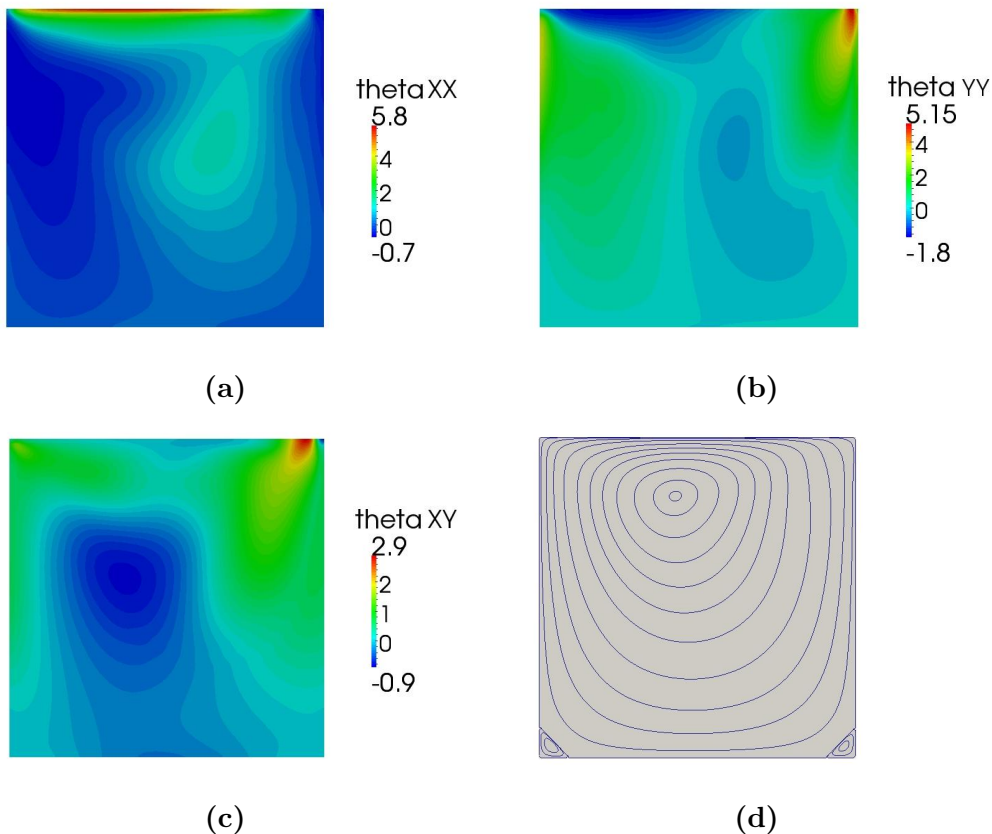


Figure 5.5: Contours of (a) Θ_{xx} , (b) Θ_{yy} and (c) Θ_{xy} . In (d), the streamlines are plotted. All the results are for $Re = 0.01$, $De = 1$, $\beta = 0.5$ and $t = 8$.

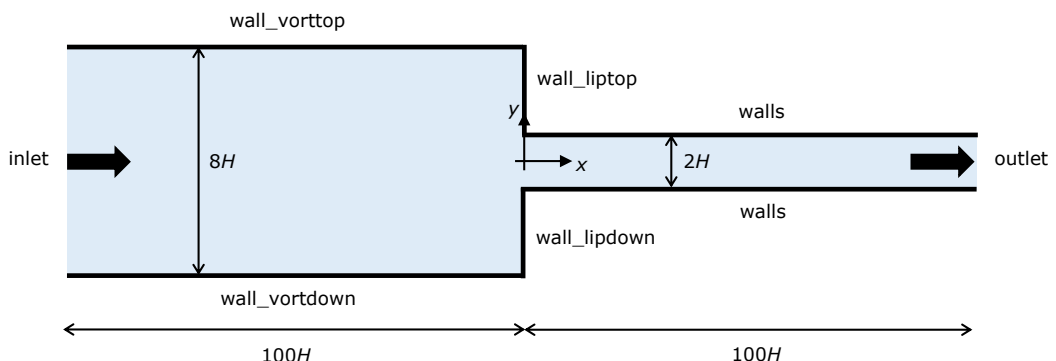


Figure 5.6: Geometry for the 4:1 planar contraction.

3-Extract \mathbf{u} and $\boldsymbol{\tau}$ at the cell centers immediately upstream and downstream of vertical line $x = 0$:

```
~$ sample
```

❖ Results

The results obtained with mesh M1 can be found in Ref. [2].

A *coded FunctionObject* returns the points where the wall-parallel velocity com-

ponent changes of sign (for both the walls near to the upper lip and corner vortices). Those points are delimiting the lip and corner vortices (if present). The user can easily add two extra *coded FunctionObjects* for the vortices in the lower-half of the contraction.

5.1.6 Case 4: flow around a confined cylinder

 `tutorials/rheoFoam/Cylinder/Oldroyd-BLog/`

❖ Overview

The planar flow past a confined cylinder is another traditional benchmark problem in computational rheology. Since this flow has no singular points and because extra-stresses can grow significantly in the wake of the cylinder, this problem is particularly well-suited to test the accuracy and stability of numerical methods. Furthermore, it is also a good problem to test the non-orthogonality handling by the algorithms, both in terms of accuracy and stability, since the grids used for this problem usually require some degree of non-orthogonality.

The Oldroyd-B model is used in this tutorial, since a reasonable amount of data is available in the literature for comparison purposes. The Reynolds number for this flow is defined as $Re = \frac{\rho UR}{\eta_0}$ and the Weissenberg number as $Wi = \frac{\lambda U}{R}$. In order to establish comparable conditions with Refs. [25, 26], the solvent viscosity ratio (β) is fixed at 0.59, the blockage ratio (diameter of cylinder/width of the channel) is 50 % and $Re = 0$ (the convective term in the momentum equation is removed). The case at $Wi = 0.7$ is simulated in this tutorial.

❖ Geometry & Mesh

The geometry used in this case is composed of a channel with a cylinder of radius R vertically centered between its walls – spaced apart $4R$ –, and placed at a distance of $20R$ from the inlet, Fig. 5.7. The length of the channel downstream of the cylinder is $60R$. The mesh for this geometry is composed of 8 blocks (upper-half), with a high cell-density near the wall of the cylinder. The minimum cell length in the radial direction of the cylinder is $0.0049R$, while in the tangential direction it is $0.0053R$.

❖ Boundary conditions

The flow is assumed to be 2D, being solved in the xy -plane. At the inlet, a uniform velocity profile with magnitude U is imposed, the polymeric extra-stresses are null and zero-gradient is assigned to pressure. Channel and cylinder walls are static (velocity is null, polymeric extra-stresses are linearly extrapolated to the walls and a zero-gradient is imposed for pressure). At the outlet, fully-developed conditions are assumed: zero-gradient for all variables, except pressure, which is fixed to a constant value, $p = 0$.

❖ Command-line

1–Create half of the mesh:

```
~$ blockMesh
```

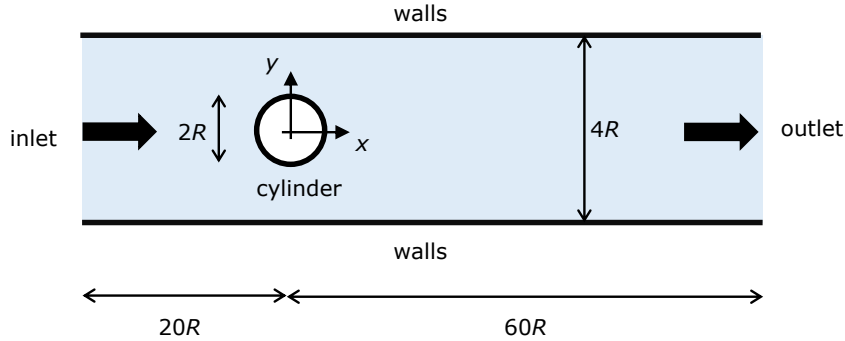


Figure 5.7: Cylinder vertically centered in a planar channel with 50 % blockage ratio.

2–Reflect the half-mesh using plane xz as mirror, to obtain the full mesh:

```
~$ mirrorMesh -noFunctionObjects
```

3–Run the solver:

```
~$ rheoFoam
```

➊ Results

Figure 5.8 presents the contour plots for the first normal stress difference and for the velocity magnitude (with superimposed streamlines), at $Re = 0$, $Wi = 0.7$ and $\beta = 0.59$, using the Oldroyd-B model with the log-conformation approach. Note that the velocity is normalized with U , time with R/U and polymeric extra-stresses with $\frac{\eta_0 U}{R}$. The drag coefficient obtained in such conditions is $C_d = 117.357$, which is in reasonable agreement with $C_d = 117.323$ [26] and $C_d = 117.315$ [25]. Refining the mesh would further increase the accuracy of the numerical solution. The drag coefficient was computed as

$$C_d = \frac{1}{\eta_0 U h} \int_S (p\mathbf{I} + \boldsymbol{\tau}') \cdot \hat{\mathbf{i}} \cdot d\mathbf{S} = \frac{1}{\eta_0 U h} \sum_{k=1}^{N_f} \mathbf{S}_f \cdot (p_f \mathbf{I} + \boldsymbol{\tau}'_f) \cdot \hat{\mathbf{i}}$$

where \mathbf{S}_f is a vector normal to each face of the cylinder boundary, whose magnitude is equal to the face's area, h is the depth of the cylinder in the neutral (empty) direction and $\hat{\mathbf{i}}$ is a unitary vector aligned with the streamwise direction. The drag coefficient is retrieved on run time by a *coded FunctionObject*, which can be found in `controlDict` dictionary.

It should be noted that, although the mesh displays some amount of non-orthogonality (run `checkMesh` to confirm it), the non-orthogonality corrector loop is not used (this is to say that only one iteration is performed) and the explicit pressure under-relaxation factor is kept relatively high (0.9). These features show the enhanced stability of the solver. However, to study for example the time evolution of the drag coefficient, the use of the non-orthogonality corrector loop,

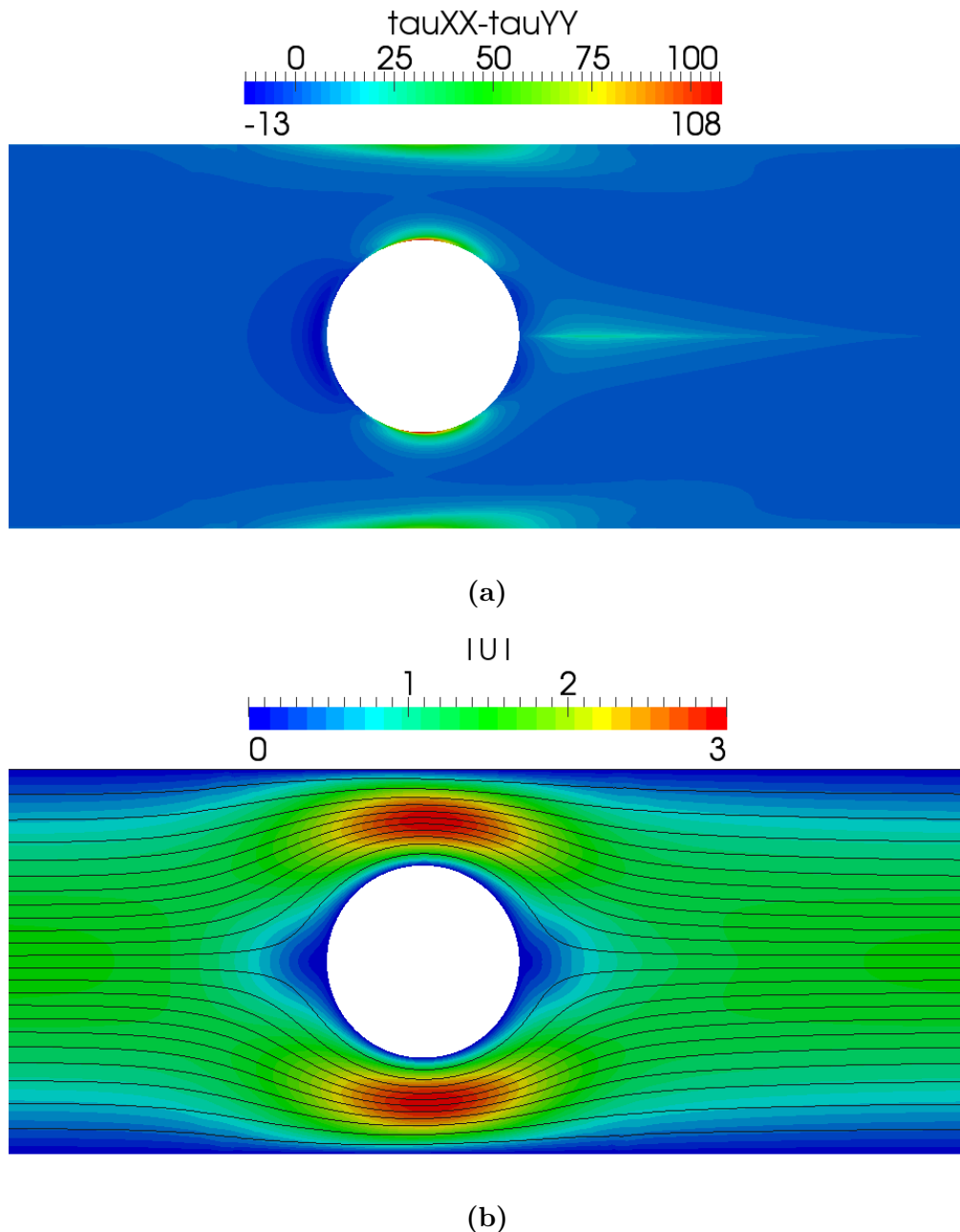


Figure 5.8: (a) First-normal stress difference and (b) velocity magnitude contours with superimposed streamlines, at $t = 15$, for $Wi = 0.7$, $Re = 0$ and $\beta = 0.59$.

combined with inner iterations, is suggested in order to increase the time accuracy (by decreasing the explicitness of the method). For a high-enough number of iterations in the non-orthogonal correction loop, under-relaxation of pressure may eventually be avoided.

5.1.7 Case 5: bifurcation in a 2D cross-slot flow

[tutorials/rheoFoam/CrossSlot/Oldroyd-BLog/](#)

❖ Overview

While the previous tutorials were based on traditional benchmark flow problems, the case selected for this tutorial is a recent benchmark: the 2D cross-slot flow [27]. For sufficiently high Deborah numbers, the flow in such geometry becomes asymmetric (steady or unsteady) [27]. At the stagnation point generated by the two opposite-flowing streams, fluid elements can remain for a virtually infinite amount of time. Because the local strain-rate is non-zero, the accumulated strain is high (theoretically infinite at the stagnation point), and this is especially problematic for models based on springs with an infinite extension – the tensile normal stress grows exponentially over time near that point. Thus, a singular point exists in this case, although not being located at a wall, as commonly seen in other geometries with singularities.

In directory `tutorials/rheoFoam/CrossSlot/`, there are four tutorials for this case, each one using a different model or solution method. The tutorial described here is the one solving the Oldroyd-B model with the log-conformation approach (`Oldroyd-BLog/`). The remaining cases are: `Oldroyd-BRootk/`, which solves the Oldroyd-B model using the root^k kernel, with $k = 8$; `Oldroyd-B-Sqrt/`, which solves the Oldroyd-B model using the square-root transformation approach; and `PTTlinearLog/`, which solves the linear PTT model with the log-conformation approach. All the tutorials with the Oldroyd-B model are for the same conditions: $De = 0.33$, $Re = 0$ and $\beta = 0$ (UCM fluid). The tutorial solving the linear PTT model is for $De = 0.6$, $Re = 0$, $\beta = 1/9$, $\varepsilon = 0.02$ and $\zeta = 0$ (simplified PTT). This group of tutorials also solves the transport equation of a passive scalar, exemplifying how this extra-feature can be used.

The dimensionless numbers for this problem are defined as: $Re = \frac{\rho UW}{\eta_0}$, $Wi = \frac{\lambda U}{W}$, $\beta = \frac{\eta_s}{\eta_0}$ and $Pe = \frac{WU}{D}$. The Péclet number (Pe) is only relevant for the scalar transport equation and D is the diffusion coefficient of the passive tracer. We set $Pe = 500$ in all the cases (representative, for example, of rhodamine-B in water flowing in a 200 μm wide channel, at 1 mm/s).

❖ Geometry & Mesh

The cross-slot geometry for this tutorial is depicted in Fig. 5.9. It consists of four identical arms (width W ; length $10W$), where the two vertically opposite arms are inlets and the remaining are outlets. Each arm is meshed as a single block with 60 cells in the streamwise direction (cells are compressed near the origin) and 51 cells uniformly distributed in the transverse direction. As a consequence, the central square block, $(x, y) \in [-0.5W, 0.5W]$, has 51x51 uniformly spaced cells. The use of an odd number of cells in both directions of the central square generates a cell exactly centered at the stagnation point, which is advantageous for the post-processing of quantities of interest at this location.

❖ Boundary conditions

The flow is assumed to be 2D, being solved in the xy -plane. At both inlets, a uniform velocity profile is specified, with magnitude U and pointing to the origin, so that those two streams are flowing in opposite directions. The polymeric extra-stresses are null and for pressure a zero-gradient is used. The walls are stationary,

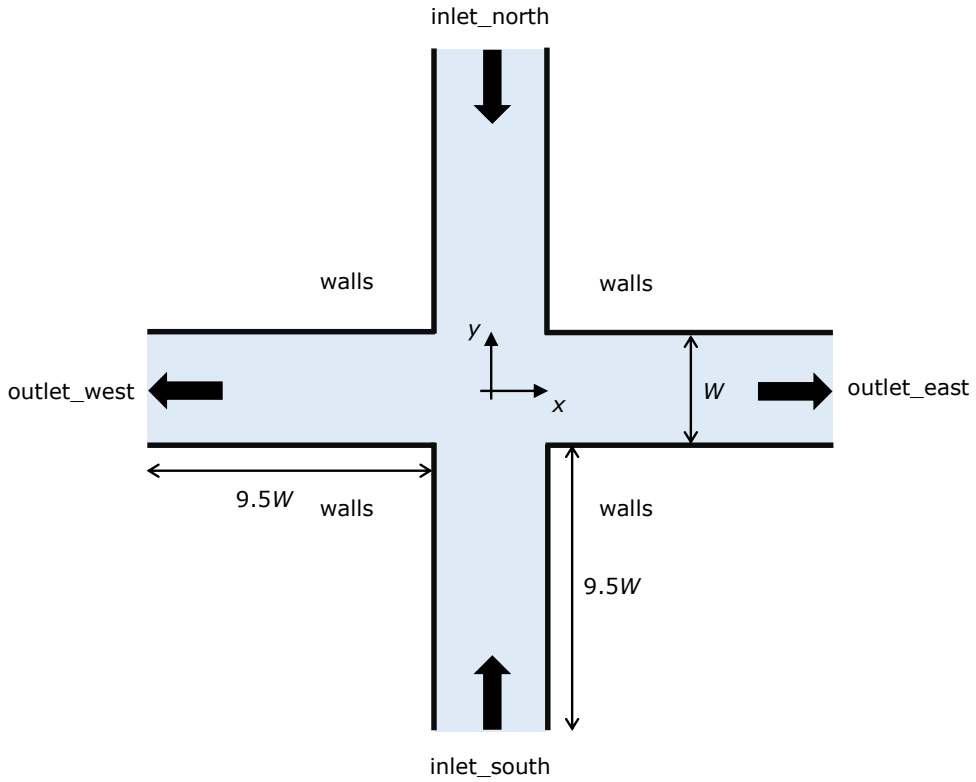


Figure 5.9: Cross-slot geometry composed of 4 arms with two balanced inlets and two outlets.

thus velocity is null, polymeric extra-stresses are linearly extrapolated and the pressure is assumed to not change in the normal direction. Fully-developed flow conditions are assigned at the outlets: null normal gradient for all variables, except pressure, which is fixed at $p = 0$.

A passive scalar (tracer field C) is added to the problem, which requires the assignment of initial and boundary conditions. We impose a continuous injection of C at *inlet_north* ($C = 1$), while no tracer is injected at *inlet_south* ($C = 0$). In the remaining boundaries, we impose null normal gradient (meaning no flux of C across the walls and fully-developed flow conditions at both outlets). At time $t = 0$, when the simulation is started, the y -positive portion of the cross-slot is filled with the tracer ($C = 1, y > 0 \wedge t = 0$).

❖ Command-line

1–Build the mesh:

```
~$ blockMesh
```

2–Create field C by copying one already present, which is not initialized in the interior domain:

```
~$ cp 0/C.org 0/C
```

3–Initialize field C in the interior domain ($C = 1, y > 0 \wedge t = 0$):

```
~$ setFields
```

4–Run the solver:

```
~$ rheoFoam
```

❖ Results

The contours for some important variables are displayed in Fig. 5.10, for $Re = 0$, $Wi = 0.33$, $\beta = 0$ (UCM model) and $Pe = 500$. The variables are normalized with U (velocity), W/U (time) and $\frac{\eta_0 U}{W}$ (stresses).

The local Weissenberg number at the origin, defined in Ref. [27] as the product of the relaxation time by the velocity gradient magnitude at the stagnation point streamlines, is $Wi_0 = 0.523$, which is close to the benchmark value obtained in a similar mesh, $Wi_0 = 0.509$ (Ref. [27], for mesh M1). The local Weissenberg number at the origin is retrieved by the solver to the case directory, through a *coded FunctionObject* that can be found in dictionary `controlDict`.

The importance of stress-velocity coupling in this case can be evaluated by re-running the tutorial with either BSD only or no stabilization method (*stabilization = none* or *BSD*, in dictionary `constitutiveProperties`).

Checkerboard fields easily develop in such conditions (this is a critical case due to the use of a UCM fluid).

Note that this tutorial makes use of a variable time-step, controlled by a maximum Courant number fixed at 0.4. This strategy is used because only steady-state results are of interest. This is also the reason to use a high tolerance in the sparse matrix solvers, in `fvSolution` dictionary – the steady asymmetry in the flow develops faster with these conditions, since the transient numerical error is higher.

5.1.8 Case 6: blood flow simulation in a real-model aneurysm

 `tutorials/rheoFoam/Aneurysm/HerschelBulkley/`

❖ Overview

The tutorial presented in this Section addresses the simulation of blood flow in a real-model aneurysm. Contrarily to the previous tutorials, this case is based on a 3D polyhedral (non-orthogonal) mesh and uses a GNF model. Furthermore, the flow is simulated for a moderate Reynolds number, which will test the robustness of the solver for such conditions, where inertia already plays an important role.

The Herschel-Bulkley model was selected to simulate the blood rheology, following Ref. [28]. The generalized Reynolds number for this model, assuming $\tau_0 = 0$ – the power-law limit –, is [28]:

$$Re_{GN} = \frac{\rho(2R_{in1})^n \bar{U}^{2-n}}{k \left(\frac{3n+1}{4n}\right)^n 8^{n-1}}$$

This tutorial simulates the flow at $Re_{GN} = 420$.

❖ Geometry & Mesh

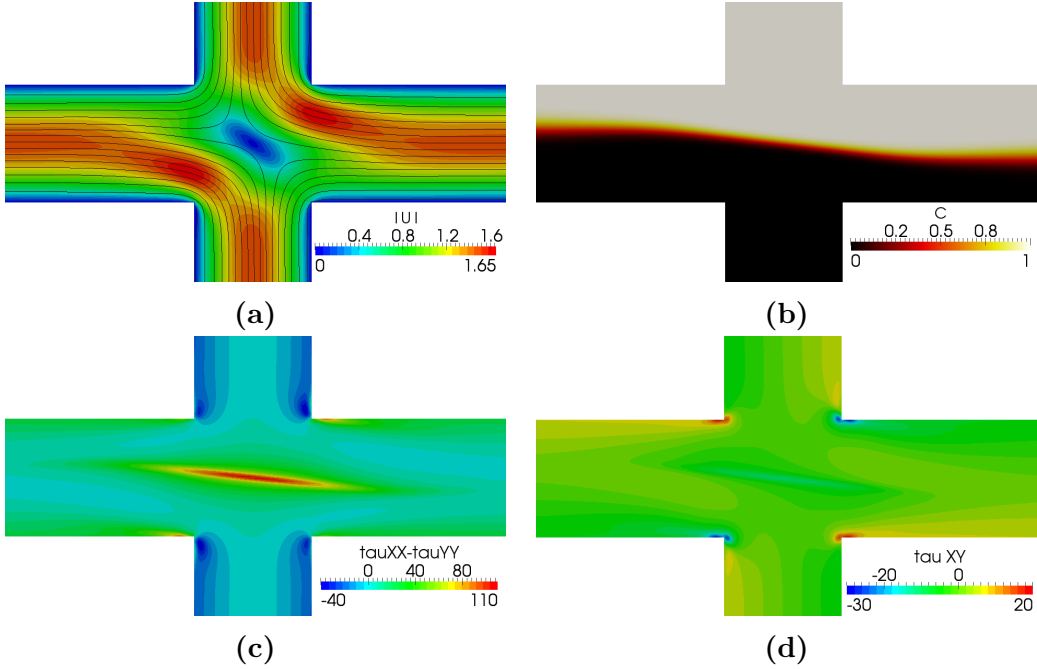


Figure 5.10: (a) Velocity magnitude contours with superimposed streamlines, (b) contours of C , (c) first-normal stress difference and (d) τ_{xy} contours, for $Re = 0$, $Wi = 0.33$, $\beta = 0$ and $Pe = 500$.

The STL file of the aneurysm surface was downloaded from a repository with real-model aneurysms [29], extracted from 3D rotational angiographies of diseased patients. From the list of available models, case ID *C0005* was selected, which refers to an aneurysm in the internal carotid artery (ICA).

The surface is composed of one main entry vessel (*in1*, the ICA), which bifurcates into two smaller vessels (*out1* and *out2*), Fig. 5.11a. The aneurysm is located near the bifurcation point. Due to the long extension of vessels upstream and downstream of the aneurysm in the original STL file, all the vessels were shortened and a cylindrical extension was connected to each one, in order to minimize entry/exit effects in the region near the aneurysm. The locations where those connections were established are highlighted in Fig. 5.11a using red arrows. The transition length between the tube connectors and the vessels is typically 10 % of the vessel radius and the radius of those tubes is equal to the equivalent radius of the vessels at the connection point. The radius of each inlet/outlet is: $R_{in1} = 1.66$ mm, $R_{out1} = 1.17$ mm and $R_{out2} = 0.95$ mm.

The mesh was built using ¹*cfMesh*, a meshing tool available in foam-extend since version 3.2. The maximum cell size was limited to 5 mm and boundary cell layers were generated near to the vessel walls in order to accurately solve the gradients developed there, Fig. 5.11b. The mesh provided with this tutorial has around 280 kcells.

❖ Boundary conditions

The boundary conditions and fluid properties used in this tutorial are based in

¹<http://cfmesh.com/>

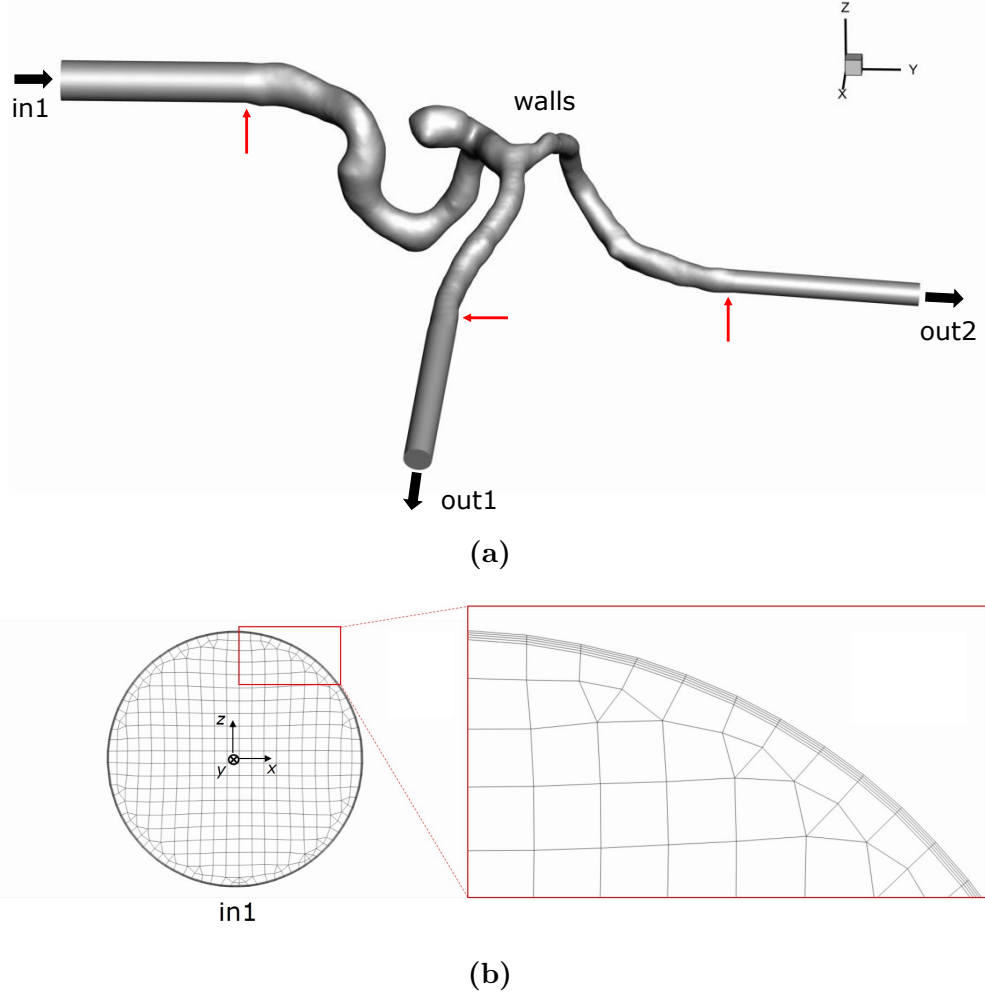


Figure 5.11: (a) Geometry of the aneurysm considered in the tutorial. Red arrows point to the transition regions between the aneurysm and the cylindrical extensions. The radius of each inlet/outlet is: $R_{\text{in}1} = 1.66 \text{ mm}$, $R_{\text{out}1} = 1.17 \text{ mm}$ and $R_{\text{out}2} = 0.95 \text{ mm}$. (b) Detailed view of the mesh on patch $\text{in}1$, zooming the cell layers near the wall. The reference axis for the geometry is centered on patch $\text{in}1$, with the normal vector of the patch pointing in the negative direction of the y -axis.

Ref. [28], where also ICA aneurysms were studied. Accordingly, blood is modeled with a Herschel-Bulkley model, with $\tau_0 = 0.0175 \text{ Pa}$, $k = 8.9721 \times 10^{-3} \text{ Pa.s}^n$, $n = 0.8601$ and $\eta_0 = 0.15 \text{ Pa.s}$. Note that η_0 (see Table 4.1) is a parameter characteristic of the model implementation in *rheoTool*, which limits the viscosity for low strain-rate values – otherwise it would generate infinite values at points with zero shear-rate. A relatively high value was attributed to η_0 in order to not affect the results. Furthermore, a density of 1050 kg/m^3 is considered.

For this fluid model, a fully-developed velocity profile is imposed at the inlet ($\text{in}1$), along with a null pressure gradient. For small τ_0 , we can use (approximately)

the fully-developed velocity profile for a power-law fluid:

$$U = \bar{U} \frac{3n+1}{n+1} \left[1 - \left(\frac{r}{R} \right)^{\frac{n+1}{n}} \right] \quad (5.4)$$

where \bar{U} is the mean velocity. In our case, \bar{U} is constant over time, thus steady conditions are simulated, instead of the cardiac cycle (this is to shorten the simulation time, since transient solutions would require a lower time-step, leading to a higher computational time). Regarding the walls, a no-slip boundary condition is imposed. At the outlets, the pressure is fixed to zero and the velocity is assumed to be fully-developed (zero gradient for velocity). Since the Reynolds number used in the tutorial is well below the critical value for transition to the turbulent regime, no special conditions need to be defined regarding turbulence modeling.

⌚ Command-line

The mesh is already built and can be found in folder `polyMesh/`.

1–Decompose the case among 2 processors to speed-up the computations (with 2 processors, it takes around 1h to reach convergence in a laptop with an Intel i5-3210M processor, 2.5 GHz):

```
~$ decomposePar
```

2–Run the solver in parallel, using 2 processors:

```
~$ mpirun -np 2 rheoFoam -parallel
```

3–Reconstruct the last time-step of the case for post-processing:

```
~$ reconstructPar -latestTime
```

⌚ Results

The results obtained at $Re_{GN} = 420$ are displayed in Fig. 5.12, where both the streamlines and the wall shear-stress magnitude ($WSSmag$) contours are shown. The wall shear-stress magnitude is computed through a `ppUtil` (described in Section 4.5.2), whose settings can be found in dictionary `fvSolution`, under subDict `PostProcessing`.

This tutorial is defined to run with an adjustable time-step, controlled by a maximum Courant number fixed at 50. The high Courant number is to quickly achieve the steady-state, without the need to cancel the time-derivatives. The non-orthogonality corrector loop was turned on, with 1 iteration *per* time-step (the pressure is also under-relaxed with a factor of 0.9), in order to avoid possible numerical issues due to non-orthogonality. The convergence can be monitored by a probe located at one of the exit vessels, downstream of the aneurysm.

5.2 *rheoTestFoam*

5.2.1 General guidelines

In Section 4.3.2, *rheoTestFoam* was presented as a testing application for the constitutive models implemented in *rheoTool*, being not a general-purpose solver. For

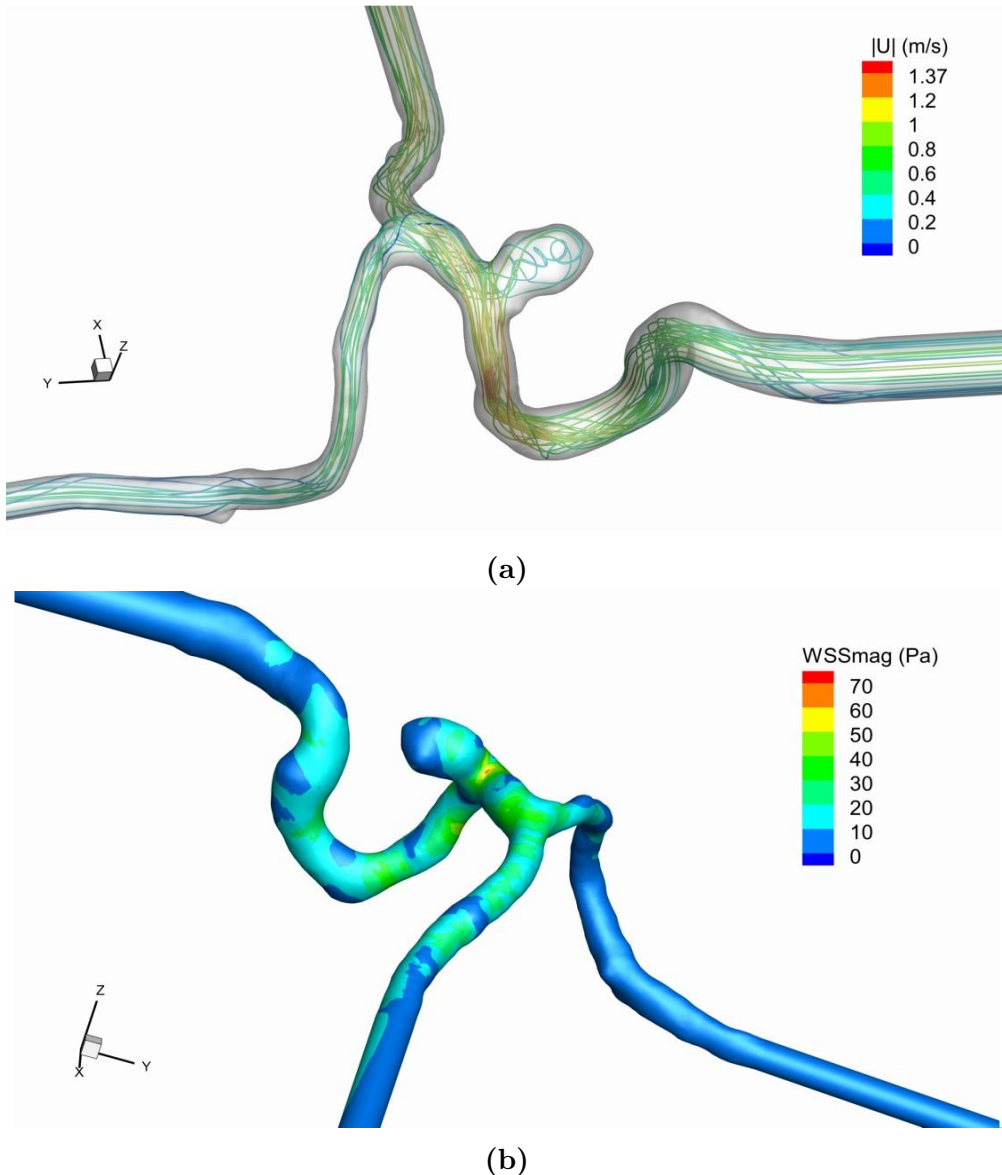


Figure 5.12: (a) Streamlines (colored with the velocity magnitude) and (b) wall shear-stress magnitude contours, at steady-state and for $Re_{GN} = 420$.

this reason, some of the steps usually required to setup a generic simulation in OpenFOAM® are not necessary with *rheoTestFoam*, while, on the other hand, extra-inputs need to be specified.

constant/

One main difference of *rheoTestFoam* cases regarding, for example, *rheoFoam* cases is in the mesh: the user should always use the same single-cell unitary mesh when working with *rheoTestFoam*. Thus, changing the mesh from case to case is unnecessary and not recommended.

The dictionary `constitutiveProperties` is composed of two subDict: `parameters` and `rheoTestFoamParameters`, as displayed in Listing 5.2. The entries in `parameters` have exactly the same meaning as previously discussed for *rheoFoam*.

However, there are two entries which remain inactive in *rheoTestFoam*: *rho* and *stabilization*. Remember from Section 4.3.2 that *rheoTestFoam* is only solving the constitutive equations for a given $\nabla\mathbf{u}$ tensor, thus those two parameters related with the momentum equation are useless. Nevertheless, they should be present (with any assigned value) to avoid a run time error. *rheoTestFoamParameters* is a subDict specific of *rheoTestFoam*, in the same way as *passiveScalarProperties* is a particular subDict of *rheoFoam*. The keyword *ramp* stands for the operation mode (see Section 4.3.2): *ramp* (*true*) or transient (*false*). The other two entries define tensor $\nabla\mathbf{u}$, since we consider $\nabla\mathbf{u} = \text{gammaEpsilonDotL}[i] \cdot \text{gradU}$, where *i* is the index representing each entry of list *gammaEpsilonDotL*. If *ramp* = *false*, the mode is transient and only one entry is expected in *gammaEpsilonDotL* – the solver is testing the transient behavior of the constitutive model, for a (single) given $\nabla\mathbf{u}$. On the other hand, in ramp mode (*ramp* = *true*), *gammaEpsilonDotL* may have as many entries as defined by the user and steady-state variables will be returned by the solver for each entry. Any combination of components is admissible for *gradU*, although only some correspond to canonical rheometric flows. The one displayed in Listing 5.2 is for a pure-shear flow: $\mathbf{u} = (\dot{\gamma}y, 0, 0)$, where $\dot{\gamma}$ is the *gammaEpsilonDotL* value.

```

1 parameters
{
3     type          Oldroyd-B;
5     etaS          etaS [1 -1 -1 0 0 0 0] 1.;
7     etaP          etaP [1 -1 -1 0 0 0 0] 1.;
9 // Place-holder variables in rheoTestFoam
11    stabilization   none;
11    rho            rho [1 -3 0 0 0 0] 0.;
}
13
13 rheoTestFoamParameters
15 {
15     ramp           false;
17     gradU          (0. 0. 0.
19                           1. 0 0.
21                           0. 0. 0.);
23     gammaEpsilonDotL
23     (
25         1.
)
}

```

Listing 5.2: Example of a *constitutiveProperties* dictionary used with *rheoTestFoam*.



When using *rheoTestFoam*, the same fields as for *rheoFoam* should be present in folder 0/. However, any value can be assigned to their internal/boundary fields,

since the solver will internally manipulate those values (only for velocity) in order to fulfill the specified $\nabla \mathbf{u}$ (Fig. 4.2). **Shortly, both the mesh and folder 0/ provided in the tutorials can be readily applied to any fluid, without any change.**

system/

When running *rheoTestFoam* in ramp mode, the user does not have control on *deltaT* (time-step), nor on the *endTime*. The time step is automatically set based on the relaxation time and strain-rate values for viscoelastic fluids or is simply set to 1 s for GNF models (in this case, the value is not important since no equation is solved implicitly). The *endTime* in ramp mode is not important, since the stopping criteria is based on an hard-coded threshold for the residuals and for the number of iterations. On the other hand, in transient mode, both variables should be specified by the user in *controlDict*. Regarding the discretization schemes (*fvSchemes* dictionary), only time-derivatives and *grad(U)* are used by the solver. The discretization of *grad(U)* should be kept as *Gauss linear*, while any valid time-scheme can be selected (except steady-state), although in ramp mode this should not make any difference, since we are looking for steady-state solutions. In dictionary *fvSolution*, the matrix solvers required by the constitutive equations must be defined and the number of inner-iterations may also be controlled if running in transient mode. Note that since the mesh has only one cell, a good time accuracy can be achieved by selecting a small time-step, without compromising the CPU time (in general, simulations will be always fast). The use of under-relaxation is not needed, as long as time-derivatives are not disabled in *fvSchemes* (this is our recommendation).

5.2.2 Case I: Herschel-Bulkley model

tutorials/rheoTestFoam/HerschelBulkley/

Overview

This tutorial illustrates the behavior of the Herschel-Bulkley model used in tutorial *Case 6* to model the blood rheology (Section 5.1.8). A steady shear flow is considered for this purpose.

Geometry & Mesh

The geometry used with *rheoTestFoam* is always the same (see Sections 5.2.1 and 4.3.2). The mesh is already built (do not change it).

Boundary conditions

The boundary conditions to be used with *rheoTestFoam* are always the same (see Sections 5.2.1 and 4.3.2). Folder 0/ should not be changed.

Command-line

1–Run the solver:

```
~$ rheoTestFoam
```

The file *Report* is created in the case directory, which contains the results.

❖ Results

For a GNF model, only the ramp mode of *rheoTestFoam* makes sense to be used, since thixotropy is not considered in any of the GNF models implemented. A steady shear flow is used, thus $\frac{\partial u}{\partial y}$ is the only non-zero component of tensor $\nabla \mathbf{u}$. For the range of shear-rates between 0.01 s^{-1} and 10000 s^{-1} , the Herschel-Bulkley model behavior is displayed in Fig. 5.13. The model predicts a shear-thinning behavior for $\dot{\gamma} > \dot{\gamma}_0$, where $\dot{\gamma}_0$ is the critical strain-rate at which $\eta = \eta_0$. For the parameters defined in this example, $\dot{\gamma}_0 = 0.13 \text{ s}^{-1}$.

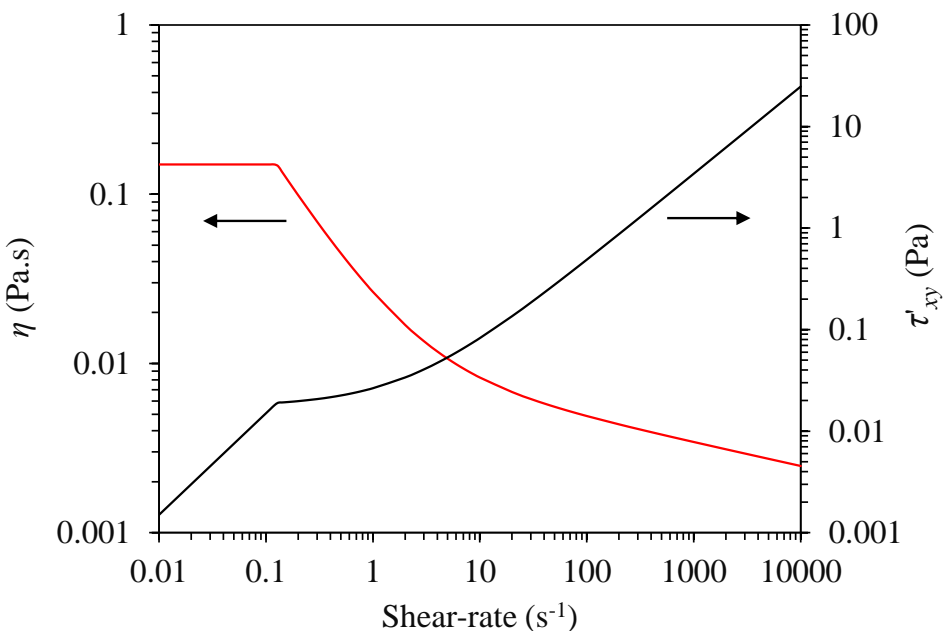


Figure 5.13: Shear viscosity and τ'_{xy} (the only non-zero component of the symmetric extra-stress tensor) as a function of the shear-rate, in a steady shear flow, for the Herschel-Bulkley model with parameters: $\tau_0 = 0.0175 \text{ Pa}$, $k = 8.9721 \times 10^{-3} \text{ Pa.s}^n$, $n = 0.8601$ and $\eta_0 = 0.15 \text{ Pa.s}$.

5.2.3 Case II: FENE-CR model

☞ [tutorials/rheoTestFoam/FENE-CR/](#)

❖ Overview

This tutorial exemplifies the use of *rheoTestFoam*, both in transient and ramp modes, with a constitutive equation for a viscoelastic fluid. The FENE-CR model is selected and its behavior will be assessed for uniaxial extensional flow.

The uniaxial extensional flow may be described by the following velocity gradient

$$\nabla \mathbf{u} = \dot{\varepsilon} \begin{bmatrix} 1 & 0 & 0 \\ 0 & -\frac{1}{2} & 0 \\ 0 & 0 & -\frac{1}{2} \end{bmatrix}$$

where $\dot{\varepsilon}$ is the extensional rate. The Weissenberg number, $Wi = \lambda\dot{\varepsilon}$, is the dimensionless group controlling the rate of stretch induced in the fluid and it was varied between 0.01 and 100, by increasing the extensional rate from 0.01 to 100 s^{-1} . The fluid properties used in the FENE-CR model are: $\eta_s = 0.1$ Pa.s, $\eta_p = 0.9$ Pa.s, $\lambda = 1$ s and different values of L^2 were tested (10, 100 and 1000). In such conditions, the extensional viscosity, defined as $\eta_E = \frac{\tau'_{xx} - \tau'_{yy}}{\dot{\varepsilon}}$, is given by [19]

$$\eta_E = 3\eta_s + \eta_p \left(\frac{2}{1 - 2\lambda\dot{\varepsilon}/f} + \frac{1}{1 + \lambda\dot{\varepsilon}/f} \right) \quad (5.5)$$

where f is the solution of the cubic equation

$$(L^2 - 3)f^3 - [(\lambda\dot{\varepsilon})(L^2 - 3) + L^2] f^2 - [2(\lambda\dot{\varepsilon})^2(L^2 - 3) - (\lambda\dot{\varepsilon})L^2 + 6(\lambda\dot{\varepsilon})^2] f + 2(\lambda\dot{\varepsilon})^2L^2 = 0 \quad (5.6)$$

❖ Geometry & Mesh

The geometry used with *rheoTestFoam* is always the same (see Sections 5.2.1 and 4.3.2). The mesh is already built (do not change it).

❖ Boundary conditions

The boundary conditions to be used with *rheoTestFoam* are always the same (see Sections 5.2.1 and 4.3.2). Folder 0/ should not be changed.

❖ Command-line

As it is, the tutorial will run in ramp mode.

1–Run the solver:

```
~$ rheoTestFoam
```

Take a look to file *Report* created in the case directory, which contains the results.

❖ Results

The results computed by *rheoTestFoam*, and displayed in Fig. 5.14a, show that the FENE-CR model is correctly implemented, since the difference to the analytical solution is negligible.

In addition to the "steady" results in Fig. 5.14a, also the transient evolution of the extensional viscosity (commonly denoted as η_E^+ in the literature) can be obtained with *rheoTestFoam*. For that purpose, simply switch the keyword *ramp* (in *constitutiveProperties*) from *true* to *false* and define the desired extensional rate as the first entry of list *gammaEpsilonDotL* (the remaining entries can be left, since they will not be read). The results obtained for $Wi = 2, 5$ and 10 are displayed in Fig. 5.14b.

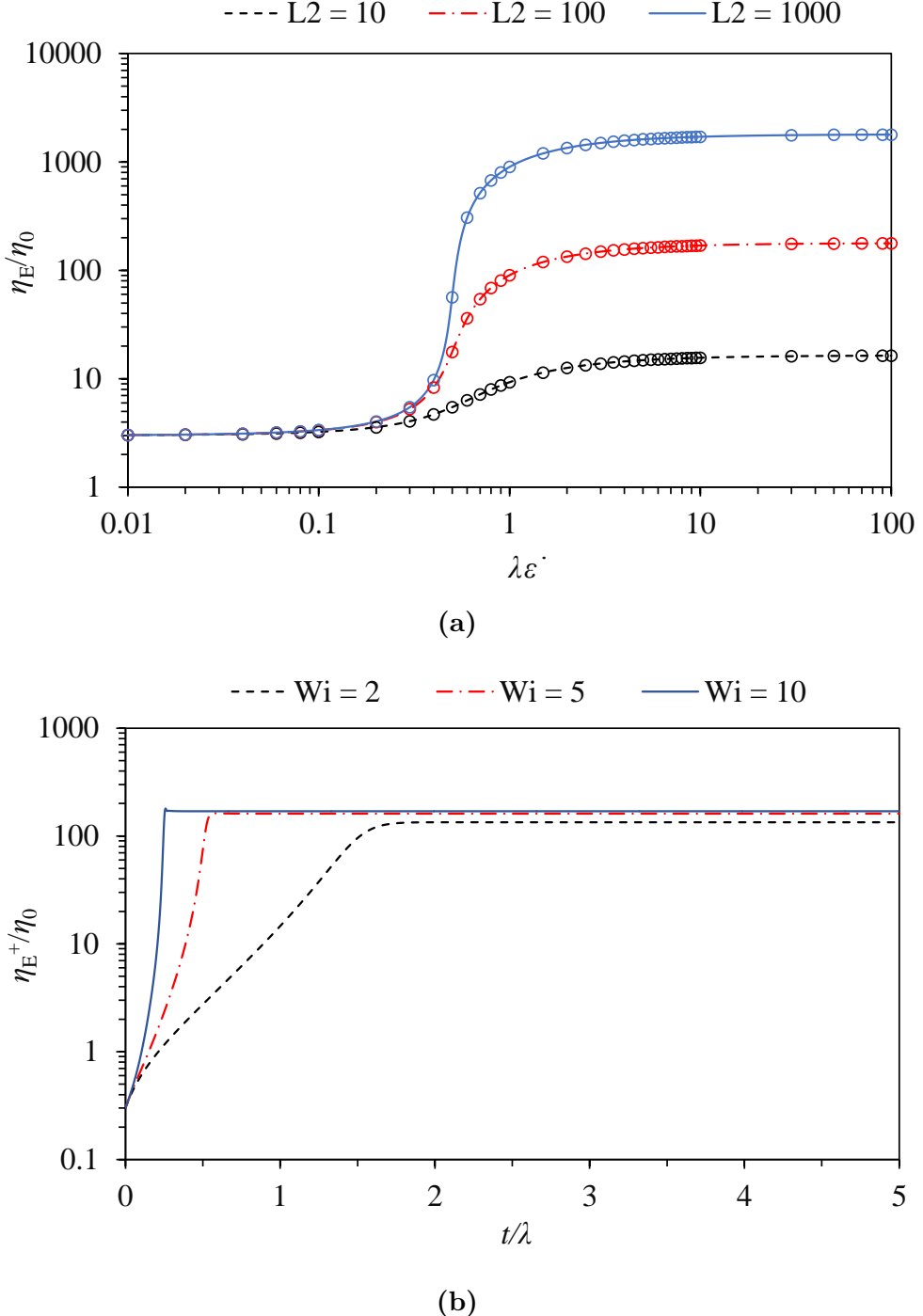


Figure 5.14: (a) Steady extensional viscosity (η_E) as a function of $Wi = \lambda\dot{\varepsilon}$, for different values of L^2 (points represent the numerical results of *rheoTestFoam* and the lines correspond to the analytical solution of Eq. 5.5); (b) transient extensional viscosity η_E^+ for different Wi , at fixed $L^2 = 100$. The remaining parameters of the FENE-CR model are $\eta_s = 0.1$ Pa.s and $\eta_p = 0.9$ Pa.s.

5.3 *rheoInterFoam*



Section 5.3 is under development.

5.3.1 General guidelines

Since most of the steps required to set up a case for *rheoInterFoam* are the same as for *rheoFoam*, only the major differences will be pointed out.

constant/

The dictionary `constitutiveProperties` should contain the same information as detailed for *rheoFoam* (Section 5.1.1), for each phase. The principle is the same as for the default two-phase solvers of OpenFOAM® (e.g. *interFoam*), where each phase owns a dictionary defining its physical properties. Importantly, `subDict passiveScalarProperties`, related with the transport of a passive scalar, is general for the two phases and should only be defined once, outside each phase. Finally, the surface tension between the two phases – parameter *sigma* – should also be present.

Note that when using default names *phase1* and *phase2* for each phase, without specifying the name of the phases in a *wordList*, then it is automatically assumed that the phases are labeled 1 and 2, respectively. Recent versions of OpenFOAM® have a slightly different behavior regarding phases labeling.

0/

In folder 0/, the internal and boundary field for the indicator (color) function used by the VOF method should be defined. The indicator has a value of 1 for one of the phases and 0 for the other phase. Ideally, and assuming that boundary conditions were correctly assigned, the indicator should remain bounded in this range. The name given to the file representing the indicator field should be consistent with the naming in dictionary `constitutiveProperties`. If the default names *phase1* and *phase2* were used, then the indicator function should be named *alpha1*. If other name was used instead, then the indicator would be named *alpha* suffixed with that name, without spaces in-between (recent versions of OpenFOAM® require a separation point). Although there are always two phases, only one indicator field should be defined, since the indicator for the other phase is computed from this one. In opposition to what is done in *rheoFoam*, the pressure field used by *rheoInterFoam* is not divided by the density, thus retaining its natural units (Pa.s).

Given that a constitutive equation is being defined and solved individually for each phase, variables *tau* and *theta* should be labeled (suffixed) with the respective phase name. Considering a viscoelastic model for each phase and default naming of phases, we would have *tau1*, *theta1* and *tau2*, *theta2*. If a multimode mode model is assigned to a given phase, then the name of each mode should also be appended.

system/

The main novelty comparing to *rheoFoam* is that when using *rheoInterFoam* the user has the possibility to choose between PIMPLE and SIMPLEC for pressure-velocity coupling. This is controlled in dictionary `fvSolution`, in subDict *PIMPLE*, where the keyword *SIMPLEC* can be assigned to *true* or *false*. Independently of the choice, the momentum equation is always solved. The variable *nCorrectors* works in its usual way (looping the pressure equation) and the variable *nInIter* assumes the same function as *nOuterCorrectors*. In a future release of *rheoInterFoam*, this workflow will most likely change. There are currently these two options because it is still not clear which one is more advantageous. Still in dictionary `fvSolution`, other keywords must be assigned in subDict *PIMPLE*, which are related with the VOF method and that the reader can found in the tutorials.

In dictionary `fvSchemes`, the discretization schemes for the two phases should be defined, as well as the discretization schemes related with the VOF method, which can also be found in the tutorials.

Besides the Courant number, the solvers using VOF, as *rheoInterFoam*, can also restrict the time-step based on an interface Courant number, which should be defined in dictionary `controlDict`.

The dictionary `setFields`, used to initialize parts of the domain with specified values, should also be present in folder `system/` whenever used.

5.3.2 Case 1: impacting drop

tutorials/rheoInterFoam/ImpactDrop/Oldroyd-BLog/

Overview

In this tutorial, a liquid drop composed of a viscoelastic fluid falls under gravity and its shape (the drop width, more precisely) is monitored before and after the drop impacts a rigid plate. Under such conditions, the drop width oscillates after the impact. This problem has been used in the literature as a benchmark case for viscoelastic two-phase flow solvers (e.g. [30, 31]).

The configuration adopted in the tutorial reproduces the conditions in Ref. [30], where an axisymmetric geometry has been used. The dimensionless numbers governing the flow are: $Fr = \frac{U_0}{\sqrt{gD}}$, $Re = \frac{\rho U_0 D}{\eta_0}$, $Wi = \frac{\lambda U_0}{D}$ and $\beta = \frac{\eta_s}{\eta_s + \eta_p}$, where U_0 is the initial velocity of the drop, g is the gravitational acceleration, D is the drop diameter, ρ is the fluid density, η_0 is the total viscosity (polymer plus solvent) and λ is the relaxation time (all these fluid properties are for the drop phase). The problem was simulated for $Fr = 2.26$, $Re = 5$, $Wi = 1$ and $\beta = 0.1$. Note that the surface tension is set to zero and we assign low (but finite) density and viscosity values to the fluid surrounding the drop.

Geometry & Mesh

The geometry is composed by a plate on its bottom, while the other patches simply act as open boundaries, representing the atmosphere. Axisymmetry is considered around the y -axis. All the dimensions are expressed as a function of the drop diameter, Fig. 5.15. The domain is big enough so that we can neglect the influence of the open boundaries location in the results.

The domain is meshed uniformly with 120 cells in both the radial and axial directions.

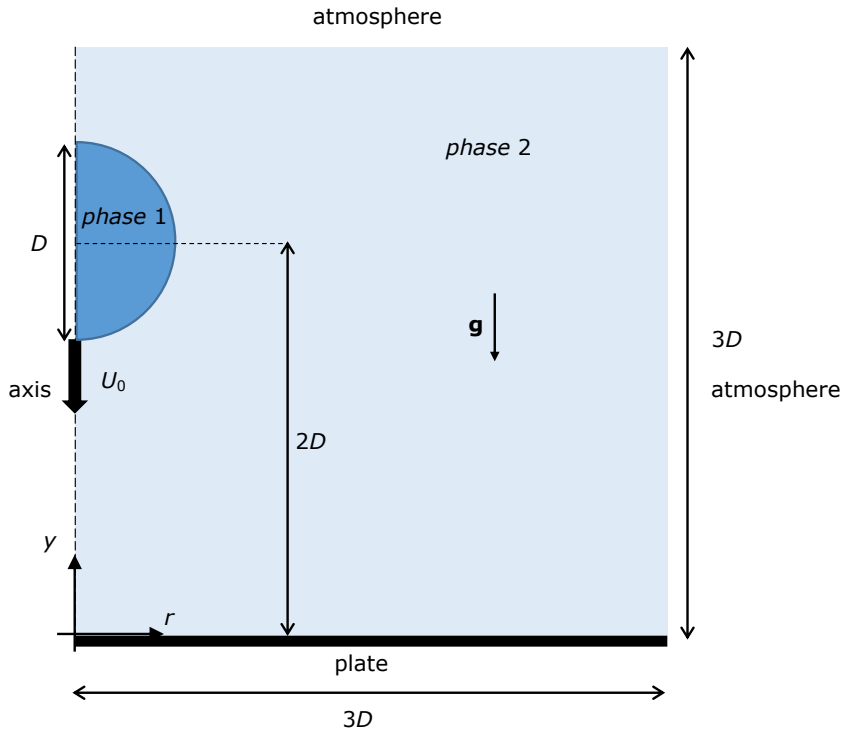


Figure 5.15: Geometry for the impacting drop problem.

❖ Boundary conditions

At the plate, no-slip boundary conditions are imposed with a null velocity, linearly extrapolated polymeric extra-stress components and zero normal gradient for the indicator field. We assign a *fixedFluxPressure* BC to the pressure, as discussed in Section 4.4.7, for multiphase flows. The patches representing the open boundaries (atmosphere) are assumed to not interfere with the dynamics of the drop, so that zero-gradient is assumed for all variables, except the pressure, which is fixed at $p = 0$.

Following Ref. [30], the drop has an initial velocity U_0 , in the vertical direction (pointing downwards), and its center of mass is at a distance $2D$ from the plate.

❖ Command-line

1–Build the mesh:

```
~$ blockMesh
```

2–Initialize the indicator and velocity fields in the drop region:

```
~$ cp 0/alpha1.org 0/alpha1
```

```
~$ cp 0/U.org 0/U
```

```
~$ setFields
```

3–Run the solver:

```
~$ rheoInterFoam
```

➊ Results

The evolution of the drop width over time is plotted in Fig. 5.16. The width is normalized with D (its initial diameter) and time with D/U_0 . The evolution of the drop width over time is written to a file by a *coded FunctionObject*.

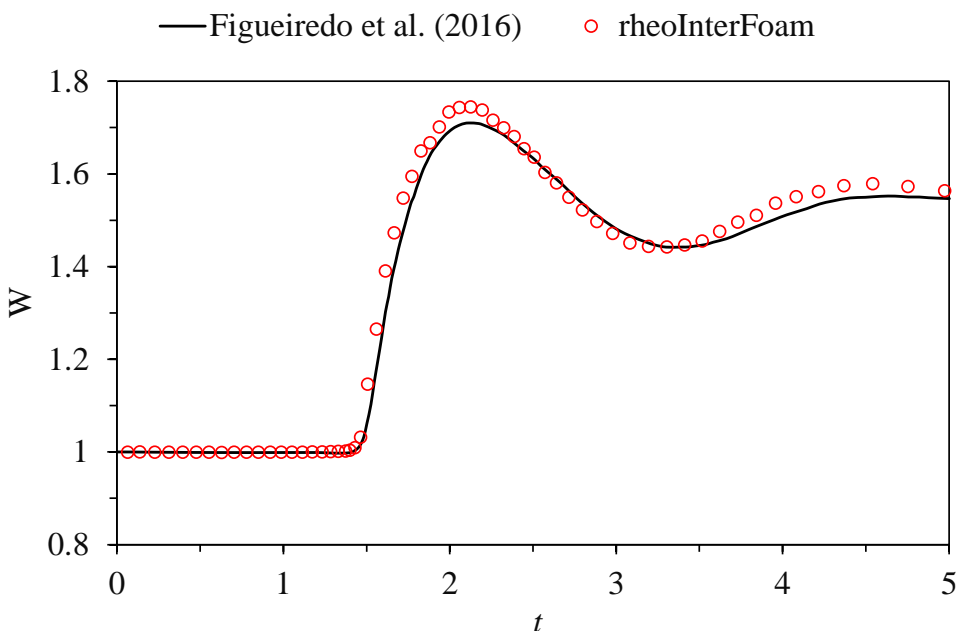


Figure 5.16: Evolution of the drop width over time for $Fr = 2.26$, $Re = 5$, $Wi = 1$ and $\beta = 0.1$. The profile obtained with *rheoInterFoam* is compared with the data of Figueiredo et al. [30].

5.3.3 Case 2: planar die swell

💻 `tutorials/rheoInterFoam/DieSwell/`

➊ Overview

A significant number of plastic objects that we use in our everyday life are produced by extrusion of molten polymers. In this process, the polymeric phase can swell significantly at the exit of the die due to the development of normal stresses. Predicting the amount of swell is important for the processing. Moreover, undesirable sharkskin defects in the extrudate surface can occur under certain conditions, and the ability to predict such conditions can potentially reduce industrial wastes.

This tutorial presents the swell of non-Newtonian fluids flowing through a planar rectangular die. The three cases provided reproduce the results obtained in Ref. [32] using *rheoTool*, for mesh M1 and three different fluids: Carreau-Yasuda

fluid with $n = 0.3$ (directory `CarreauYasuda/`); Oldroyd-B fluid with $\beta = \frac{1}{9}$ and $Wi = 2$ (directory `Oldroyd-BLog/`); Giesekus fluid with $\beta = \frac{1}{9}$, $\alpha = 0.5$ and $Wi = 4$ (directory `GiesekusLog/`). The viscoelastic fluid models are solved with the log-conformation approach. Note that both gravity and surface-tension effects are neglected in this tutorial. In addition, only the steady-state solution is of interest.

❖ Geometry & Mesh

The geometry for this case is displayed in Fig. 5.17. The mesh corresponds to mesh M1 of Ref. [32]. Note that this is a kind of stick-slip configuration, which represents a die with negligible wall thickness. Accordingly, patch `wallOut` overlaps part of the `wallIn` patch.

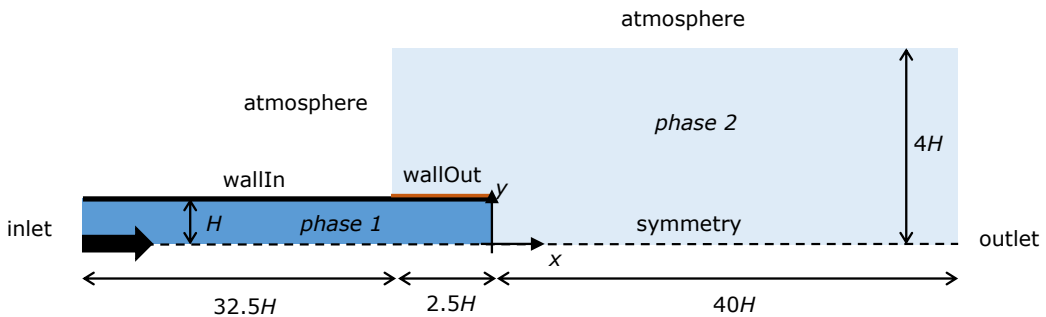


Figure 5.17: Geometry for the planar die swell tutorial.

❖ Boundary conditions

The boundary conditions used are described in Ref. [32]. In order to avoid the definition of an analytical solution at the `inlet`, a long entrance channel is used.

❖ Command-line

1–Build the mesh:

```
~$ blockMesh
```

2–Initialize the color function field:

```
~$ cp 0/alpha1.org 0/alpha1
```

```
~$ setFields
```

3–Run the solver:

```
~$ rheoInterFoam
```

❖ Results

The results obtained with mesh M1 can be found in Ref. [32]. The users of the foam-extend version (*fe40*) will notice an instability in the extrudate surface close to the die exit, which eventually vanishes with time. Such instability is not present in the OpenFOAM® versions.

Several methods can be used to compute the amount of swell far from the die exit. Assuming that the free-surface of the extrudate corresponds to $\alpha = 0.5$, for $\alpha \in [0, 1]$, this isoline can be directly extracted with Paraview. Another option is to extract the profile of the color function (α) over a vertical line far from the die exit, using the *sample* utility of OpenFOAM®. Then, the value $\alpha = 0.5$ can be simply interpolated from the nearest values. A more complex, still more versatile option is to code a *ppUtil* function (Section 4.5.2) retrieving in run time the maximum free-surface position in a predefined region. This would also allow to check for convergence of the free-surface position. Slight differences can be found among the results from the different methods.

5.4 *rheoEFoam*

5.4.1 General guidelines

The first steps to set up a case for *rheoEFoam* are the same as for *rheoFoam* (Section 5.1.1). After that, the hydrodynamic component of the problem will be ready, and only the electric component will remain to be defined – this is the subject of this section.

constant/

The *electricProperties* dictionary should be added to folder *constant/*. It contains most of the information about the EDF model to be used, as shown in Listing 5.3, illustrating an example for the PNP model.

```

parameters
2 {
    type          NernstPlanck;
4
    T             T [ 0 0 0 1 0 0 0 ] 298;
6    relPerm       relPerm [ 0 0 0 0 0 0 0 ] 80.1;

8    psiContrib    true;
extraEField      extraEField [ 1 1 -3 0 0 -1 0 ] (5000 0
0);
10
    species
12 (
        cCation
14     {
            z           z [ 0 0 0 0 0 0 0 ] 1;
16     D           D [ 0 2 -1 0 0 0 0 ] 1e-9;
        }
18
        cAnion
20     {
```

```

22           z
22           D
22       }
24   );
}

```

Listing 5.3: Example of a `electricProperties` dictionary used with `rheoEFoam` – the settings displayed are for the PNP model.

The electric properties in dictionary `electricProperties` are defined inside a subDict named *parameters* (line 1, Listing 5.3). The EDF model is selected through keyword *type*, where the *TypeName* of any model in Table 4.2 can be used (the user may type any random word to get the list of all available EDF models). Apart from the *type* keyword, all the remaining entries are model-specific. In the case of the PNP model in Listing 5.3, *T* is the absolute temperature and *relPerm* corresponds to the relative permittivity (dielectric constant) of the electrolyte, ϵ_R , such that $\epsilon = \epsilon_R \epsilon_0$, where ϵ_0 is the vacuum permittivity. In line 8, the entry *psiContrib* set to *true* indicates that variable *psi* (either Ψ or ψ) should contribute to the electric field used in the definition of the electric body-force. The default behavior, i.e., if the entry is not defined, is *psiContrib* = *true*. The next line (line 9) is also optional and allows the user to define an additional uniform electric field, *extraEField* (units are in SI, as always). This electric field will **only** enter in the computation of the electric body-force in the momentum equation ($\mathbf{f}_E = \rho_E(\mathbf{E} + \text{extraEField})$; **extraEField** corresponds to vector \mathbf{E}_a in Table 4.2). Then, from line 11 to 24 each specie of the electrolyte is defined. In the example, only two species are modeled: *cCation* and *cAnion*, each having its own charge valence (*z*) and diffusivity (*D*). Note that the charge valence is a signed integer: positive for cations and negative for anions. The user can add as many species as desired to the list, for the model under analysis. The name given to each specie is user-defined, but consistence must be kept when further defining the respective fields, as explained next.

The example in Listing 5.3 should not be generalized to all the EDF models, as stated before. The best way for the user to know how the `electricProperties` dictionary should look like for a given EDF model is to analyze a tutorial provided for that model (at least one tutorial is provided for each model).

0 /

In addition to the fields related with the hydrodynamics (pressure, velocity and eventually extra-stress), when using `rheoEFoam` for EDFs, the fields specific to the given EDF model should be specified in folder 0 / (or the equivalent starting time folder when different from 0).

For the PNP model illustrated in Listing 5.3, we need to define 3 or 4 fields, depending if we use one single electric potential or two, respectively. In the first case, the fields would be *psi* (in this guide represented by Ψ), *cCation* and *cAnion* (in this guide represented by c_i). In the second case, field *psi* would be replaced by *psi* (in this guide represented by ψ) and *phiE* (in this guide represented by ϕ_{Ext}). Note that although having the same name in both cases, field *psi* has different meanings for each one: it is either the total, unique electric potential (Ψ),

or the intrinsic electric potential (ψ) – in practice, the Poisson equation to be solved is different in each case. The selection between both cases is made through variable `phiE`: when present, `psi` is considered the intrinsic electric potential, ψ . It is important to highlight that the fields representing the concentration of each specie (in mol/m³) should keep the name defined in dictionary `electricProperties`, in a one-to-one correspondence for each specie. These names are user-defined, in opposition to the names for the electric potential variables, which are fixed: `psi` and `phiE`.

The PNP model is the only to require the definition of fields for the concentration of each ionic specie. The other EDF models only require the electric potential (one or two variables, depending on the model and on the user's choice) to be defined. The exception is the Ohmic model, which also requires a field for the conductivity (`sigma`, in this guide represented by σ). Still for this model, only one electric potential variable may exist and its name should be `phiE`. In case of doubt, checking the tutorials is always a good starting point.

system/

Since additional equations are solved for EDFs (comparing to pressure-driven flows), the discretization schemes for the terms entering these equations need to be defined, as well as the sparse matrix solvers and respective settings.

The discretization schemes are defined in dictionary `fvSchemes`. The new entries to add to the dictionary are model-dependent and can be found in the tutorials. If the discretization scheme for any term is missing, an error will be retrieved complaining for it.

Regarding dictionary `fvSolution`, keep in mind when defining the matrix solvers for the new fields that Poisson-type equations require, in general, a symmetric matrix solver, while generic transport equations (including advection) are usually handled with an asymmetric matrix solver. Regarding under-relaxation, our recommendations are the same as the ones expressed for `rheoFoam`: by default, do not use under-relaxation, except, eventually for pressure in non-orthogonal grids, if needed. Note that the Nernst-Planck equations for each specie in the PNP model are collectively solved under the name `ci`, instead of the name given to the specie (this should be taken into account when defining the matrix solver and the under-relaxation factors).

Still in dictionary `fvSolution`, a new subDict needs to be defined for EDFs, named `electricControls`, Listing 5.4. In the code sample analyzed in Section 4.2.4, we have seen that each equation of a given EDF model is solved inside a *while* loop, controlled by a maximum allowable number of iterations and the initial residual of the equation being solved (the loop is exited when the first of the two criteria is met). These loops are intended to converge explicit terms inside each equation, since this can be critical for some EDFs. Thus, the controlling parameters of these cycles – the maximum number of iterations and the threshold residual – are defined in subDict `electricControls`. This needs to be done for each equation, or default values are assumed otherwise (`maxIter: 50; residuals: 10-7`). For non-stiff problems and when the mesh non-orthogonality is kept low, 1 iteration can be enough. When the PNP model is used, the number of electrokinetic coupling iterations (see Section 4.2.3) can also be defined in this subDict, as shown in line 3

of Listing 5.4 (if not defined, $nIterPNP = 2$ is assumed by default). As mentioned in Section 4.2.3, we recommend a minimum of 2 electrokinetic coupling iterations for any generic case using this model.

```

1 electricControls
{
3   nIterPNP          2;
5   phiEEqn
{
7     residuals 1e-7;
8     maxIter    1;
9   }

11  psiEqn
{
13    residuals 1e-7;
14    maxIter    1;
15  }

17  ciEqn
{
19    residuals 1e-7;
20    maxIter    1;
21  }
}
```

Listing 5.4: Example of an *electricControls* subDict in dictionary fvSolution – the settings displayed are for the PNP model.

5.4.2 Case I: EDF of power-law and PTT fluids in a microchannel

Our first tutorial for *rheoEFoam* is aimed to predict the velocity profile for a purely EDF of a power-law fluid (**Part A**) and for the mixed pressure-/electrically-driven flow of a linear PTT fluid (**Part B**) in a slit microchannel. The numerical profiles are compared with analytical solutions.

➊ Part A - Power-law fluid

⬇️ [tutorials/rheoEFoam/channelEDF/PowerLaw/PoissonBoltzmann](#)

⌚ Overview

The analytical solution for the EDF of a power-law fluid in a slit microchannel can be found in Ref. [33] for a generic flow behavior index (n) of the power-law model, under the Debye-Hückel approximation. For fully-developed flow conditions, the velocity profiles depend on n and on $\tilde{\kappa} = \kappa H = \frac{H}{\lambda_D} = \sqrt{\frac{2(zH)^2 e c_0 F}{\varepsilon k T}}$, where λ_D is the Debye length for a binary, symmetric electrolyte, as defined in Eq. (3.32), and H is the channel half-width. Although we will only present results for the PB model, we also provide the corresponding cases for the PNP and DH

models – as you will see, the results are indistinguishable between the models, for the conditions simulated.

❖ Geometry & Mesh

The geometry is a 2D (slit) microchannel with half-width H , Fig. 5.18. Due to the periodic boundary conditions assumed on the inlet/outlet, the mesh has one single cell in the x -direction and 300 non-uniformly distributed cells in the y -direction, normal to the applied electric field.

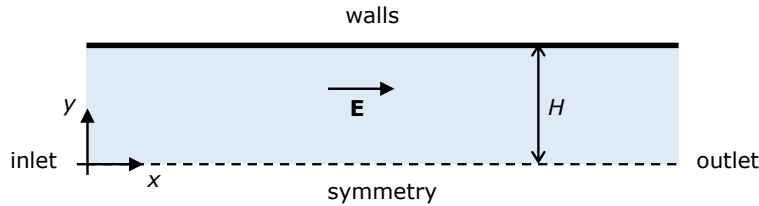


Figure 5.18: Planar channel geometry.

❖ Boundary conditions

The flow is 2D in the xy -plane. At both the inlet and outlet, periodicity is imposed. Thus, we assume from the beginning that this condition will retrieve the fully developed profiles for an infinitely long microchannel. A symmetry condition is imposed at $y = 0$. The walls are impermeable ($\mathbf{u} = \mathbf{0}$ and zero-gradient for pressure) and have a fixed intrinsic electric potential. Due to the simple geometry of the channel, the flow is generated by imposing a uniform electric field throughout the channel, parallel to the walls (\mathbf{E}). Therefore, there is no need to solve for the external electric potential variable (ϕ_{IE}): the electric field is directly imposed through the `extraField` entry of dictionary `electricProperties`. These boundary conditions hold for both the PB and DH models. In order to use the PNP model, a boundary condition must be defined at the wall for the ionic species. Since Boltzmann equilibrium holds and only the steady-solution is sought, the easiest way is to simply compute the ionic concentration from the potential distribution (check the `boltzmannEquilibrium` boundary condition described in Section 4.4.3). The flow is initially at rest and the intrinsic electric potential is zero.

❖ Command-line

1–Build the mesh:

```
~$ blockMesh
```

2–Run the solver:

```
~$ rheoEFoam
```

3–Extract the profile of \mathbf{u} along the vertical direction:

```
~$ sample -latestTime
```

❖ Results

The velocity profiles over the y -direction are depicted in Fig. 5.19 for varying $n = 0.25, 0.5, 0.75, 1$ and 1.5 , at fixed $\tilde{\kappa} = 15$. The velocity profiles are normalized by the velocity at the centerline of the channel, while the spatial coordinate is normalized by the channel half-width. The numerical results reproduce accurately the analytical solution [33] and show that shear-thinning fluids ($n < 1$) display an apparently compressed EDL, while the opposite is observed for shear-thickening fluids ($n > 1$).

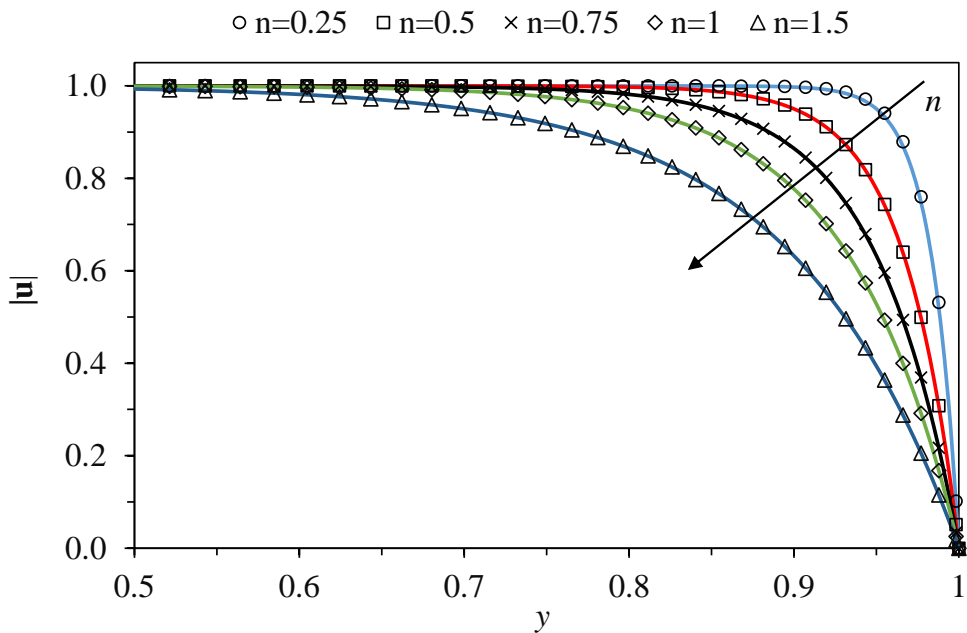


Figure 5.19: Velocity magnitude over the direction transverse to the applied electric field for a power-law fluid with different flow behavior index, at fixed $\tilde{\kappa} = 15$. The points represent numerical values, while the lines are the analytical solution [33]. Note that the x -scale has been truncated and only represents one-quarter of the channel width (this is to have a zoomed view near the wall).

As aforementioned, the same results would be obtained with the PNP and DH models and the user may confirm that from the cases provided. All the cases are prepared for $n = 0.75$ (this can be easily changed in dictionary `constitutiveProperties`) and will converge in the total time of simulation defined in `controlDict`. However, we should note that for low n , where $n = 0.25$ can be included, the simulation will take a much longer time to reach the steady-state, because of the low viscosity that develops near the wall, where the shear-rate attains very high values (it becomes even worse for higher $\tilde{\kappa}$). Furthermore, care should be taken in defining the upper and lower bounds for the viscosity (check the power-law model implementation in Table 4.1), since stringent bounds may influence the numerical solution.

⌚ Part B - linear PTT fluid

 `tutorials/rheoEFoam/channelEDF/PTTlinear/DebyeHuckel`

❖ Overview

Afonso et al. [34] derived an analytical expression for the mixed pressure-electrically-driven flow of simplified ($\zeta = 0$) linear PTT fluids in slit channels with an homogeneous zeta-potential at the walls, under the Debye-Hückel approximation. For creeping flow conditions ($Re = 0$), the velocity profiles depend on $\Gamma = -\frac{H^2}{\epsilon\psi_0} \frac{|\nabla p|}{|\mathbf{E}|}$ (ratio between pressure and electric forcing), $\tilde{\kappa} = \kappa H = \frac{H}{\lambda_D} = \sqrt{\frac{2(zH)^2 ec_0 F}{\varepsilon kT}}$ and $\sqrt{\varepsilon} De = \sqrt{\varepsilon} \lambda \kappa U$, where ε is the extensibility parameter of the PTT model, $U = -\frac{\epsilon\psi_0 |\mathbf{E}|}{\eta_0}$ is the Helmholtz-Smoluchowski velocity and ψ_0 is the zeta-potential at the wall. Both ∇p and \mathbf{E} only have a single non-zero component, in our case, the x -component. Note that in this tutorial we use exceptionally ϵ to represent the electric permittivity (instead of ε), in order to distinguish it from ε that we use to represent the extensibility parameter of the PTT model.

In this tutorial, we analyze the effect of varying Γ , while keeping the remaining dimensionless parameters fixed.

❖ Geometry & Mesh

The geometry is similar to the one used in **Part A** for the power-law fluid example. However, the physical dimensions are different and, importantly, we do not consider periodicity between the *inlet* and *outlet*. Instead, the flow is also solved in the x -direction. We note that this is not mandatory and that cyclic conditions would also provide the right solution. However, considering the full channel in the x -direction eases the definition of the pressure gradient, at the expense of having a higher number of cells in the mesh. Several options would allow to keep the cyclic patches and to impose directly the pressure gradient in the momentum equation, as the *fvOptions* tool, but we consider them less straightforward than our choice (at least for less experienced users).

❖ Boundary conditions

The boundary conditions are similar to the ones used in **Part A**, with some modifications required by the use of a viscoelastic model and due to the different conditions assigned to patches *inlet* and *outlet*. Since pressure gradients are allowed, we fix the pressure at the *outlet* and adjust the *inlet* pressure as required to get the desired Γ . Remember that in *rheoEFoam* field p represents the pressure divided by the density. A zero-gradient condition is imposed for the remaining variables at those two patches. Regarding the wall, the polymeric extra-stresses are linearly extrapolated.

❖ Command-line

1–Build the mesh:

```
~$ blockMesh
```

2–Run the solver:

```
~$ rheoEFoam
```

3—Extract the profile of \mathbf{u} along the vertical direction for the latest time (the x -position of the sampling line should not be important):

```
~$ sample -latestTime
```

❖ Results

Fig. 5.20 shows the velocity profiles under different forcing ratios. The velocity is normalized by the Helmholtz–Smoluchowski velocity (U , defined above), while the spatial coordinate is normalized by the channel half-width. Note that for a Newtonian case and $\Gamma = 0$ (pure EDF), the (normalized) velocity profile at the centerline would have a value very close to 1 (the higher $\tilde{\kappa}$, the closer it is) and we can see that this value is significantly higher for a linear PTT fluid due to shear-thinning.

The parameters provided in the tutorial are for $\Gamma = 4$.

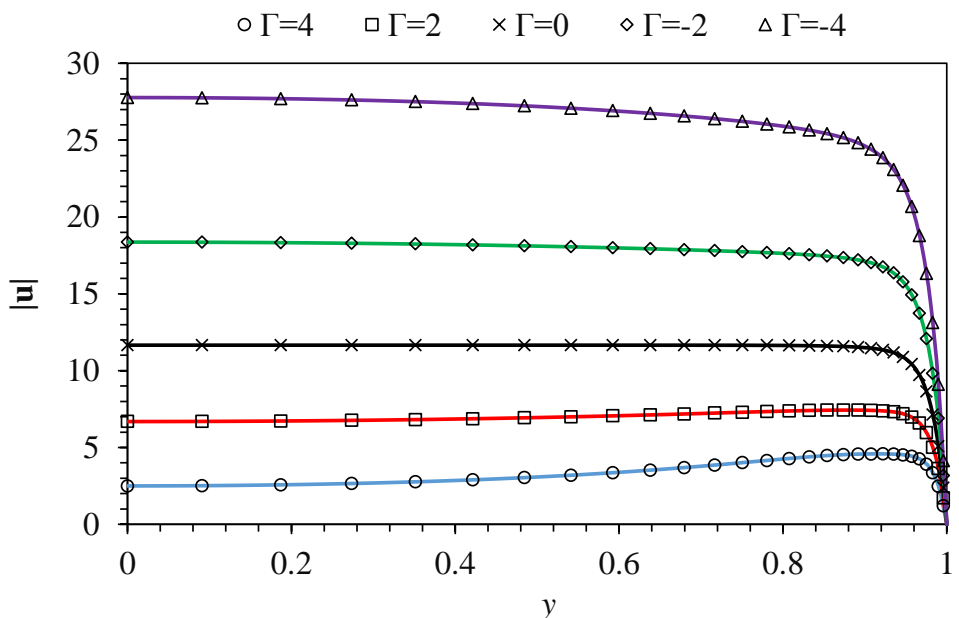


Figure 5.20: Velocity magnitude along the direction transverse to the applied electric field and pressure gradient for a simplified linear PTT fluid, at different forcing ratios Γ , for $\tilde{\kappa} = 20$ and $\sqrt{\varepsilon}De = 4$. The points represent numerical values, while the lines are the analytical solution [34].

5.4.3 Case II: induced-charge electroosmosis around a cylinder

☛ `tutorials/rheoEFoam/ICEO/NernstPlanck`

❖ Overview

This tutorial analyzes the DC induced-charge electroosmosis (ICEO) around a conducting cylinder. We have investigated this problem in Ref. [3] and we present in this tutorial the setup used for $\tilde{V} = 0.01$ and $\tilde{\kappa} = 10$, in mesh M1.

In directory `tutorials/rheoEFoam/ICED/`, the same case is available under different EDF models (PNP, PB and DH). For the conditions aforementioned, all give similar results in steady-state. The case for the PNP model uses one potential (Ψ), while the remaining cases are solved under the splitting approach for the electric potential (both ϕ_{Ext} and ψ are defined). For the last ones, you can also see the use of the *inducedPotential* boundary condition described in Section 4.4.4.

❖ Geometry & Mesh

The geometry used in this tutorial is displayed in Fig. 5.21, being the same as in Ref. [3]. The mesh corresponds to mesh M1 of that work, and more details on the problem definition can be found therein.

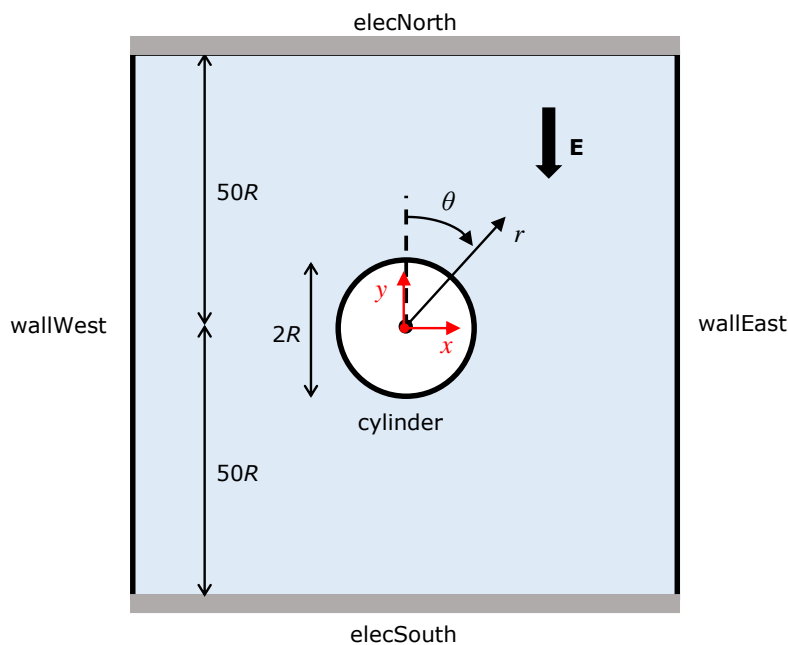


Figure 5.21: Metallic cylinder placed over an electric field. The surrounding domain is square (edge size: $100R$) and the cylinder lays on its center. The cylindrical coordinate system (r, θ) is plotted in black, while the Cartesian coordinate system (x, y) is represented in red (remember that OpenFOAM® uses the Cartesian system for computations).

❖ Boundary conditions

The boundary conditions are described in detail in Ref. [3]. It is worth to note that the boundary conditions of this tutorial, for the PNP model, are different between the versions of *rheoTool*. Indeed, we set a *zeroGradient* BC for the pressure at the cylinder surface in versions *of222* and *fe40*. However, in version *of40* we use the more accurate *fixedFluxExtrapolatedPressure* BC, which is not available in the other versions (see Section 4.4.7). In order to keep the code of *rheoEFoam* unchanged, this BC applied in the specific context of this problem – the pressure field needs an internal reference value/point, because no Dirichlet BC is defined

for it – requires that at least one of the remaining boundaries does not fix the velocity ($\mathbf{u} = \mathbf{0}$ is used in *of222* and *fe40*). A simple workaround to this situation, which would allow to keep the no-slip BC in all the boundaries (without violating continuity), would be to comment the line where function *adjustPhi()* is called in *rheoEFoam* (file *pEqn.H*). In practice, both the methods retrieve similar solutions, since the bounding domain is significantly larger than the cylinder radius. In addition, the major difference between using *zeroGradient* (*of222* and *fe40*) or *fixedFluxExtrapolatedPressure* (*of40*) for the pressure on the cylinder surface is essentially observed in the velocity values in the first 2–3 cells adjacent to the cylinder (more evident at $\theta = 0$ and 180°). Farther away from the surface, the effect is barely detected. The differences are more noticeable at higher voltages, but they vanish with mesh refinement, since this compensates the low-order accuracy of the *zeroGradient* BC.

❖ Command-line

1–Build the mesh:

```
~$ blockMesh
```

2–Run the solver:

```
~$ rheoEFoam
```

3–Extract profiles of \mathbf{u} along the line $\theta = 45^\circ$:

```
~$ sample -latestTime
```

❖ Results

You may find the following relation useful in converting the velocity from the Cartesian base where it is computed, to the cylindrical base used in Ref. [3] to display the results:

$$\begin{bmatrix} U_r \\ U_\theta \end{bmatrix} = \begin{bmatrix} \sin(\theta) & \cos(\theta) \\ \cos(\theta) & -\sin(\theta) \end{bmatrix} \begin{bmatrix} U_x \\ U_y \end{bmatrix} \quad (5.7)$$

Note that two *ppUtil* (cf. Section 4.5.2) are used in this tutorial, returning both the global balance of ions (*calcBalance*) and the current density through the cylinder surface (*calcJpatch*). The latter allows to verify, in this specific case, that the no-flux boundary conditions for the two ionic species is working as expected, since a *quasi-null* current density is retrieved at the boundary where it is assigned.

5.4.4 Case III: charge transport across an ion-selective membrane

 `tutorials/rheoEFoam/selecMembrane/NernstPlanck`

❖ Overview

This tutorial presents the charge transport across an ion-selective membrane and will show the development of the so-called electroconvective instabilities (e.g. [35]). We addressed this EDF in Ref. [3] and we present in this tutorial the setup used for $\tilde{V} = 120$, in mesh M1. The case is adjusted to run until $\tilde{t} = 0.01$, but this time can be easily increased in *controlDict*.

❖ Geometry & Mesh

The geometry for this tutorial is displayed in Fig. 5.22, being the same as in Ref. [3]. The mesh corresponds to mesh M1 of that work, and more details on the problem definition can be found therein.

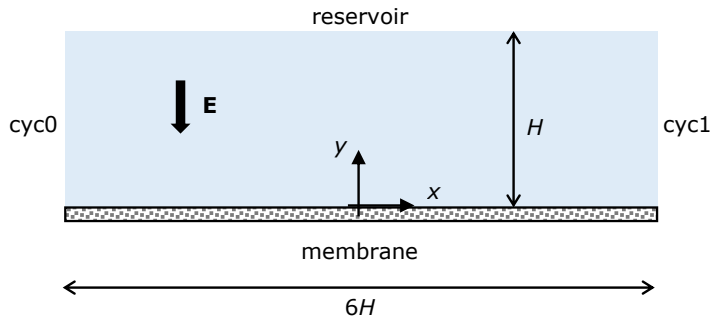


Figure 5.22: Planar reservoir with an ion-selective membrane (only permeable to cations) on its bottom.

❖ Boundary conditions

The boundary conditions were described in detail in Ref. [3]. For the users of OpenFOAM® v4.x, if the *fixedFluxExtrapolatedPressure* is intended to be used at the membrane boundary – this is the most correct option –, then the function *adjustPhi()* must be disabled in solver *rheoEFoam*, as discussed in Section 4.4.7 and in the previous tutorial (again, because no Dirichlet BC is used for pressure, which automatically enables function *adjustPhi()*). Since this would require a permanent change in the solver, we have chosen to use a *zeroGradient* BC in replacement. The degree of approximation, as well as the differences between the two approaches, are the same as for the tutorial in the previous Section (see the comments therein).

❖ Command-line

This tutorial is slightly different from the previous ones regarding the command-line sequence to run. This is because the problem is first solved in a 1D configuration and the resulting solution is then disturbed and used as the starting solution of the 2D configuration. Thus, we recommend to use directly the *Allrun* script to run this tutorial, although we also explain next the main steps accomplished by that script.

Firstly, in the directory of the main case you will find a folder named *solution1D/*. This is where the 1D problem is solved – script *Allrun* inside this folder is the first call of the *Allrun* in the main directory. Computing the 1D solution is relatively straightforward in what respects the commands to be executed, since it only requires building the mesh (*blockMesh*) and running the solver (*rheoEFoam*). You may note that the hydrodynamic component of the solver is switched off through the *solveFluid* keyword in dictionary *fvSolution*,

which is set to *false*. Thus, only the Poisson and Nernst-Planck equations are being solved. Furthermore, we note that underrelaxation is being used to compute the 1D solution in order to enable the use of high time-steps. Under the current settings, the lower the voltage on patch *reservoir*, the higher the time for the 1D solution to converge (the *endTime* should be increased accordingly in these situations). Our criteria for convergence relies in the monitor for the current density.

After the 1D solution is computed, the resulting fields are mapped to the 2D domain (also created with *blockMesh* beforehand), using the *mapFields* utility available by default in OpenFOAM®. Then, the fields for the cationic and anionic concentration are locally disturbed by a 1 % random perturbation. This is accomplished by a pre-processing utility named *rndPerturbation*, which has been specifically created for this task and that can be found in directory `src/libs/preProcessing/rndPerturbation/`. The case is ready to be run with *rheoEFoam*, noticing that now *solveFluid* = *true*.

While the case is running, a *ppUtil* (cf. Section 4.5.2) is simultaneously being executed (*calcJpatch*), which retrieves the surface-averaged current density over time on both the *reservoir* and *membrane* patches (Fig. 5.22).

⌚ Results

The current density can be plotted over time and the contours of charge density can be computed and visualized in Paraview (these are just some suggestions).

The electric field intensity can be controlled by changing the voltage in file `solution1D/0/psi`, under the entry for patch *reservoir*. Note that any change in the initial/boundary conditions of any field must be done in the files inside folder `solution1D` due to the mapping procedure. By running the `Allrun` script in the main folder, the 1D solution will be always computed first.

5.4.5 Case IV: electrokinetic instabilities in a flow-focusing device

 `tutorials/rheoEFoam/EKI/Ohmic`

⌚ Overview

This tutorial aims to reproduce qualitatively the electrokinetic instabilities arising in a flow-focusing device, when electrolytes of different conductivity join at the converging region. The problem has been extensively studied in Ref. [36], both experimentally and theoretically.

The use of the Ohmic model is illustrated in this tutorial, which also includes the transport of a passive, neutral scalar.

As shown by Posner et al. [36], the dynamics of the problem is essentially governed by three dimensionless numbers: the electric Rayleigh number, $Ra_E = \frac{\epsilon E_a^2 h^2}{\eta D}$, the conductivity ratio $\gamma = \frac{\sigma_W}{\sigma_S}$ and the voltage ratio $\beta = \frac{V_W}{V_S}$. The indices refer to the north (N), south (S), west (W) and outlet (O) arms of the flow-focusing device and $h = 0.8H$ is the channel depth. Furthermore, an apparent electric field is computed as $E_a = \frac{V_N - V_O}{L_N + L_O}$, where the denominator of E_a represents the summed distance of the north and east arms (distance between the ends of each arm, passing

by the center of the geometry: $L_N + L_O = 24H$ in this tutorial). The parameters of the tutorial are chosen in order to simulate $Ra_E = 839$, $\gamma = 10$ and $\beta = 1.05$.

❖ Geometry & Mesh

The geometry is a 3D flow-focusing device (Fig. 5.23) composed of three converging inlets and one outlet. The width and the depth of the channel are uniform over all the geometry: $2H$ and $0.8H$, respectively. The inlet arms (west, south and north) are all $8H$ long, while the outlet arm (east) is $16H$ long.

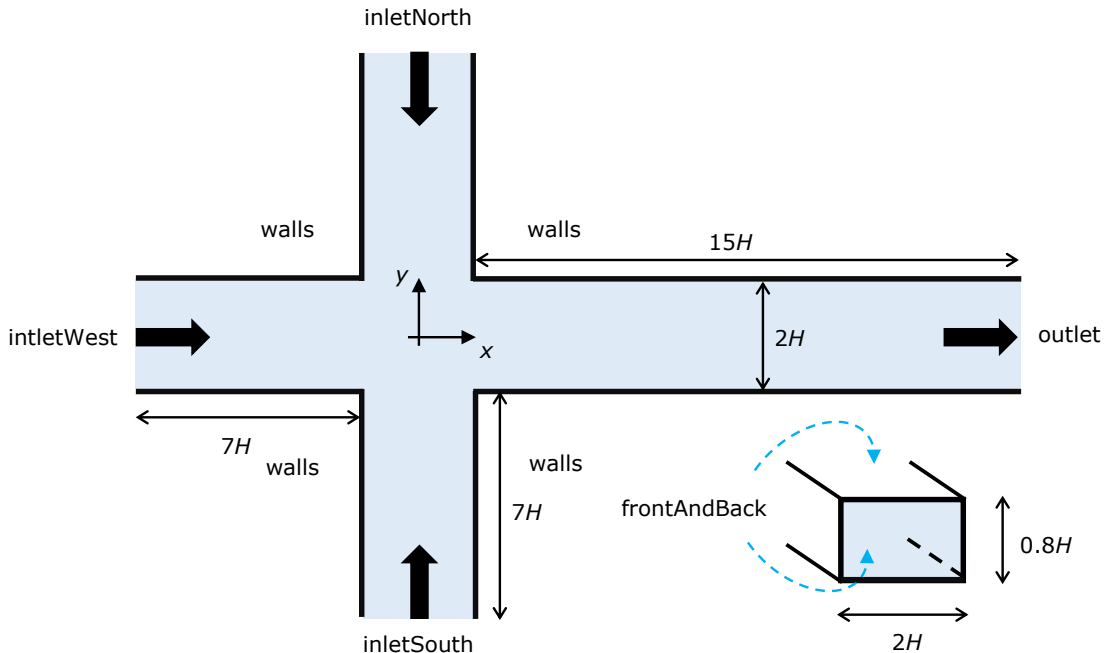


Figure 5.23: Three-dimensional flow-focusing device.

The geometry is divided into 12 blocks for meshing purposes. The dimensions of the cells at the junction corners are approximately: $(\Delta x, \Delta y, \Delta z) \approx (0.1, 0.1, 0.07)H$.

❖ Boundary conditions

Since the Ohmic model is used in this simulation, we have to define boundary conditions for pressure, velocity, electric potential and conductivity. We consider that all the arms are open to the atmosphere, thus $p = 0$ and a zero-gradient is assumed for the velocity. At *inletNorth* and *inletSouth*, the conductivity of the fluid entering those arms is the same, but ten times lower than the conductivity of the fluid entering *inletWest* ($\gamma = 10$). A passive scalar (neutral dye) is also entering the geometry through *inletWest*, only. A zero-gradient condition is imposed for both the conductivity and the passive-scalar concentration at the *outlet*. At the *walls* we assume zero-gradient for all variables, except the velocity. As discussed in Section 3.5.6, the Ohmic model is usually complemented with a conductivity-dependent slip velocity (Eq. 3.40). In this tutorial, we use $m = -0.3$ for the

power-law index (see Section 4.4.6). Regarding the electric potential, the *outlet* is grounded, while the potential at *inletNorth* and *inletSouth* are the same, being adjusted in order to impose the desired Ra_E . The potential at *inletWest* is set according to β .

Note that the passive-scalar (dye) has a diffusivity which is one order of magnitude lower than the diffusivity of the ions (conductivity), in agreement with typical real conditions.

❖ Command-line

1–Build the mesh:

```
~$ blockMesh
```

2–Create fields *C* and *sigma* by copying the ones already present, but which are not initialized in the interior domain:

```
~$ cp 0/C.org 0/C
```

```
~$ cp 0/sigma.org 0/sigma
```

3–Initialize fields *C* and *sigma* in the interior domain ($C = 1 \wedge \sigma = \sigma_W$ for $x < -H$ and $t = 0$):

```
~$ setFields
```

4–Run the solver:

```
~$ rheoFoam
```

5–Post-process in Paraview (hint: slice the channel at the midplane in the *z*-direction and plot the contours of *C*):

```
~$ paraFoam
```

❖ Results

The contours for the passive-scalar are displayed in Fig. 5.24 at the mid-plane in *z*, for different Ra_E . The reader will probably note similarities between these instabilities and von-Kármán vortex streets.

The patterns are qualitatively similar to those obtained in Ref. [36] (see Fig. 4 therein, although our Ra_E is defined differently from the one used in that work). The periodicity or the chaotic behavior of the instabilities can be further evaluated by looking to the probes of *C* and *U*.

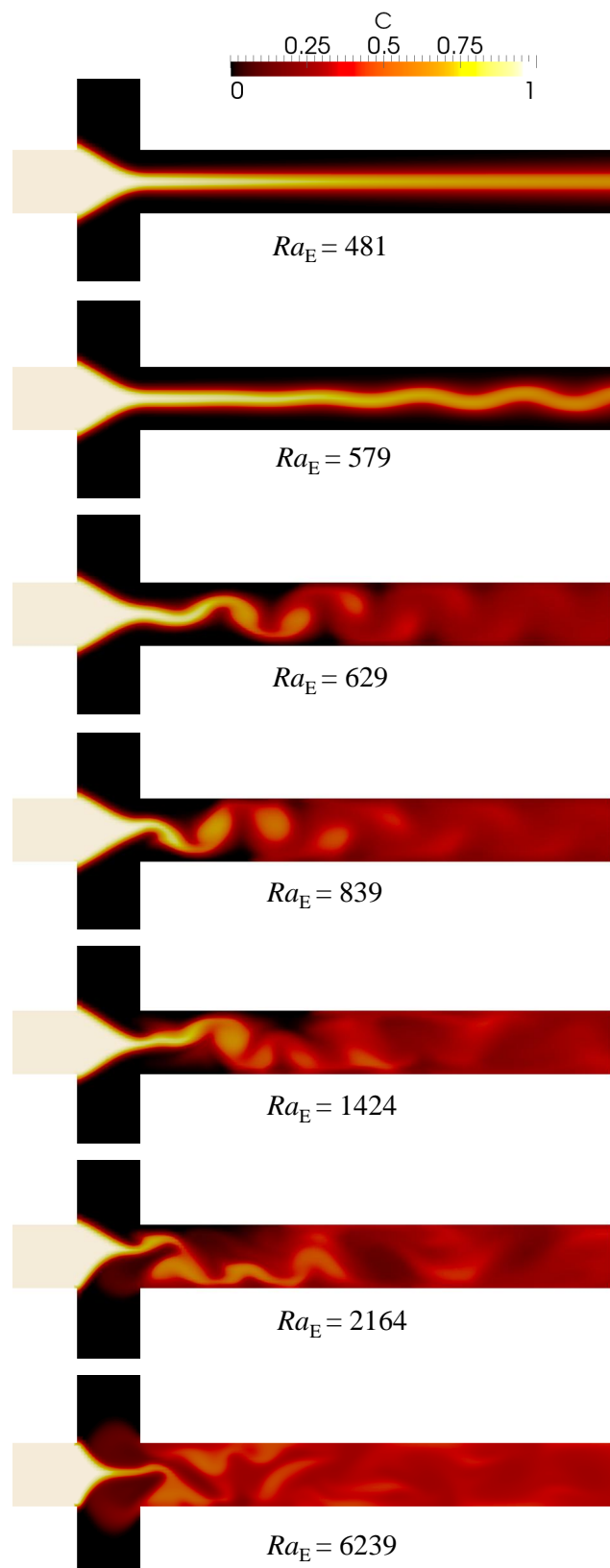


Figure 5.24: Instantaneous contours of C at the mid-plane in z for different Ra_E ($\gamma = 10$ and $\beta = 1.05$). The case provided in the tutorial is for $Ra_E = 839$ and the remaining ones can be easily obtained by simply scaling the applied voltage (ϕ_{IE}) at the inlets (see the definition of Ra_E).

Note that we do not use exactly the same parameters as in Posner et al. [36], since our purpose was solely to illustrate the qualitative behavior of electrokinetic instabilities, through a fast-running case. The large time-step used (Courant-controlled, with $Co = 1.5$) is also inadequate to capture accurately the transient behavior of this case.

5.4.6 Case V: electrokinetic mixer

 `tutorials/rheoEFoam/EKmixer/slipSmoluchowski`

❖ Overview

The main purpose of this tutorial is to illustrate the use of the *slipSmoluchowski* EDF model (see Section 3.5.5 and Table 4.2). Although simple, this model is very useful to simulate Newtonian fluid flows in complex geometries, being accurate for thin EDL and low intrinsic potentials. In addition, in this tutorial we also use AC fields, combined with the transport of a passive-scalar.

The case that we propose is an electrokinetic-based micromixer, inspired on the work of Coleman et al. [37]. In that work, the authors showed that a flow-focusing geometry followed by an expansion can achieve a good degree of mixing between two fluids, under AC-driven injection.

Note that this tutorial does not reproduce exactly the same geometrical dimensions, nor the same operating conditions of Ref. [37].

❖ Geometry & Mesh

The 2D electrokinetic mixer is shown in Fig. 5.25 (the user can check the dimensions by opening the mesh in Paraview or by inspecting the corresponding `blockMeshDict` file). The device consists of a flow-focusing region where one fluid is injected through `inletWest` and the other fluid is injected in `inletNorth`. The geometry is made symmetric relative to the x -axis and an expansion region exists downstream to the flow-focusing, which is where the mixing mainly occurs.

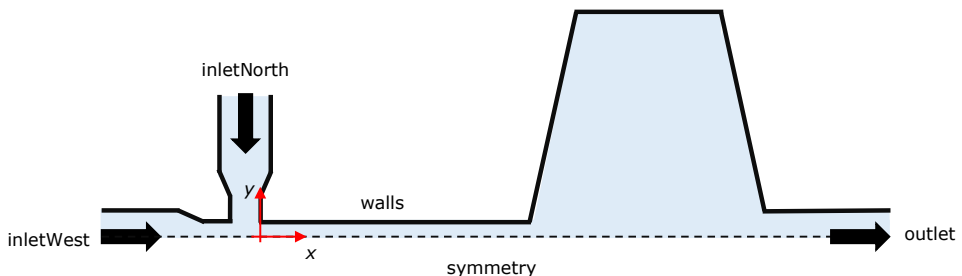


Figure 5.25: Electrokinetic mixer similar to the device used by Coleman et al. [37].

❖ Boundary conditions

We consider a purely EDF, thus $p = 0$ at both inlets and outlet boundaries, and a zero-gradient condition is simultaneously assigned to the velocity. Regarding the

externally applied potential, it is fixed at 0 V in the *outlet* and a custom sinusoidal boundary condition is imposed at each inlet,

$$\phi_{\text{Ext}}(t) = \phi_{\text{Ext, DC}} + \phi_{\text{Ext, AC}} \sin(2\pi ft + \theta) \quad (5.8)$$

As long as $\phi_{\text{Ext}}(t) > 0$ at each inlet, there is a unidirectional net flow of fluid in the region $x > 0$, although the fluid can move both forward and backward in the region $x \leq 0$, which constitutes the injecting mechanism of the mixer [37]. By changing $\phi_{\text{Ext, DC}}$, $\phi_{\text{Ext, AC}}$, f and/or θ at each inlet, different degrees of mixing can be achieved. At the wall, zero-gradient is considered for pressure and electric potential and the Helmholtz-Smoluchowski equation (Eq. 3.33) is used for the slip velocity.

A passive-scalar is injected at *inletWest* and the purpose of the mixer is precisely to achieve the perfect mixing of the passive-scalar stream (*inletWest*), with the stream devoid of that scalar (*inletNorth*) – perfect mixing means $C = 0.5$ for a passive-scalar in the range $[0, 1]$. Note that, as stated in Ref. [37], the operating conditions can be also tuned in order to obtain a pre-defined degree of mixture different than a 0.5/0.5 stream at the outlet.

⌚ Command-line

Since the list of commands to run is rather extensive, we recommend the user to simply run the script `Allrun`. The commands executed by `Allrun` that might seem new, regarding what has been done in the previous tutorials, are `topoSet` and `refineMesh`. Those commands select the cells in the expansion region and perform a refinement in the y -direction, respectively.

⌚ Results

Fig. 5.26 shows the contours of the passive-scalar when either the stream devoid of C , or rich in C , are injected. Both snapshots were taken after the system has reached a periodic state. As can be seen, the conditions defined ensure a good mixing between the streams, since $C \approx 0.5$ at the outlet.

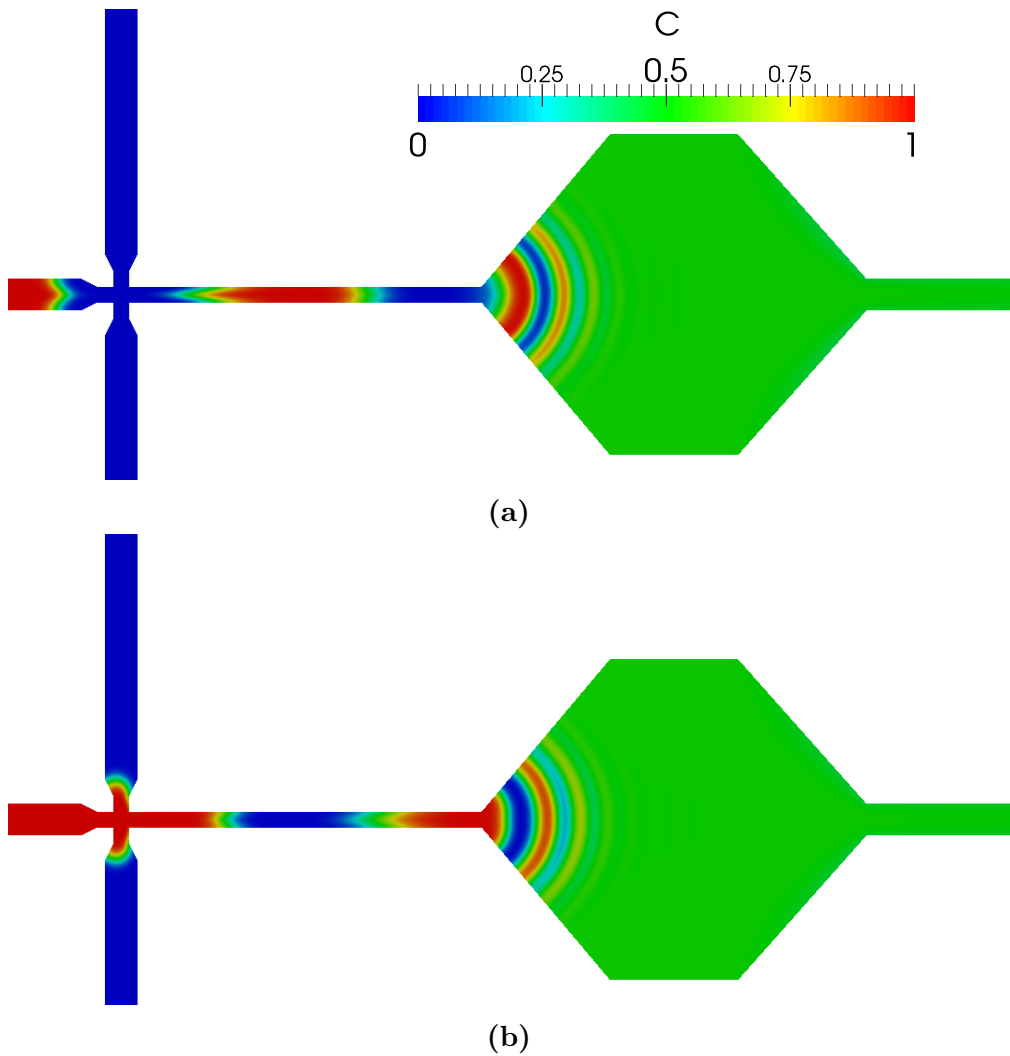


Figure 5.26: Snapshots of the passive scalar concentration field at different instants: (a) injecting the phase devoid of C (*inletNorth*) and (b) injecting the phase rich in C (*inletWest*). Note that the geometry has been reflected relative to the x -axis (in Paraview) for presentation purposes – only the upper-half of the geometry is simulated.

The user can play with the several degrees of freedom of the electric potential boundary conditions in order to achieve different degrees of mixing. Note that the time-step used in the tutorial has been adjusted to obtain results in a reasonable amount time, but it should be lowered to achieve higher accuracy in time. Such a high time-step, as well as the "coarse" mesh used, would not be possible to use if, for instance, the full PNP model was used instead – the simulation would most likely diverge due to stability issues.

5.4.7 Case VI: electro-elastic instabilities in cross-shaped geometries

[tutorials/rheoEFoam/EEI/PoissonBoltzmann/](#)

❖ Overview

The electrically-driven flow of high-molecular weight polyacrylamide solutions in cross-slot and flow-focusing devices was seen to become unstable after a threshold electric potential is exceeded [38]. This tutorial addresses the numerical simulation of such phenomena, as presented in Ref. [38]. This tutorial merges electrically-driven flows with viscoelastic fluid models, where the electric charge distribution is computed by the Poisson-Boltzmann model and the extra-stress tensor of the viscoelastic fluid is evolved using the Oldroyd-B model ($\beta = 0.4$). The settings of the tutorial reproduce the case with $\Delta V = 160$ V, $Wi_B = 2.06$, $Wi_\kappa = 103$ (CrossSlot/) and $\Delta V = 160$ V, $Wi_B = 1.03$, $Wi_\kappa = 154$ (FlowFocusing/) of Ref. [38]. The physical time of the simulations is $t_f = 0.5$ s = 10λ .

❖ Geometry & Mesh

The geometry for this case is displayed in Fig. 5.27. Both the geometry and the mesh correspond to the ones used in Ref. [38]. The flow is assumed to be 2D, being solved in the xy -plane. Note that the patch names for the cross-slot and flow-focusing geometries differ in the west arm, which is either an outlet or an inlet (Fig. 5.27).

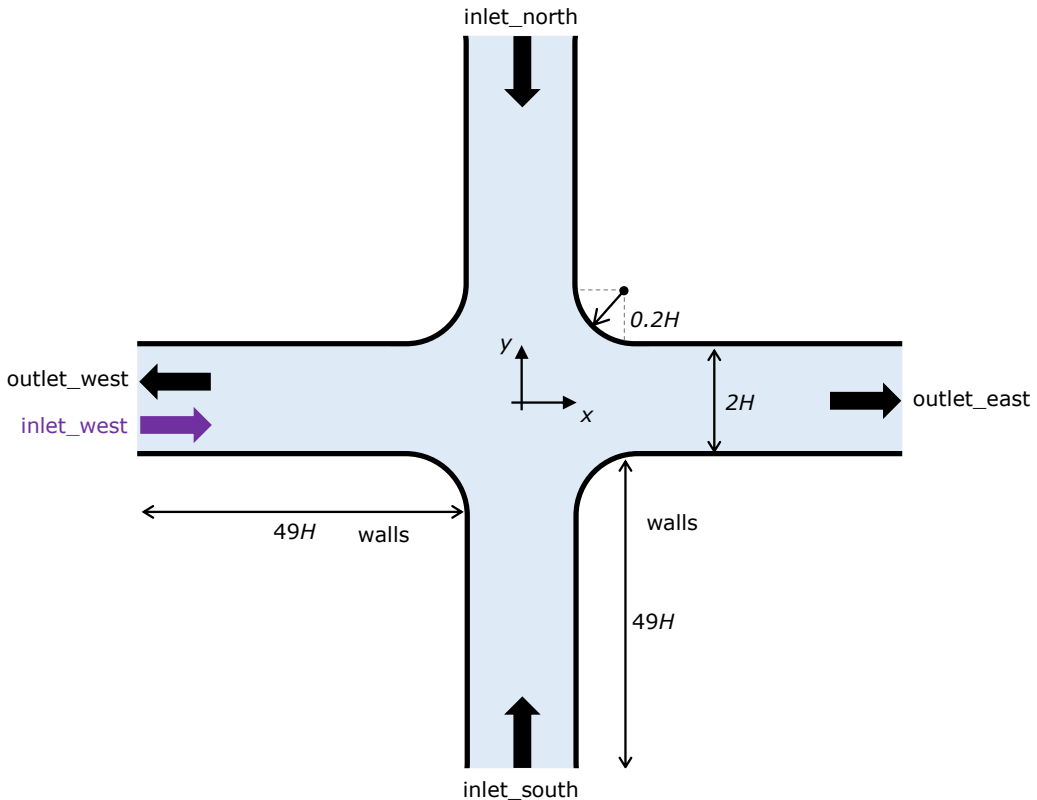


Figure 5.27: Cross-slot and flow-focusing geometries. In the west arm, the black arrow is for the cross-slot configuration (*outlet_west*) and the purple arrow is for the flow-focusing configuration (*inlet_west*). In the tutorial, $H = 5 \times 10^{-5}$ m.

❖ Boundary conditions

The boundary conditions used are described in Ref. [38]. The tutorials also include the transport of a passive tracer. Note that the pressure extrapolation boundary condition at the wall is replaced by a zero-gradient condition in versions *of222* and *fe40*, since it is not available therein.

⌚ Command-line

Before presenting the command line sequence, it is worth to note that the mesh for this case is built in a slightly different way. Indeed, the `blockMesh` application only builds one-quarter of the geometry/mesh, the one in the first quadrant (+,+). The remaining of the geometry/mesh is built by 2 sequential mirroring operations (`mirrorMesh`): first using the Oyz plane and then using the Oxz plane. Afterwards, patches should be renamed accordingly, which requires selecting, splitting and removing faces of already existing patches (`topoSet`) and creation of new ones (`createPatch`).

1–Build the mesh:

```
~$ blockMesh
~$ cp system/mirrorMeshDict0 system/mirrorMeshDict
~$ mirrorMesh
~$ cp system/mirrorMeshDict1 system/mirrorMeshDict
~$ mirrorMesh
~$ topoSet
~$ createPatch -overwrite
```

2–Initialize field C in the interior domain:

```
~$ cp 0/C.org 0/C
~$ setFields
```

3–Run the solver:

```
~$ rheoEFoam
```

⌚ Results

The dye patterns (field C) of the unstable flows can be visualized in Paraview.

Appendix A

Parameters and variables in *rheoTool*

Table A.1: List of some relevant parameters and variables used by *rheoTool* and correspondence with the nomenclature used in this guide.

| Name in the guide | Name in the code | Dimensions [kg m s K mol A cd] | Definition |
|-------------------|------------------|--------------------------------|---|
| α | alpha | [0 0 0 0 0 0] | Anisotropy parameter of Giesekus and eXtended Pom-Pom models (scalar) |
| α | alpha | [0 0 0 0 0 0] | Parameter of the piecewise-linear HRS functions (scalar) |
| α | alpha | [0 0 0 0 0 0] | Indicator/Color function of the VOF method (scalar) |
| A | A | [0 0 0 0 0 0] | Conformation tensor (symmTensor) |
| a | a | [0 0 0 0 0 0] | Dimensionless parameter of Carreau-Yasuda and White-Metzner models (scalar) |
| a | a | [0 0 0 0 0 0] | Variable of FENE-P model (scalar) |
| - | AK_- | [0 0 0 0 -1 0 0] | Avogadro's constant (scalar) |
| β | beta | [0 0 0 0 0 0] | Parameter of the piecewise-linear HRS functions (scalar) |
| β | beta | [0 0 0 0 0 0] | CCR coefficient of Rolie-Poly model (scalar) |

| | | | |
|----------------------|---------------|-------------------|---|
| b | b | [0 0 0 0 0 0] | Dimensionless parameter of White-Metzner model (scalar) |
| - | b | [0 0 0 0 0 0] | Square-root conformation tensor of Ref. [10], for the <i>Oldroyd-B</i> <i>Sqrt</i> model (symmTensor) |
| χ_{\max} | chiMax | [0 0 0 0 0 0] | Maximum stretch ratio in Rolie-Poly model (scalar) |
| - | C | [0 0 0 0 0 0] | Passive scalar (scalar) |
| c_i | - | [0 -3 0 0 1 0 0] | Concentration of specie i in mol/m ³ (scalar) |
| c_0 | c0 | [0 -3 0 0 1 0 0] | Reference ionic concentration (scalar) |
| δ | delta | [0 0 0 0 0 0] | Exponent of Rolie-Poly model (scalar) |
| D | D | [0 2 -1 0 0 0 0] | Diffusion coefficient in the passive scalar transport equation (scalar) |
| D_i | Di | [0 2 -1 0 0 0 0] | Diffusion coefficient of ionic specie i (scalar) |
| μ | elecMobility | [-1 0 2 0 0 1 0] | Electroosmotic mobility (scalar) |
| μ_0 | elecMobility0 | [-1 0 2 0 0 1 0] | Electroosmotic mobility at a reference conductivity (scalar) |
| ε | epsilon | [0 0 0 0 0 0] | Extensibility parameter of PTT-type models (scalar) |
| ε | - | [-1 -3 4 0 0 2 0] | Electric permittivity (scalar) |
| ε_0 | epsilonK_- | [-1 -3 4 0 0 2 0] | Electric permittivity of vacuum (scalar) |
| η | eta | [1 -1 -1 0 0 0 0] | Newtonian viscosity (scalar) |
| $\eta(\dot{\gamma})$ | eta | [1 -1 -1 0 0 0 0] | Shear-rate dependent viscosity from a GNF model (scalar) |
| η_0 | eta0 | [1 -1 -1 0 0 0 0] | Zero shear-rate viscosity (scalar) |
| η_0 | eta0 | [1 -1 -1 0 0 0 0] | Limiting viscosity in the Herschel-Bulkley model (scalar) |

| | | | |
|----------------|-------------|-------------------|--|
| η_∞ | etaInf | [1 -1 -1 0 0 0 0] | Infinite shear-rate viscosity (scalar) |
| η_{\max} | etaMax | [1 -1 -1 0 0 0 0] | Upper bound for the viscosity in the power-law model (scalar) |
| η_{\min} | etaMin | [1 -1 -1 0 0 0 0] | Lower bound for the viscosity in the power-law model (scalar) |
| η_p | etaP | [1 -1 -1 0 0 0 0] | Polymeric viscosity coefficient (scalar) |
| η_s | etaS | [1 -1 -1 0 0 0 0] | Solvent viscosity (scalar) |
| Λ | eigVals | [0 0 0 0 0 0 0] | Eigenvalues obtained in the diagonalization of \mathbf{A} (tensor) |
| \mathbf{R} | eigVecs | [0 0 0 0 0 0 0] | Eigenvectors obtained in the diagonalization of Θ and \mathbf{A} (tensor) |
| e | eK_- | [0 0 1 0 0 1 0] | Elementary charge (scalar) |
| \mathbf{E}_a | extraEFIELD | [1 1 -3 0 0 -1 0] | Constant and uniform extra electric field (vector) |
| f | f | [0 0 0 0 0 0 0] | Variable of FENE-type models (scalar) |
| F | FK_- | [0 0 1 0 -1 1 0] | Faraday's constant (scalar) |
| k | k | [1 -1 -1 0 0 0 0] | Consistency index of power-law model (scalar) |
| k | k | [0 0 1 0 0 0 0] | Time-scale in the Carreau-Yasuda model (scalar) |
| K | K | [0 0 1 0 0 0 0] | Time-scale for η_p in the White-Metzner model (scalar) |
| k | kbK_- | [1 2 -2 -1 0 0 0] | Boltzmann's constant (scalar) |
| λ | lambda | [0 0 1 0 0 0 0] | Relaxation time (scalar) |
| λ_B | lambdaB | [0 0 1 0 0 0 0] | Relaxation time of the backbone tube orientation (scalar) |
| λ_D | lambdaD | [0 0 1 0 0 0 0] | Reptation time (scalar) |
| λ_R | lambdaR | [0 0 1 0 0 0 0] | Rouse or stretch time (scalar) |
| λ_S | lambdaS | [0 0 1 0 0 0 0] | Relaxation time for the tube stretch (scalar) |

| | | | |
|-------------------------------|--------------|-------------------|--|
| L | L | [0 0 1 0 0 0 0] | Time-scale for λ in the White-Metzner model (scalar) |
| L^2 | L2 | [0 0 0 0 0 0 0] | Extensibility parameter of FENE-type models (scalar) |
| m | m | [0 0 0 0 0 0 0] | Dimensionless parameter of White-Metzner model (scalar) |
| m | m | [0 0 0 0 0 0 0] | Power-law exponent for the conductivity-dependent Helmholtz-Smoluchowski velocity (scalar) |
| n | n | [0 0 0 0 0 0 0] | Flow behavior index for shear-rate dependent viscosity models (scalar) |
| ϕ_{Ext} | phiE | [1 2 -3 0 0 -1 0] | Externally-applied electric potential (scalar) |
| Ψ | psi | [1 2 -3 0 0 -1 0] | Total electric potential (scalar) |
| ψ | psi | [1 2 -3 0 0 -1 0] | Intrinsic electric potential (scalar) |
| p | p | [1 -1 -2 0 0 0 0] | Pressure, in <i>rheoInterFoam</i> (scalar) |
| $\frac{p}{\rho}$ | p | [0 2 -2 0 0 0 0] | Pressure divided by the density, in <i>rheoFoam</i> and <i>rheoEFoam</i> (scalar) |
| $\mathbf{u} \cdot \mathbf{S}$ | phi | [0 3 -1 0 0 0 0] | Face fluxes (scalar) |
| q | q | [0 0 0 0 0 0 0] | Amount of arms at the end of the polymer backbone (scalar) |
| ρ | rho | [1 -3 0 0 0 0 0] | Density (scalar) |
| ρ_E | - | [0 -3 1 0 0 1 0] | Charge density (per unit volume) (scalar) |
| ε_R | relPerm | [0 0 0 0 0 0 0] | Relative electric permittivity or dielectric constant (scalar) |
| σ | sigma | [-1 -3 3 0 0 2 0] | Electric conductivity (scalar) |
| σ_0 | sigma0 | [-1 -3 3 0 0 2 0] | Reference electric conductivity (scalar) |
| $\dot{\gamma}$ | strainRate() | [0 0 -1 0 0 0 0] | Shear-rate (scalar) |

| | | | |
|--------------------------------|-------|-------------------|---|
| τ | tau | [1 -1 -2 0 0 0 0] | Polymeric extra-stress tensor (symmTensor) |
| τ_0 | tau0 | [1 -1 -2 0 0 0 0] | Yield stress (scalar) |
| - | tauMF | [1 -1 -2 0 0 0 0] | Polymeric extra-stress tensor weighted by the indicator function in <i>rheoInterFoam</i> (symmTensor) |
| Θ | theta | [0 0 0 0 0 0 0] | Natural logarithm of the conformation tensor (symmTensor) |
| T | T | [0 0 0 1 0 0 0] | Absolute temperature (scalar) |
| \mathbf{u} | U | [0 1 -1 0 0 0 0] | Velocity (vector) |
| ζ | zeta | [0 0 0 0 0 0 0] | Slip parameter of PTT-type models (scalar) |
| z_i | zi | [0 0 0 0 0 0 0] | Charge valence of specie i (scalar) |

Bibliography

- [1] J. Favero, A. Secchi, N. Cardozo, and H. Jasak, “Viscoelastic fluid analysis in internal and in free surface flows using the software OpenFOAM,” *Computers & Chemical Engineering*, vol. 34, no. 12, pp. 1984 – 1993, 2010. 10th International Symposium on Process Systems Engineering, Salvador, Bahia, Brasil, 16-20 August 2009.
- [2] F. Pimenta and M. Alves, “Stabilization of an open-source finite-volume solver for viscoelastic fluid flows,” *Journal of Non-Newtonian Fluid Mechanics*, vol. 239, pp. 85 – 104, 2017.
- [3] F. Pimenta and M. Alves, “Simulation of electrically-driven flows using OpenFOAM®,” *arXiv:1802.02843*, 2018.
- [4] R. Fattal and R. Kupferman, “Constitutive laws for the matrix-logarithm of the conformation tensor,” *Journal of Non-Newtonian Fluid Mechanics*, vol. 123, no. 2–3, pp. 281 – 285, 2004.
- [5] R. Bird and O. Hassager, *Dynamics of Polymeric Liquids: Fluid mechanics*, vol. 1-2 of *Dynamics of Polymeric Liquids*. Wiley, 1987.
- [6] G. Guennebaud, B. Jacob, *et al.*, “Eigen v3.” <http://eigen.tuxfamily.org>, 2010.
- [7] X. Chen, H. Marschall, M. Schäfer, and D. Bothe, “A comparison of stabilisation approaches for finite-volume simulation of viscoelastic fluid flow,” *International Journal of Computational Fluid Dynamics*, vol. 27, no. 6-7, pp. 229–250, 2013.
- [8] R. Fattal and R. Kupferman, “Time-dependent simulation of viscoelastic flows at high weissenberg number using the log-conformation representation,” *Journal of Non-Newtonian Fluid Mechanics*, vol. 126, no. 1, pp. 23 – 37, 2005.
- [9] A. Afonso, F. Pinho, and M. Alves, “The kernel-conformation constitutive laws,” *Journal of Non-Newtonian Fluid Mechanics*, vol. 167–168, pp. 30 – 37, 2012.
- [10] N. Balci, B. Thomases, M. Renardy, and C. R. Doering, “Symmetric factorization of the conformation tensor in viscoelastic fluid models,” *Journal of Non-Newtonian Fluid Mechanics*, vol. 166, no. 11, pp. 546 – 553, 2011. XVIth International Workshop on Numerical Methods for Non-Newtonian Flows.

- [11] Ž. Tuković and H. Jasak, “A moving mesh finite volume interface tracking method for surface tension dominated interfacial fluid flow,” *Computers & Fluids*, vol. 55, pp. 70 – 84, 2012.
- [12] H. Jasak, “Pressure-velocity coupling in FOAM, Consistent derivation for steady and transient flow solvers.” OFW11, Guimarães, Portugal, 2016.
- [13] F. Moukalled, A. A. Aziz, and M. Darwish, “Performance comparison of the NWF and DC methods for implementing high-resolution schemes in a fully coupled incompressible flow solver,” *Applied Mathematics and Computation*, vol. 217, no. 11, pp. 5041 – 5054, 2011.
- [14] H. Jasak, H. Weller, and A. Gosman, “High resolution NVD differencing scheme for arbitrarily unstructured meshes,” *International Journal for Numerical Methods in Fluids*, vol. 31, no. 2, pp. 431 – 449, 1999.
- [15] A. Afonso, F. Pinho, and M. Alves, “Electro-osmosis of viscoelastic fluids and prediction of electro-elastic flow instabilities in a cross slot using a finite-volume method,” *Journal of Non-Newtonian Fluid Mechanics*, vol. 179–180, pp. 55 – 68, 2012.
- [16] C.-H. Chen, H. Lin, S. K. Lele, and J. G. Santiago, “Convective and absolute electrokinetic instability with conductivity gradients,” *Journal of Fluid Mechanics*, vol. 524, pp. 263–303, 2005.
- [17] A. Persat and J. G. Santiago, “An ohmic model for electrokinetic flows of binary asymmetric electrolytes,” *Current Opinion in Colloid & Interface Science*, vol. 24, pp. 52 – 63, 2016.
- [18] K. K. Kabanemi and J.-F. Hétu, “Nonequilibrium stretching dynamics of dilute and entangled linear polymers in extensional flow,” *Journal of Non-Newtonian Fluid Mechanics*, vol. 160, no. 2–3, pp. 113 – 121, 2009.
- [19] P. J. Oliveira, “Asymmetric flows of viscoelastic fluids in symmetric planar expansion geometries,” *Journal of Non-Newtonian Fluid Mechanics*, vol. 114, no. 1, pp. 33 – 63, 2003.
- [20] W. H. Press, B. P. Flannery, S. A. Teukolsky, and W. T. Vetterling, “Numerical recipes (FORTRAN version),” *Press Syndicate of the University of Cambridge, Cambridge, UK*, 1989.
- [21] F. Habla, A. Woitalka, S. Neuner, and O. Hinrichsen, “Development of a methodology for numerical simulation of non-isothermal viscoelastic fluid flows with application to axisymmetric 4:1 contraction flows,” *Chemical Engineering Journal*, vol. 207, no. Supplement C, pp. 772 – 784, 2012. 22nd International Symposium on Chemical Reaction Engineering (ISCRE 22).
- [22] Z. Wu and D. Li, “Mixing and flow regulating by induced-charge electrokinetic flow in a microchannel with a pair of conducting triangle hurdles,” *Microfluidics and Nanofluidics*, vol. 5, no. 1, pp. 65–76, 2008.

- [23] S. Xue and G. W. Barton, “An unstructured finite volume method for viscoelastic flow simulations with highly truncated domains,” *Journal of Non-Newtonian Fluid Mechanics*, vol. 233, pp. 48 – 60, 2016. Papers presented at the Rheology Symposium in honor of Prof. R. I. Tanner on the occasion of his 82nd birthday, in Vathi, Samos, Greece.
- [24] Y. Na and J. Y. Yoo, “A finite volume technique to simulate the flow of a viscoelastic fluid,” *Computational Mechanics*, vol. 8, no. 1, pp. 43–55, 1991.
- [25] M. A. Hulsen, R. Fattal, and R. Kupferman, “Flow of viscoelastic fluids past a cylinder at high weissenberg number: Stabilized simulations using matrix logarithms,” *Journal of Non-Newtonian Fluid Mechanics*, vol. 127, no. 1, pp. 27 – 39, 2005.
- [26] M. Alves, F. Pinho, and P. Oliveira, “The flow of viscoelastic fluids past a cylinder: finite-volume high-resolution methods,” *Journal of Non-Newtonian Fluid Mechanics*, vol. 97, no. 2–3, pp. 207 – 232, 2001.
- [27] F. Cruz, R. Poole, A. Afonso, F. Pinho, P. Oliveira, and M. Alves, “A new viscoelastic benchmark flow: Stationary bifurcation in a cross-slot,” *Journal of Non-Newtonian Fluid Mechanics*, vol. 214, pp. 57 – 68, 2014.
- [28] A. Valencia, A. Zarate, M. Galvez, and L. Badilla, “Non-newtonian blood flow dynamics in a right internal carotid artery with a saccular aneurysm,” *International Journal for Numerical Methods in Fluids*, vol. 50, no. 6, pp. 751–764, 2006.
- [29] Aneurisk-Team, “AneuriskWeb project website, <http://ecm2.mathcsemory.edu/aneuriskweb>.” Web Site, 2012.
- [30] R. Figueiredo, C. Oishi, A. Afonso, I. Tasso, and J. Cuminato, “A two-phase solver for complex fluids: Studies of the weissenberg effect,” *International Journal of Multiphase Flow*, vol. 84, pp. 98 – 115, 2016.
- [31] C. Oishi, F. Martins, M. Tomé, and M. Alves, “Numerical simulation of drop impact and jet buckling problems using the extended pom-pom model,” *Journal of Non-Newtonian Fluid Mechanics*, vol. 169–170, pp. 91 – 103, 2012.
- [32] R. Comminal, F. Pimenta, J. H. Hattel, M. A. Alves, and J. Spangenberg, “Numerical simulation of the planar extrudate swell of pseudoplastic and viscoelastic fluids with the streamfunction and the VOF methods,” *Journal of Non-Newtonian Fluid Mechanics*, vol. 252, pp. 1 – 18, 2018.
- [33] C. Zhao and C. Yang, “An exact solution for electroosmosis of non-newtonian fluids in microchannels,” *Journal of Non-Newtonian Fluid Mechanics*, vol. 166, no. 17–18, pp. 1076 – 1079, 2011.
- [34] A. Afonso, M. Alves, and F. Pinho, “Analytical solution of mixed electroosmotic/pressure driven flows of viscoelastic fluids in microchannels,” *Journal of Non-Newtonian Fluid Mechanics*, vol. 159, no. 1–3, pp. 50 – 63, 2009.

- [35] C. L. Druzgalski, M. B. Andersen, and A. Mani, "Direct numerical simulation of electroconvective instability and hydrodynamic chaos near an ion-selective surface," *Physics of Fluids*, vol. 25, no. 11, p. 110804, 2013.
- [36] J. D. Posner and J. G. Santiago, "Convective instability of electrokinetic flows in a cross-shaped microchannel," *Journal of Fluid Mechanics*, vol. 555, pp. 1–42, 05 2006.
- [37] J. T. Coleman, J. McKechnie, and D. Sinton, "High-efficiency electrokinetic micromixing through symmetric sequential injection and expansion," *Lab Chip*, vol. 6, pp. 1033–1039, 2006.
- [38] F. Pimenta and M. Alves, "Electro-elastic instabilities in cross-shaped microchannels," *Submitted for publication*, 2018.